Journal of Applied Hydrography

HYDROGRAPHISCHE NACHRICHTEN 03/2026 HN 133

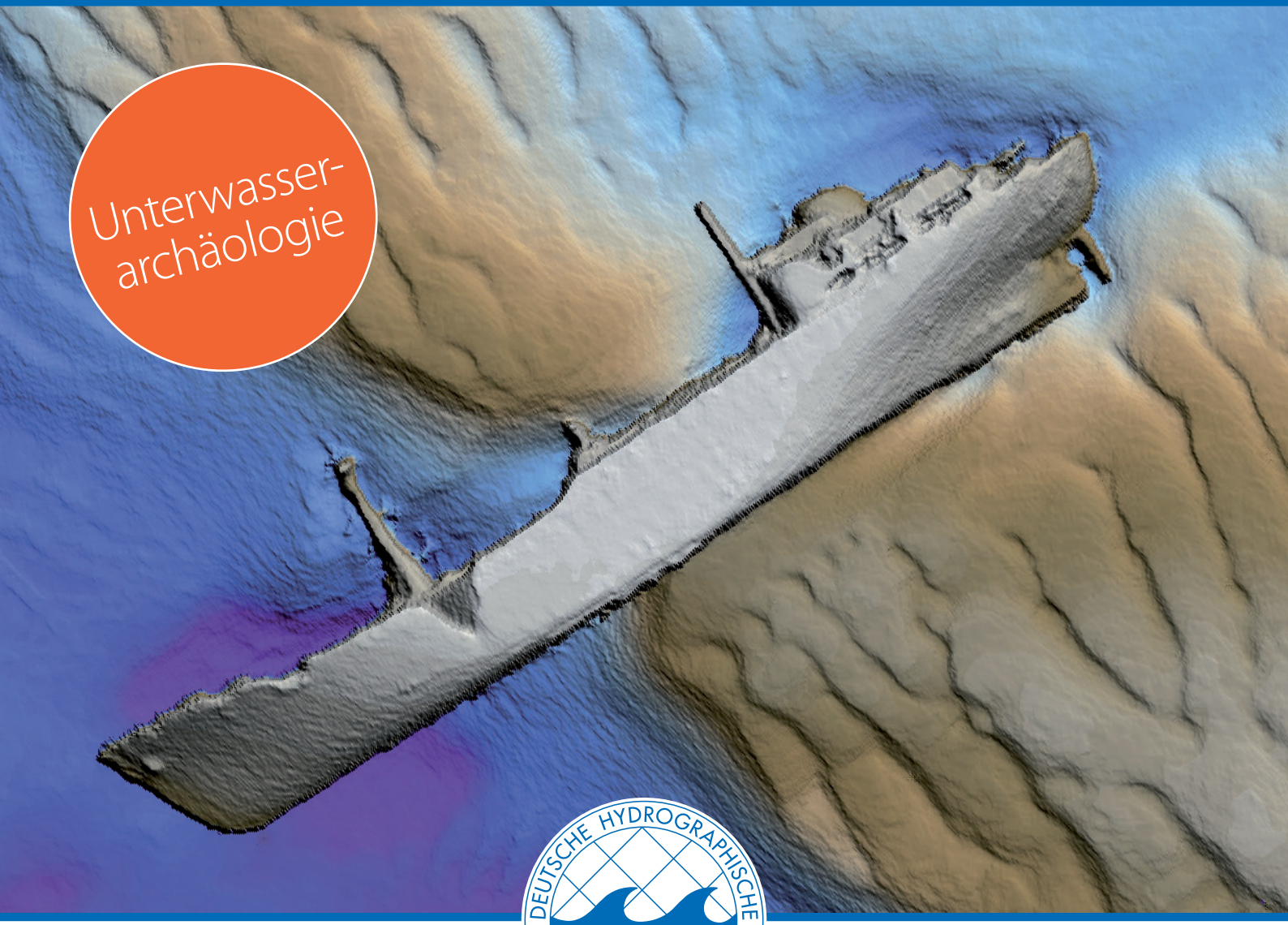

DEUTSCHE HYDROGRAPHISCHE GESELLSCHAFT e.V.
DHyG

pyroscience
sensor technology

AquapHOx Loggers & Transmitters

for optical oxygen sensors

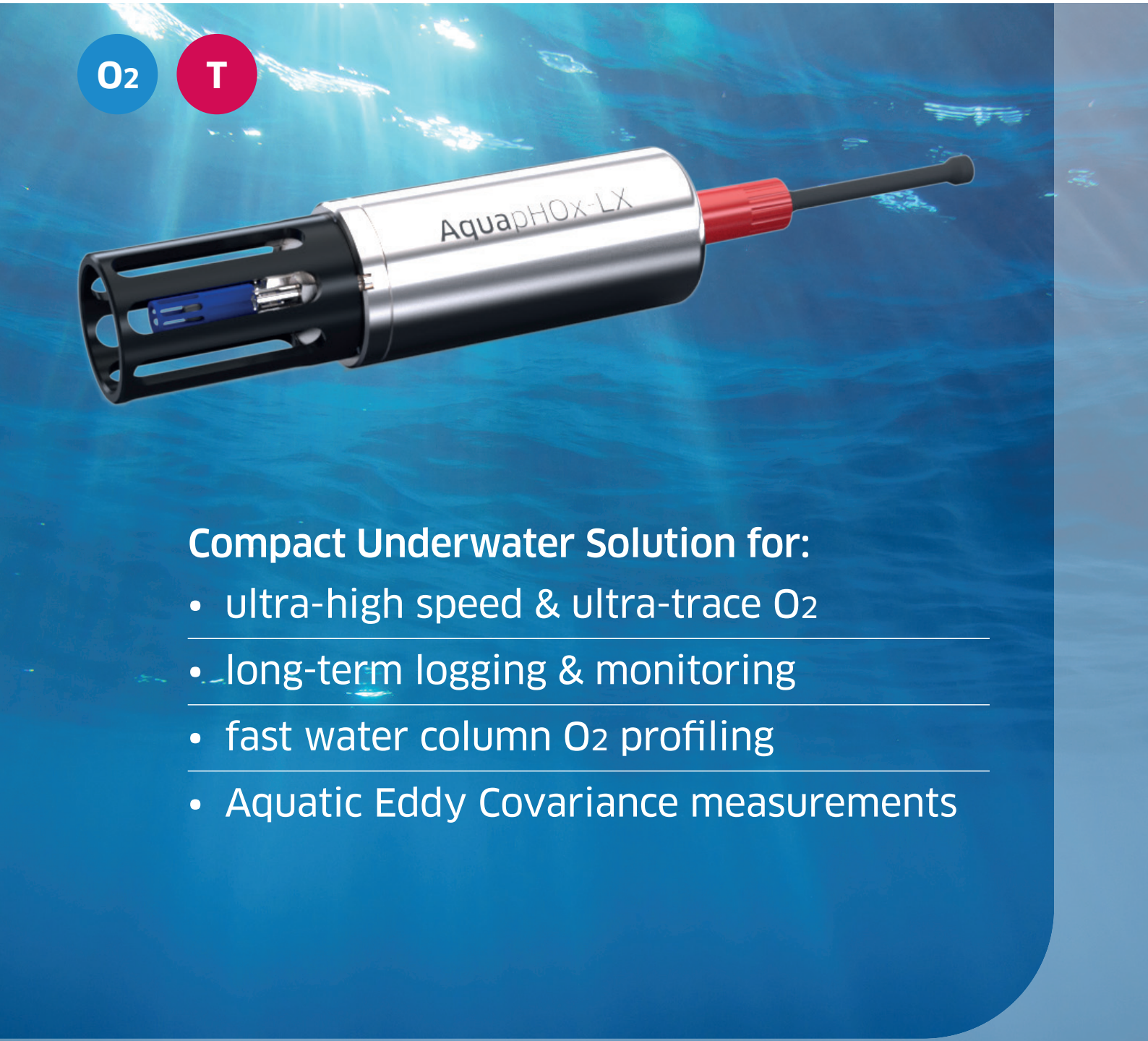

Compact Underwater Solution for:

- ultra-high speed & ultra-trace O_2
- long-term logging & monitoring
- fast water column O_2 profiling
- Aquatic Eddy Covariance measurements

www.pyroscience.com

Liebe Leserinnen und Leser,

wenn ich dieses Heft als Jugendlicher in die Hände bekommen hätte, wäre ich vielleicht Unterwasserarchäologe geworden. Aus den Fachbeiträgen spricht so viel Begeisterung für die geschilderten Tätigkeiten und Aufgaben – das ist geradezu ansteckend. Angereichert wird das Ganze mit tollen Bildern, die das, was unsichtbar unter Wasser liegt, sichtbar machen.

In den Beiträgen geht es zum einen um die Prospektion archäologischer Funde, zum anderen um die Dokumentation des Gefundenen. Berichtet wird von Zufallsfunden (S. 6, S. 30 und S. 46), aber auch von systematischen Vermessungsaktivitäten, um im Boden Verborgenes zu untersuchen (S. 16 und S. 24). Das Instrument der Wahl für die Erkundung ist ein parametrisches Sedimentecholot mit mehreren Kanälen (S. 16 und S. 24). Zur Dokumentation hingegen wird die Unterwasserphotogrammetrie eingesetzt, die sich immer raffinierterer Methoden bedient (S. 34).

Die vielen Autoren der Beiträge zur Unterwasserphotogrammetrie – darunter nur zwei Autorinnen – mahnen, das unter Wasser Vorgefundene besser zu dokumentieren, damit es uns erhalten bleibt – und zwar in Worten, Zahlen und Bilden sowie als virtuelles Modell –, auch wenn die Funde die Zeit im Sediment nicht überstehen. Durch regelmäßige Dokumentation lassen sich auch Veränderungen nachvollziehen. Zur Rekonstruktion der Funde werden immer häufiger 3D-Modelle angefertigt, die durchaus geeignet sind, noch mehr Begeisterung für die Unterwasserarchäologie zu wecken, auch bei der Öffentlichkeit.

Zeigen Sie dieses Heft Ihren Kindern und deren Freundinnen und Freunden. Die müssen ja nicht alle plötzlich Unterwasserarchäologie als Berufswunsch haben, auch ein Job in der Hydrographie wäre okay. Schließlich gilt: ohne die hydrographische Vermessung wäre die Archäologie aufgeschmissen. So drückt es Jens Auer, der Landesarchäologe von Mecklenburg-Vorpommern, im Wissenschaftsgespräch aus (S. 52).

Mit Begeisterung bei der Sache waren auch drei Studierende der HafenCity Universität in Hamburg. Ob es nun um die Verteilung von Sedimenten im Hamburger Hafen geht (S. 58), um Meeresströmungen, die möglicherweise von Seamounts beeinflusst werden (S. 68), oder um Daten aus der Satellitenaltimetrie, die vielleicht etwas über die Morphologie von Seamounts verraten (S. 74) – immer sticht das besondere Engagement und die Leidenschaft für das gewählte Fach hervor. Die Autorinnen der beiden Seamount-Artikel erhielten übrigens von der DHyG eine Förderung, die es ihnen ermöglicht hat, an der Forschungsfahrt teilzunehmen, von der sie berichten.

Ich wünsche Ihnen, dass Sie bei der Lektüre ein paar interessante und unerwartete Fundstellen entdecken.

Lars Schiller

Impressum

Journal of Applied Hydrography
HN 133 – März 2026

HYDROGRAPHISCHE NACHRICHTEN

Offizielles Organ der Deutschen Hydrographischen Gesellschaft – DHyG

Herausgeber
Deutsche Hydrographische Gesellschaft e. V.
c/o Innomar Technologie GmbH
Schutower Ringstraße 4
18069 Rostock

ISSN: 0949-5657 (Print), **1866-9204** (Online-Ausgabe)

Chefredakteur Lars Schiller
E-Mail: lars.schiller@dhyg.de

Redaktion
Dipl.-Ing. Peter Dugge; Ellen Heffner, M.Sc.;
Dr. Jens Schneider von Deimling; Dr.-Ing. Patrick Westfeld

Hinweise für Autoren und Inserenten
www.dhyg.de > Journal of Applied Hydrography > Mediadaten und Hinweise

Alle Ausgaben im Archiv
www.dhyg.de > Journal of Applied Hydrography > Archiv

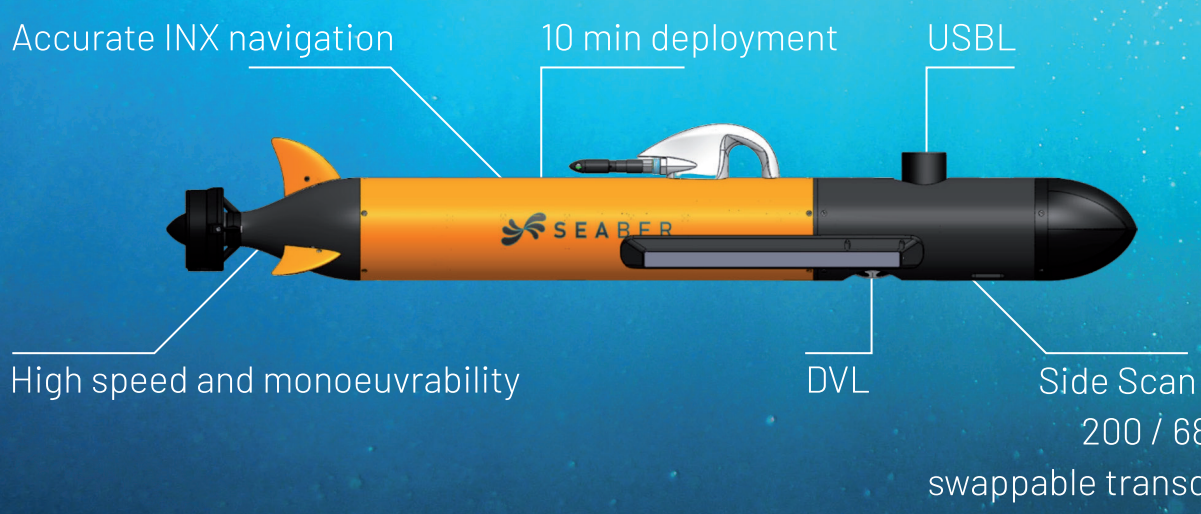

MARVEL-SCAN

MARVEL-SCAN is the most compact AUV with side scan sonar and acoustic positioning.

Your new way to use AUVs.

Photo: Chrijstian Palmer

FEATURES

- » INX Navigation system
- » DVL
- » SEAPLAN Software
- » Embedded rechargeable batteries
- » SEACOMM
- » Field case and accessories
- » Acoustic positioning and communication module
- » Autonomous buoy with USBL unit and dual antenna GNSS-RTK module

FURTHER INFORMATION

Nautilus MARINE SERVICE GmbH

Nautilus Marine Service GmbH
Alter Postweg 30 · D-21614 Buxtehude
Expert: Wibke Dünkel · Phone: +49 (0) 4161 / 55 903-13
sales@nautilus-gmbh.com · nautilus-gmbh.com

Aus dem Inhalt

DOI: 10.23784/HN133-01

Unser unsichtbares Erbe

Archäologische Fundstellen in der Ostsee

Ein Beitrag von JENS AUER

Dieser Beitrag beleuchtet das reiche archäologische Erbe am Grund der Ostsee vor Mecklenburg-Vorpommern. Von steinzeitlichen Jagdstrukturen wie dem »Blinkerwall« bis hin zu mittelalterlichen Schiffswracks und Relikten des Zweiten Weltkriegs bietet die Unterwasserarchäologie einzigartige Einblicke in die Menschheitsgeschichte, die an Land oft verloren gehen. Am Beispiel einer Notbergung, eines spätmittelalterlichen Klinkerfahrzeugs im Jahr 2021, wird der Prozess von der zufälligen Entdeckung eines Wracks, über die Ausgrabung, bis hin zur digitalen Rekonstruktion und anschließenden Deponierung am Meeresgrund aufgezeigt. Abschließend wird die Bedeutung digitaler Visualisierungsmethoden hervorgehoben, um dieses »unsichtbare« Erbe der Öffentlichkeit zugänglich zu machen.

Unterwasserarchäologie | Ostsee | Schiffswracks | Photogrammetrie | Mecklenburg-Vorpommern
underwater archaeology | Baltic Sea | wrecks | photogrammetry | Mecklenburg-West Pomerania

This article explores the rich archaeological heritage on the Baltic Sea floor off the coast of Mecklenburg-West Pomerania. Ranging from Stone Age hunting structures like the »Blinkerwall« to medieval shipwrecks and World War II relics, underwater archaeology provides unique insights into human history that are often lost on land. Using the 2021 rescue excavation of a late medieval clinker-built vessel as a case study, the archaeological process from discovery to excavation and recording, digital reconstruction and subsequent reburial on the seabed is illustrated. Finally, the importance of digital visualisation methods is highlighted as a means to make this »invisible« heritage accessible to the public.

Autor
Dr. Jens Auer ist Landesarchäologe beim Landesamt für Kultur und Denkmalpflege Mecklenburg-Vorpommern in Schwerin.

j.auer@lakd-mv.de

Touristen schätzen den Strand in Mecklenburg-Vorpommern für seine Ruhe und die Weite der Ostsee – doch wirft man einen Blick unter die scheinbar endlose Wasseroberfläche, ergibt sich schnell ein anderes Bild (Abb. 1). Mehr als 4000 registrierte archäologische Fundstellen – Tendenz steigend – zeugen am Meeresgrund von der bewegten Geschichte des Ostseeraums. Dabei reicht das Spektrum der archäologischen Fundplätze von steinzeitlichen Siedlungsplätzen bis hin zu Schiffs- und Flugzeugwracks der letzten Kriege (Auer et al. 2020).

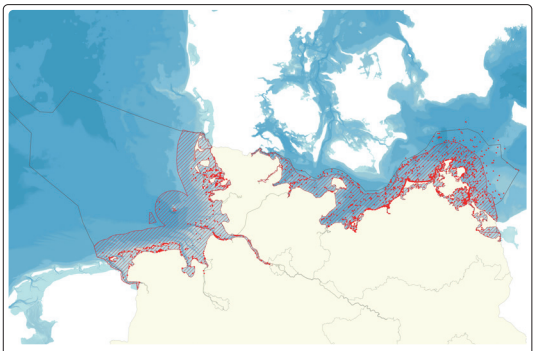

Hintergrundkarte: © GeoBasis-DE/BKG 2020 und BSH (Digitales Geländemodell des Meeresbodens der deutschen Nord- und Ostsee)

Abb. 1: Karte der bekannten Unterwasserfundplätze vor den drei norddeutschen Küstenländern. Der rot schraffierte Bereich markiert das Küstenmeer (Auer et al. 2020, basierend auf Auszügen aus den Denkmaldatenbanken der norddeutschen Küstenländer)

Bis vor etwa 10 000 Jahren lag der Meeresspiegel erheblich tiefer als heute. Sowohl in der Nord- als auch in der Ostsee erstreckte sich nach der Eiszeit begehbares Gebiet, dessen steinzeitliche Bewohner vielfältige Spuren in der Landschaft hinterlassen haben. Doch der steigende Meeresspiegel nach der letzten Eiszeit ließ diese Küstenlandschaften untergehen, sodass sie nun, häufig von jüngeren Sedimenten überdeckt, hervorragend bewahrt am Meeresgrund liegen (Abb. 2). Verschiedene Forschungsprojekte haben in den letzten Jahrzehnten eindrucksvoll die exzellenten Erhaltungsbedingungen dokumentiert und das Potenzial dieser Fundstellen für die Forschung aufgezeigt (Lübke 2014; Schmölcke et al. 2006; Bailey et al. 2020). Als Beispiel kann hier der Fund einer geschäfteten Feuersteinklinge auf einem mittelsteinzeitlichen Fundplatz vor der Insel Poel dienen (4400 bis 4100 v. Chr.). Während im trockenen Milieu an Land höchstens die Klinge selbst erhalten geblieben wäre, konnte bei diesem Unterwasserfund auch der hölzerne Griff mit seiner kunstvollen Bastbindung dokumentiert werden (Abb. 3).

Für besondere Aufmerksamkeit sorgte im Jahr 2022 der Fund einer mehr als 900 m langen

Abb. 2: Meeresspiegelanstieg und landschaftliche Veränderungen während des Holozäns in Nordeuropa (von links nach rechts: 9700 bis 9200 v. Chr. (Präboreal); 8700 bis 8000 v. Chr. (Boreal); 6500 bis 4500 v. Chr. (Atlantikum). Heutige Küstenlinien und die Grenzen der Bundesländer sind grau hinterlegt, Land ist grün dargestellt, Meere und Seen sind blau markiert und Gletscher erscheinen weiß

(Karten zusammengestellt vom ZBSA nach: Björck 1995; Brooks et al. 2011; Cohen et al. 2017; Edwards/Brooks 2008; Harff et al. 2017; Lericolais 2017; Moscon et al. 2015; Pasa-nen et al. 2010; Påsse/Andersson 2005; Patton et al. 2017; Seguinot et al. 2018; Stroevenet al. 2016; Subetto et al. 2017; Weaver et al. 2003)

Steinstruktur, dem sogenannten Blinkerwall, am Grunde der Mecklenburger Bucht durch ein Forschungsteam der Christian-Albrechts-Universität zu Kiel (Supka et al. 2025). Die regelmäßige Anordnung der Steine spricht gegen eine natürliche Entstehung. Die momentane Arbeitshypothese ist daher, dass es sich hier um eine von steinzeitlichen Jägern errichtete Jagdarchitektur handelt, mit deren Hilfe Rentierherden zu Jagdzwecken in die Enge getrieben werden konnten (Abb. 4a und Abb. 4b). In diesem Fall wäre der Steinwall vor etwa 11 000 bis 12 000 Jahren errichtet worden, als nach der letzten Eiszeit Rentierherden durch die noch nicht von der Ostsee überfluteten Landschaften zogen. Ähnliche Strukturen sind z. B. aus dem Lake Huron in den Vereinigten Staaten bekannt. Sollte sich diese Hypothese bestätigen, so würde es sich beim Blinkerwall um eines der ältesten von Menschen geschaffenen Bauwerke in der Ostsee handeln (Geersen et al. 2024).

Doch nicht nur steinzeitliche Jäger und Sammler haben Spuren am Meeresgrund hinterlassen. Tausende am Grund liegende Wracks, Wrackteile und Schiffsladungen zeugen ebenso von einem regen Seehandel, wie auch von kriegerischen Auseinandersetzungen auf See. Das Spektrum der bekannten Fundstellen reicht dabei von vorzeitlichen Einbäumen über hölzerne Handelsschiffe bis hin zu Schiffen und Flugzeugen, die während der beiden Weltkriege ihre letzte Ruhestätte vor den deutschen Küsten fanden.

Abb. 3: Der Fund einer geschäfteten Feuersteinklinge auf dem mittelsteinzeitlichen Siedlungsplatz Timmendorf Nordmole in der Ostsee vor der Insel Poel ist ein eindrucksvolles Beispiel für die gute Erhaltung von organischem Material auf submarinen Fundplätzen

(A. Paasch, LAKD-MV, 2020)

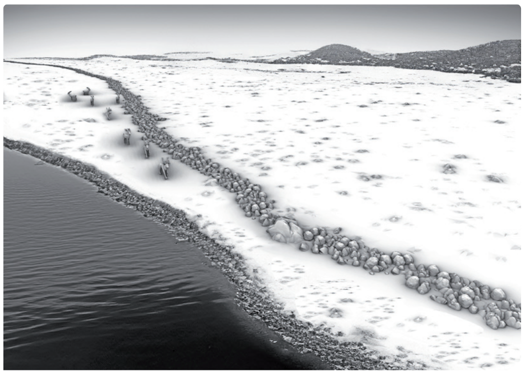

Abb. 4a: Künstlerische Rekonstruktion des Blinkerwalls als Treibjagdstruktur

(Grabowski 2024)

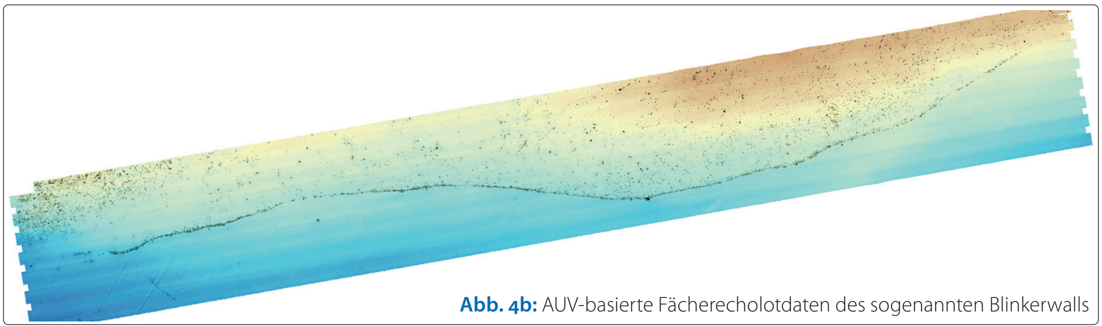

Abb. 4b: AUV-basierte Fächerecholotdaten des sogenannten Blinkerwalls

(Geersen et al. 2024)

(O. Braasch, LAKD M-V, 1994)

Abb. 5: Auf dem Luftbild ist das Wrack der englischen Brigg *Water Nymph* am Strand vor dem Badeort Ahrenshoop deutlich sichtbar

Lange Zeit galten Wasserfahrzeuge als die fortschrittlichsten Fortbewegungsmittel ihrer Zeit, sodass sich in ihnen häufig das technische Know-how einer Gesellschaft widerspiegelt. Ein zu einem bestimmten Zeitpunkt mit Inventar und Ladung gesunkenes Wrack gleicht regelrecht einer Zeitkapsel, die einen bestimmten Moment in der Vergangenheit festhält und detaillierte Einblicke in Handelsbeziehungen und das soziale Gefüge an Bord liefert. In diesem Zusammenhang können selbst einzelne Ausrüstungsgegenstände, wie beispielsweise ein verlorener Anker, überaus wertvolle Hinweise auf maritime Praxis, Herstellungsverfahren oder Ereignisse in der Vergangenheit liefern.

Dabei müssen Wracks nicht immer in großen Wassertiefen liegen. So können aufmerksame Schwimmer bei guter Sicht am Strand vor dem Ostseebad Ahrenshoop in wenigen Metern Wassertiefe die Umrisse eines 30 m langen Handelsschiffs des 19. Jahrhunderts ausmachen (Abb. 5). Archivrecherchen haben ergeben, dass es sich hier um die Überreste der 35 Jahre alten britischen Brigg *Water Nymph* handelt, die im August 1875 im Sturm an der Küste strandete. Die Strandung des Schiffs, die Rettung der Besatzung und vor allem auch die Bergungsversuche werden in Briefen des örtlichen Strandhauptmanns lebendig beschrieben. Besondere Aufmerksamkeit erfährt dabei der unfreundliche englische Kapitän und Eigner des Schiffs, William Peck, der jeden Bergungsversuch unterbindet – möglicherweise motiviert von der lockenden Versicherungsprämie. So endet der letzte Brief des Strandhauptmanns in dieser Sache mit den Worten: Empfehlen dürfte es sich, wenn dem K. Peck klar gemacht würde, dass solche Willkürhandlungen, und ich möchte sagen, Verhöhnungen von Beamten auf deutschem Boden auch selbst einem Engländer nicht gestattet sind (Auer und Belasus 2008).

Auch die Überreste von Wasserbauten wie Hafenanlagen oder Verteidigungsanlagen können in den Küstengewässern erhalten bleiben. So sind im Hafen von Wismar Konzentrationen von archäologischen Funden entdeckt worden, welche die Existenz eines Reedeplatzes wahrscheinlich machen (Förster 2000). Ein im Schlick der Schlei erhaltenes, bis zu 1,6 km langes Kastenbauwerk des 8. Jahrhunderts war vermutlich ein Teil des Danewerks, einer durch die Schleswiger Landenge verlaufenden Befestigungsanlage, welche die Grenze zwischen Dänemark und dem Fränkischen Reich sicherte (Abb. 6) (Auer et al. 2016).

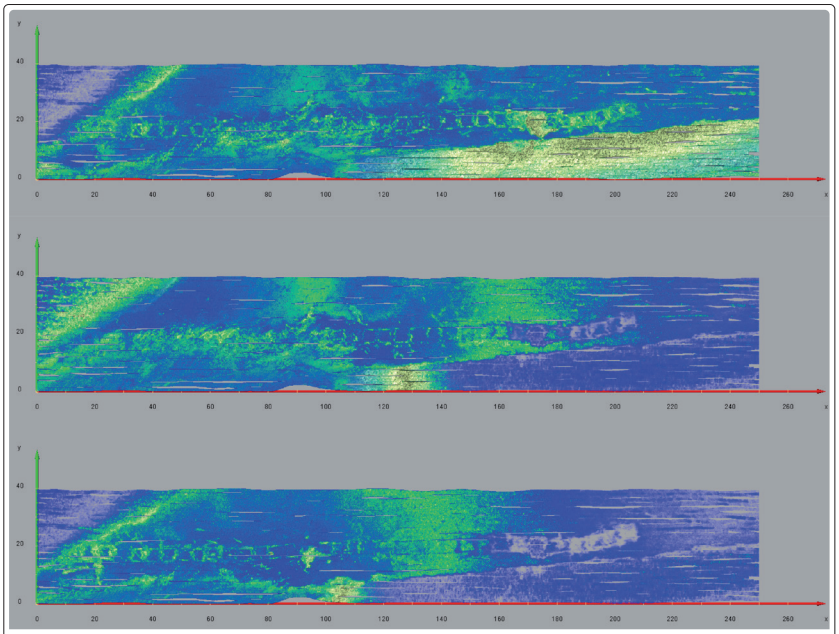

(Innomar 2014)

Abb. 6: Sedimentsonaraufnahmen der Kastenkonstruktionen in der Schlei östlich von Reesholm. Die in verschiedenen Tiefen durch den Datensatz gelegten Schnitte zeigen deutlich den Verlauf der im weichen Sediment verborgenen Holzkästen. Nur ein Teil der Kästen ist oberflächlich sichtbar

Funde von Flugzeugwracks in Nord- und Ostsee stehen meist im Bezug zum Zweiten Weltkrieg. Auch wenn Abstürze häufig zu ausgedehnten Trümmerfeldern am Meeresgrund führten, bieten die Fundstellen von Flugzeugwracks oft Einblicke in technische Aspekte von Konstruktion und Einsatz. Sie legen aber auch ein beredtes Zeugnis vom Kriegsgeschehen ab (Abb. 7).

Eine relativ junge Fundgruppe, welche vor allem im Greifswalder Bodden und in der Ostsee vor Peenemünde auf der Insel Usedom auftritt, sind Relikte der Entwicklung von Lenkwaffen und Raketen aus dem Zweiten Weltkrieg, welche in den Peenemünder Versuchsanstalten entwickelt und getestet wurden. Da kaum schriftliche Dokumentation für diese Arbeiten erhalten ist, stellen die gut erhaltenen Unterwasserfunde nun eine wichtige Quelle für dieses dunkle Kapitel der deutschen Geschichte dar (Abb. 8) (Teschendorff et al. 2021).

Wie wird das archäologische Kulturerbe am Meeresgrund erfasst?

Die Bezeichnung ›unsichtbares Erbe‹ wirft schnell die Frage auf, wie archäologische Fundplätze

unter Wasser inventarisiert werden. Wer findet Wracks und andere Bodendenkmale und wo werden diese registriert?

In Deutschland sind die archäologischen Fachbehörden der Bundesländer auf Basis der jeweiligen Denkmalschutzgesetze für die Inventarisierung von Bodendenkmalen zuständig. Dies gilt sowohl für den Festlandbereich, als auch für das Küstenmeer. In Mecklenburg-Vorpommern registriert das Landesamt für Kultur und Denkmalpflege alle archäologischen Fundstellen in einem webbasierten geografischen Informationssystem, dem sogenannten DenkmalGIS. Allerdings erfolgt keine flächendeckende aktive Erfassung durch die Behörde, stattdessen werden Informationen aus verschiedenen Quellen ausgewertet, geprüft und zusammengeführt. Schiffswracks, als prominenteste Vertreter des Unterwasserkulturerbes seit dem Mittelalter, vermehrt jedoch in der Neuzeit, fanden immer wieder Eingang in historische Quellen in Form von Verklarungen, Gerichtsunterlagen oder Zeitungsnachrichten. Grund dafür war häufig der Wert der Ladung bzw. deren Versicherung, die Frage nach Schuld oder Verursacher des Seeunglücks oder aber die Gefährdung der Schifffahrt durch Wracks oder Wrackteile. Informationen zur Verortung des Unglücks bzw. zum weiteren Verlauf sind dabei aber häufig sehr ungenau oder stellen nur eine Randnotiz dar. Eine systematische Publikation von Seeunglücken und den resultierenden Schiffswracks vor den deutschen Küsten mit dem Ziel, die Sicherheit der Seefahrt zu erhöhen, erfolgte erst ab der Mitte des 19. Jahrhunderts durch die heute vom Bundesamt für Seeschifffahrt und Hydrographie veröffentlichten *Nachrichten für Seefahrer* (NfS) und ihre Vorgängerpublikationen. Eine systematische Suche, Erfassung und Überwachung von Schifffahrtshindernissen, unter anderem also auch Schiffswracks, begann in Deutschland jedoch erst nach dem Zweiten Weltkrieg, da die hohe Anzahl von im Krieg versenkten Fahrzeugen in den Schifffahrtswegen die Sicherheit der Schifffahrt massiv beeinträchtigte. Diese Aufgabe wurde in der Deutschen Demokratischen Republik vom Seehydrographischen Dienst und in der Bundesrepublik Deutschland vom Deutschen Hydrographischen Institut wahrgenommen. Heute stellt die sogenannte Wracksuche eine feste Aufgabe des Bundesamtes für Seeschifffahrt und Hydrographie (BSH) dar. Dabei werden bekannte Schifffahrtshindernisse regelmäßig mit geophysikalischen Methoden und durch Taucher untersucht, um Zustand und die potenzielle Gefährdung der Schifffahrt einzuschätzen. Die Ergebnisse fließen in die vom BSH verwaltete Datenbank der Unterwasserhindernisse ein und stellen eine der wichtigsten Quellen zu Schiffswracks und anderen am Seegrund sichtbaren Arten von Unterwasserkulturerbe dar.

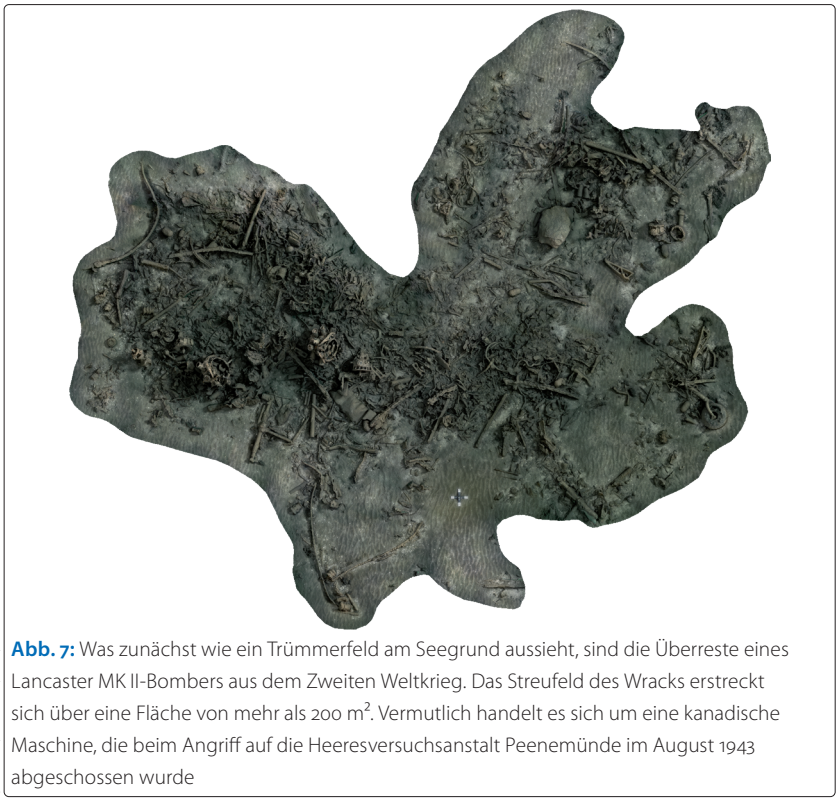

(P. Stencel, LAKD M-V, 2019)

Abb. 7: Was zunächst wie ein Trümmerfeld am Seegrund aussieht, sind die Überreste eines Lancaster MK II-Bombers aus dem Zweiten Weltkrieg. Das Streufeld des Wracks erstreckt sich über eine Fläche von mehr als 200 m^2. Vermutlich handelt es sich um eine kanadische Maschine, die beim Angriff auf die Heeresversuchsanstalt Peenemünde im August 1943 abgeschossen wurde

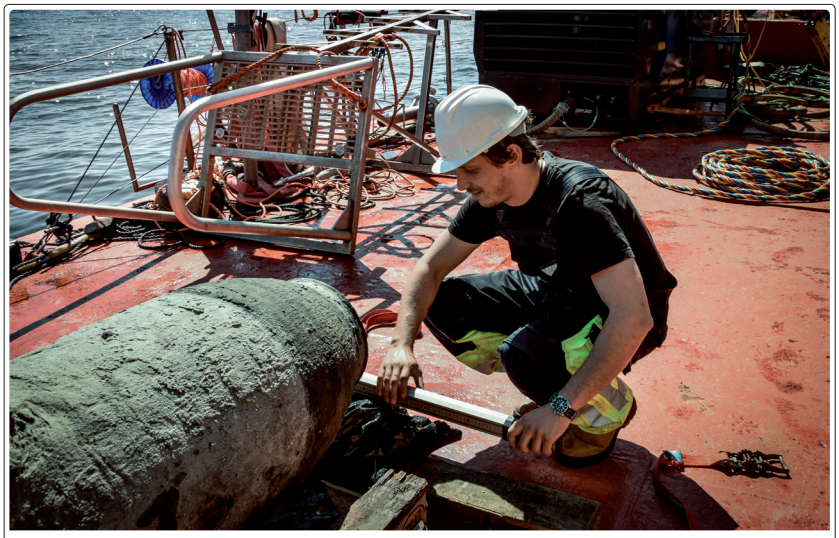

(M. Grabowski, 2018)

Abb. 8: Archäologe bei der Vermessung des Testmodells einer Henschel Hs 293-Gleitbombe an Bord eines Munitionsbergungsschiffes

Eine weitere wichtige Quellengruppe sind Fundmeldungen durch ehrenamtliche Bodendenkmalpfleger und Strandspaziergänger. In Mecklenburg-Vorpommern wird ein großer Teil der strandnahen archäologischen Fundstellen durch die systematische Suche regionaler ehrenamtlicher Bodendenkmalpfleger erfasst.

Aber auch Touristen und Strandspaziergänger melden immer wieder an den Strand gespülte Schiffshölzer oder steinzeitliche Artefakte. Dabei führt die zunehmende Intensität von Sturmereignissen der letzten Jahre und die damit einhergehende Erosion an den Sandstränden des Landes

Abb. 9: Im Jahr 2021 entdeckte ein Strandspaziergänger am Darßer Weststrand Überreste eines großen geklinkerten Schiffs aus der Slawenzeit (922 n. Chr.). Die Schiffsteile wurden geborgen und werden nun im LAKD M-V konserviert

(A. Weidemann, 2021)

zu einem deutlichen Zuwachs von archäologischen Fundmeldungen (Abb. 9).

Geschützt? Aber wie?

Archäologische Fundplätze, die die Kriterien der jeweiligen Denkmalschutzgesetze erfüllen, sind in den Küstenmeeren durch die Denkmalschutzgesetze der Länder geschützt, allerdings gibt es außerhalb der 12-Meilen-Zone, in der sogenannten Ausschließlichen Wirtschaftszone (AWZ), noch keine vergleichbare Regel. Das liegt daran, dass Kultur – dazu gehören auch das Kulturerbe und die Archäologie – ausschließlich Sache der Länder ist. Zwar hat das Unterwasserkulturerbe inzwischen Eingang in eine Vielzahl an Richtlinien und Gesetzen gefunden, die dessen Schutz einfordern, aber diese gelten nur mittelbar und regeln keine Zuständigkeiten, Schutzgebiete, Verbote oder Genehmigungserfordernisse. Die Inkraftsetzung des UNESCO-Übereinkommens zum Schutz des Unterwasserkulturerbes von 2001 durch Deutschland wäre hier ein bedeutender Fortschritt.

Allerdings kennen wir bisher nur einen Bruchteil der real existierenden archäologischen Fundplätze, was den effektiven Schutz zu einer Herausforderung macht. Denn vor allem mit der Ausweitung von Bautätigkeiten im Offshore-Bereich wird auch die Frage nach dem Schutz submariner Fundplätze immer relevanter. Der Schlüssel liegt hier in frühzeitigem Handeln und systematischem Vorgehen in den verschiedenen Planungs- und Bauphasen.

Erhalten oder bergen? Der Umgang mit archäologischen Bodendenkmalen am Meeresgrund

Das öffentliche Bild der Archäologie ist stark von Ausgrabungen geprägt – fälschlicherweise, denn jede Ausgrabung bedeutet am Ende auch eine Störung oder Zerstörung des Fundzusammenhangs und damit auch einen Informationsverlust, der nur durch sorgfältige Dokumentation ausgeglichen werden kann. Das wichtigste Ziel der Bodendenkmalpflege ist daher zunächst immer die Erhaltung des Bodendenkmals an Ort und Stelle und die Vermeidung von Eingriffen. Eine Ausgrabung oder Bergung sollte immer erst die letzte Handlungsoption darstellen.

Daher sind die Denkmalschutzbehörden der Küstenländer bemüht, frühzeitig mit Planern und Investoren von Bauvorhaben ins Gespräch zu kommen. Wie bei anderen Schutzgütern auch, sollten die möglichen Auswirkungen des geplanten Bauvorhabens auf das Unterwasserkulturerbe im Rahmen von Umweltprüfungen beschrieben und bewertet und notwendige Schutzmaßnahmen erläutert werden. Dabei ist es wichtig, alle Auswirkungen von Eingriffen zu bedenken. Auch Ausspülungen durch veränderte Strömungsverhältnisse an Fundamenten von Windrädern oder Leitungen können archäologische Fundplätze beschädigen.

Eine wichtige Rolle bei der Erfassung des Unterwasserkulturerbes nimmt gerade bei geplanten Baumaßnahmen die archäologische Auswertung und Interpretation geophysikalischer und geotechnischer Daten ein. Schließlich können frühzeitig erkannte Fundstellen in die Planung nicht nur mit einbezogen werden, sondern auch von vornherein vermieden bzw., wenn nötig, durch archäologische Ausschlusszonen oder auch Abdeckungen geschützt werden. Ein erster Schritt ist dabei die archäologische Auswertung der durch den Vorhabenträger erhobenen geophysikalischen Daten. Die Ergebnisse dieser Auswertung werden dann mit weiteren Quellen, wie z. B. Wrackregistern oder Verzeichnissen von Schiffsverlusten abgeglichen, um ein möglichst klares Bild der möglicherweise im Untersuchungsgebiet vorhandenen Fundstellen zu bekommen. Um Aussagen zu potenziell vorhandenen Spuren urgeschichtlicher Besiedlung zu treffen, ist ein gutes Verständnis der geomorphologischen Entwicklung im Untersuchungsraum notwendig. Auch hier bilden geophysikalische und geotechnische Untersuchungen eine wichtige Grundlage.

Allerdings bleibt auch nach einer gründlichen Datenanalyse immer ein gewisses Restrisiko, während Voruntersuchungen oder Bauarbeiten auf bisher unbekannte Fundstellen zu treffen. Ein Beispiel hierfür ist vor allem die Suche nach Kampfmitteln, wo engmaschige Prospektionsmethoden eingesetzt werden, um magnetische Anomalien im Seegrund aufzuspüren. Dadurch werden immer wieder archäologische Fundstellen entdeckt. Aber auch bei Baggerarbeiten kann es noch zu solchen Zufallsfunden kommen, z. B. wenn hölzerne Wracks im Sediment begraben liegen und keine nennenswerte magnetische Anomalie darstellen. Gerade wenn Eingriffe in den Boden vor-

(B. Kluz, Archcom, 2021)

Abb. 10: Wrackteile in der Baggerschaufel. Dieses Bild bot sich der baubegleitenden Archäologin bei der Auffindung des Schiffswracks

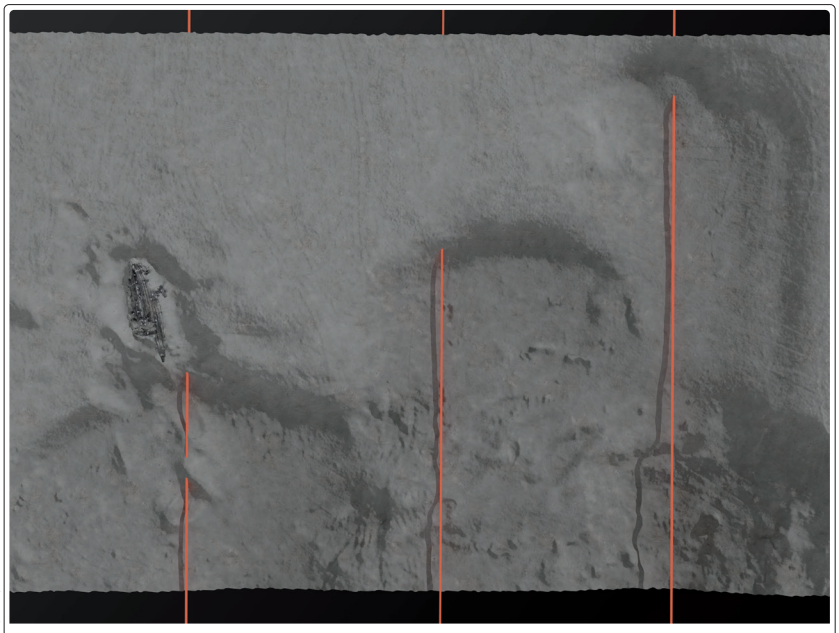

(P. Stenzel, Archcom, 2021)

Abb. 11: In diesem 3D-Modell der Fundsituation ist die Lage des Schiffswracks in unmittelbarer Nähe zur geplanten Kabeltrasse gut zu erkennen. Das Wrack liegt am Rand des bereits ausgebaggerten Bereiches in direkter Nähe zur geplanten Kabeltrasse

genommen werden, sollte daher eine Baubegleitung durch Archäologen erfolgen, um Fundstellen schnell erkennen zu können und notwendige weitere Schritte zu deren Schutz zu planen.

Hölzer in der Baggerschaufel!

Wie wichtig eine solche Baubegleitung ist, zeigt der überraschende Fund eines hölzernen Schiffswracks im Anlandungsbereich einer Kabeltrasse im Jahr 2021 (Auer und Grabowski n.d.).

Bei Baggerarbeiten tauchen während der Nachtschicht Schiffshölzer in der Baggerschaufel auf (Abb. 10). Die baubegleitende Archäologin reagiert sofort: Die Baggerarbeiten werden an der Fundstelle eingestellt und eine archäologische Ausschlusszone wird um den Fundpunkt herum definiert um weitere mögliche Hölzer am Seegrund zu schützen.

Holzdokumentation im Morgengrauen

Noch im Morgengrauen erfolgt eine erste Dokumentation und Einschätzung der Holzfunde und eine Fundmeldung an die zuständige Denkmalschutzbehörde. Es handelt sich um Planken und Spanten eines geklinkerten Fahrzeugs aus Eiche. Verschiedene Baumerkmale deuten auf eine Datierung in das späte Mittelalter hin.

Um zu klären, was am Seegrund nach dem Eingriff erhalten ist, wird eine archäologische Fachfirma vom Bauherrn damit beauftragt, den Umfang der Fundstelle festzustellen und diese zu bewerten. Schnell stellt sich heraus, dass sich die ca. 9 m langen Reste eines Klinkerfahrzeugs noch kieloben liegend am Meeresgrund befinden (Abb. 11). In der Umgebung des Wracks werden im Sediment vereinzelte Hölzer sowie ein größeres zusammenhängendes Teil einer Schiffsseite festgestellt, eingemessen und geborgen.

Das Wrack befindet sich direkt im Anlandungsbereich der geplanten Seekabeltrasse. Eine Umgehung und damit die Erhaltung in situ sind unmöglich, ein weiterer Eingriff in das Bodendenkmal lässt sich nicht vermeiden. Daher wird unmittelbar mit der Planung der archäologischen Dokumentation und Bergung begonnen. Diese soll in enger Zusammenarbeit mit dem Bauherrn schnellstmöglich durchgeführt werden, um den Fortlauf der Kabelverlegung zu gewährleisten und eine weitere Beschädigung des nun im flachen Wasser teilweise exponierten Schiffswracks durch Wellengang zu vermeiden.

Ein Team aus sechs Unterwasserarchäologinnen und -archäologen legt die Wrackstelle mit Hilfe von Unterwassersaugern zunächst vorsichtig frei. Alle Hölzer werden mit aus der Landwirtschaft stammenden Ohrenmarken für Rinder markiert. Im Anschluss wird das Wrack photogrammetrisch dokumentiert und ein 3D-Modell erstellt (Abb. 12). Aufgrund der schlechten Unterwassersicht von teilweise weniger als 50 cm, kommt hierzu eine GoPro-Videokamera zum Einsatz. Nach der Erstellung eines ersten Übersichtsplans wird das Schiffswrack vorsichtig in seine Einzelteile zerlegt (Abb. 13). Dabei arbeiten die Archäologen in umgekehrter Baureihenfolge, das heißt, die Hölzer werden Schicht

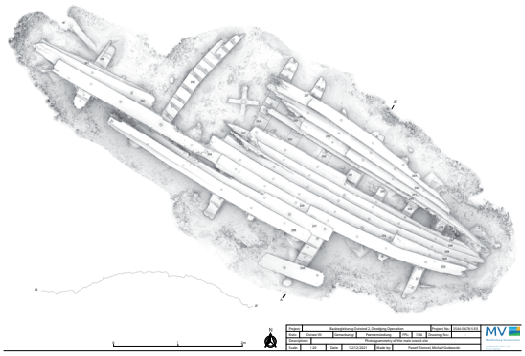

(M. Grabowski und P. Stencel, Archcom, 2021)

Abb. 12: Das kieloben liegende Wrack wurde nach der Freilegung mit Hilfe einer GoPro-Kamera photogrammetrisch dokumentiert. Die einzelnen Schiffshölzer wurden vor der Dokumentation mit deutlich sichtbaren Rinderohrenmarken gekennzeichnet

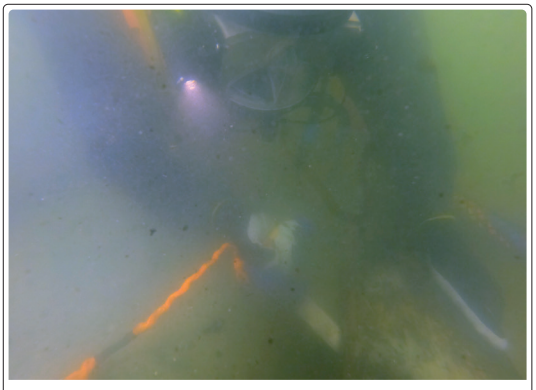

(M. Grabowski, Archcom, 2021)

Abb. 13: Taucher beim Zerlegen des Schiffswracks unter Wasser. Die Holznägel, mit welchen die Spanten in der Rumpfschale befestigt sind, werden mit einer Handsäge durchtrennt

(A. Paasch, LAKD M-V, 2021)

Abb. 14: Eine der eichenen Klinkerplanken wird mit dem Artec Leo-Scanner dreidimensional erfasst

(M. Grabowski, 2022)

Abb. 15: 3D-Modell einer Bodenwrange des Wracks, links mit Textur, rechts als annotierte Umzeichnung in Vorbereitung für die Ausgabe im archäologischen Befundkatalog

für Schicht gelöst und entfernt. Holznägel, mit denen die Spanten des Schiffs an den Planken befestigt sind, müssen dabei mit Handsägen durchtrennt werden. Alle geborgenen Hölzer werden mit Hilfe einer Plattform an Deck gehoben und zunächst nass zwischengelagert. Ein Austrocknen der Hölzer muss unbedingt vermieden werden, da ansonsten gleich eine Verformung bzw. ein Verfall der Oberfläche einsetzt.

Da aufgrund der Lage des Wracks die Erhaltung von Inventar und Ladung in der Rumpfschale möglich ist, wird der Innenbereich vorsichtig freigesaugt. Bis auf einen deutlich jüngeren Georgstaler aus dem Umfeld kommen allerdings keine weiteren archäologischen Funde zutage. Nach einer gründlichen Umfeldsuche kann die Ausgrabung nach zehn Tagen beendet und die Baufreigabe erteilt werden.

Ein hölzernes Puzzlespiel

Die archäologische Arbeit ist damit allerdings noch lange nicht beendet. Sorgfältig verpackt werden die 111 geborgenen Schiffshölzer in die Konservierungswerkstätten des Landesamtes für Kultur und Denkmalpflege in Schwerin transportiert. Nach der Reinigung werden Proben von Kalfatmaterial, Anhaftungen und eventuellen Anstrichen genommen. Die gereinigten Hölzer werden mit Hilfe eines Artec Leo-Scanners dreidimensional erfasst (Abb. 14), interpretiert und anschließend in der Software Rhinoceros3D beschrieben.

Die so erzeugten detaillierten 3D-Modelle (Abb. 15) bilden die Grundlage der archäologischen Holzdokumentation und helfen, den Schiffbauprozess zu verstehen. Werkzeugspuren und Markierungen sind im Modell deutlich zu erkennen. Zudem lassen sich die Modelle in beliebigem Maßstab als 3D-Modell ausdrucken. Aus den im Maßstab 1 : 10 gedruckten Hölzern wird ein dreidimensionales »Puzzle«. In mühsamer Kleinarbeit wird nun versucht, die vielen im Umfeld des Wracks geborgenen Einzelhölzer und Holzbruchstücke wieder in den Wrackzusammenhang einzuordnen.

So entsteht langsam ein Arbeitsmodell des Schiffswracks, wie es vor dem Eingriff mit der Baggerschaufel am Grund der Ostsee lag. Dieses Mo-

(M. Grabowski, 2022)

Abb. 16: Die im Maßstab 1 : 10 aus PLA gedruckten Hölzer werden mit kleinen Schrauben zu einem ersten Arbeitsmodell zusammengesetzt. Als Anhaltspunkt dient dabei die Unterwasserdokumentation des Fundplatzes

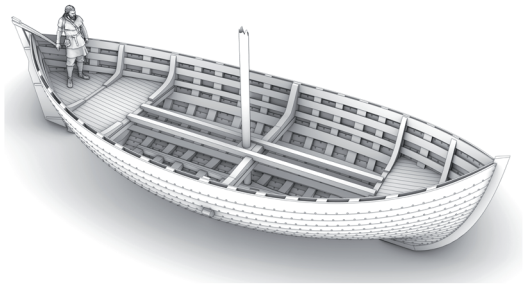

(M. Grabowski, 2022)

Abb. 17: Die visuelle Rekonstruktion des Schiffsfundes (Peenemündung, Ostsee VII, Fpl. 136) gibt einen ersten Eindruck vom möglichen Aussehen des Küstenseglers. Als Ausgangspunkt diente das Arbeitsmodell, mit dessen Hilfe versucht wurde, die geborgenen Schiffsteile und Sektionen in den Fundzusammenhang einzuordnen

dell dient als Grundlage für eine Rekonstruktion des Fahrzeugs (Abb. 16).

Das kieloben aufgefundene Schiffswrack war fast über seine gesamte Länge erhalten. Der eichene Kiel war ursprünglich 9 m lang, wurde aber bei den Baggerarbeiten stark beschädigt. Vorder- und Achtersteven des Schiffs konnten nicht aufgefunden werden. Von der Außenhaut aus geklinkerten Eichenplanken sind an der Steuerbordseite 13 Gänge erhalten, an der Backbordseite allerdings nur vier. Die aus Eiche radial gespaltenen Außenplanken waren durch auf rechteckigen Nietplatten vernietete, eiserne Klinkernägel miteinander verbunden. Als Dichtmaterial in Laschen und Landungen wurde durchgängig in Teer getränkte Schafswolle genutzt. Die eichenen Spanten waren mit sorgfältig zugearbeiteten Holznägeln an der Außenhaut befestigt. Ein massiver Querbalken ragte durch eine rechteckige Öffnung in der Außenhaut und verband die beiden Schiffseiten vor dem Mast. Der Querbalken wurde, möglicherweise bei einer Reparatur, mit geteerten Resten eines gefärbten Wollstoffs abgedichtet. Wie die dendrochronologische Auswertung zeigt, stammen die Schiffbauhölzer aus dem westlichen Schweden und wurden zwischen 1437 und 1438 gefällt. Eine der beprobten Planken wies allerdings deutliche Spuren einer Zweitverwendung auf und stammt aus dem südlichen Ostseeraum. Vermutlich wurde das Schiff in seiner Lebenszeit mindestens einmal aufwendig repariert.

Die gesammelten Daten erlauben eine vorsichtige Rekonstruktion des Wracks und liefern erste Hinweise auf Aussehen und Verwendung des Fahrzeugs. Der in Schweden gebaute einmastige Küstenfahrer hatte eine Länge von ungefähr 11 m und war bis zu 4 m breit bei einer Seitenhöhe von ca. 2,7 m. Die Tragfähigkeit betrug zwischen 13 und 14 Tonnen. Das Boot hatte sicherlich ein Heckruder, welches von einem Halbdeck im Achterbereich bedient werden konnte. Die Ladung konnte in einem offenen Laderaum in der Schiffsmitte verstaut werden (Abb. 17).

Das im Greifswalder Bodden gefundene Schiff weist viele Ähnlichkeiten mit dem sogenannten *Kalmar 1*-Wrack auf, einem kleinen mittelalterlichen Lastensegler, der in den 1930er-Jahren bei Entwässerungsarbeiten vor dem Schloss im südschwedischen Kalmar entdeckt wurde (Åkerlund 1951).

Ein Küstenfahrer ohne Ladung

Doch wie gelangte das Wrack an seinen Fundort? Und wo sind Ladung und Inventar?

Bewuchsspuren an den erhaltenen Schiffshölzern zeigen deutlich, dass der Schiffsfund ursprünglich auf ebenem Kiel liegend im Sediment eingebettet war. Wann und wie das Fahrzeug kieloben an seinen Fundort gelangte, bleibt unklar. Es ist möglich, dass das Wrack durch Sturm oder menschliche Eingriffe bei früheren Bauarbeiten in seiner Lage gestört wurde und schließlich im flachen Wasser des Boddens wieder mit Sediment bedeckt wurde. Ladungsreste konnten aber trotz intensiver Suche nicht im Umfeld entdeckt werden. Allerdings sind im Greifswalder Bodden einige spätmittelalterliche Schiffsladungen bekannt. So wurden am Eingang des Boddens Ansammlungen von bearbeitetem schwedischem Kalkstein gefunden, in deren Umfeld keine Wrackhölzer entdeckt werden konnten. Möglicherweise kenterte der Küstenfahrer an einem stürmischen Tag im Bodden und verlor Ladung und Inventar in tiefem Wasser, während der Schiffsrumpf ins Flachwasser gespült wurde. Vielleicht liefert eine Analyse der organischen Ablagerungen auf der Rumpfinnenseite weitere Informationen zu einer möglichen Ladung des Bootes.

Auch wenn viele Analysen noch ausstehen, zeigen die vorläufigen Ergebnisse schon eindrucksvoll, wie viele Informationen zu Schiffbau und Nutzung im Spätmittelalter auch ein unerwarteter Zufallsfund noch zu liefern vermag, wenn er rechtzeitig erkannt wird und eine archäologische Notbergung erfolgen kann.

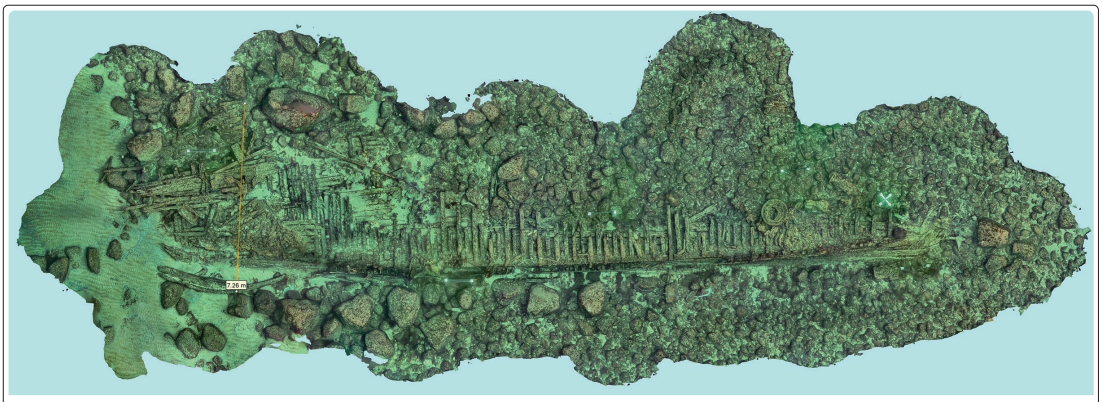

(Unterwasseraufnahmen: H. Phoenix, 3D Modell: R. Obst, Archaeomare e.V., 2026)

Abb. 18: Beispiel einer photogrammetrischen Dokumentation eines hölzernen Schiffswracks vor dem Gellort auf Rügen (Wittow, Ostsee VI, Fpl. 26)

Die Konservierung von Nasshölzern ist zeitaufwendig und mit hohen Kosten verbunden. Eine vollständige Konservierung von großen Funden, wie z. B. Schiffswracks, wird daher meist nur dann angestrebt, wenn entweder eine Ausstellung geplant ist oder aber die wissenschaftliche Auswertung eine ständige direkte Zugänglichkeit erfordert. In diesem Fall wurde ein anderer Weg gewählt. Nach der vollständigen Dokumentation wurden alle Schiffshölzer systematisch unter einer Sandabdeckung von 1,5 m in einem Depot am Meeresgrund eingelagert. Hier kann das Wrack in einer sauerstoffarmen Umgebung sicher lagern und bleibt für eine spätere Konservierung verfügbar.

Das Unsichtbare sichtbar machen

Während die beschriebene archäologische Ausgrabung eine Möglichkeit bietet, verborgenes Kulturerbe sichtbar und zugänglich zu machen, bleibt dieser Weg die Ausnahme. Ein weitaus schonenderer Ansatz ist die digitale ›Sichtbarmachung‹ durch die Erstellung präziser 3D-Modelle von Schiffswracks direkt am Meeresgrund (Abb. 18).

Dank technologischer Fortschritte in den letzten Jahren sind Unterwasserdokumentations- und -visualisierungsmethoden – allen voran die Photogrammetrie – deutlich anwenderfreundlicher geworden. Dies führt dazu, dass immer mehr Taucher ihre Entdeckungen systematisch erfassen und auf Plattformen wie Sketchfab der Öffentlichkeit zugänglich machen. Beeindruckende Beispiele für Wrackmodelle aus Nord- und Ostsee finden sich etwa auf der Website des Ingenieurs Holger Buss (www.dive3d.eu).

Auch in Mecklenburg-Vorpommern leisten ehrenamtliche Bodendenkmalpfleger und engagierte Sporttaucher einen wesentlichen Beitrag zur Dokumentation und Visualisierung von Unterwasserfundstellen. Beispielhafte Arbeiten hierzu präsentieren die Gesellschaft für Schiffsarchäologie in Rostock (www.gfs-rostock.de/3d) sowie der Verein Archaeomare (www.archaeomare.de/kompetenzen/structur-frome-motion-photogrammetrie).

Diese dokumentierten Wracks werfen eindrucksvolle Schlaglichter auf das einzigartige kulturelle Erbe des Ostseeraums, das bislang unter der Wasseroberfläche verborgen lag. //

Literatur

Åkerlund, Harald (1951): Fartygsfynden i den forna hamnen i Kalmar. Almqvist & Wiksells boktryckeri, Uppsala

Auer, Jens; Mike Belasus (2008): The British Brig ›Water Nymph‹ or … even an Englishman cannot take the liberty to deride a civil servant on German soil. International Journal of Nautical Archaeology, DOI: 10.1111/j.1095-9270.2007.00168.x

Auer, Jens; Michal Grabowski (n.d.): So much from so little. Proceedings of the Seventeenth International Symposium on Boat and Ship Archaeology – ISBSA 17, forthcoming

Auer, Jens; Detlef Jantzen; Marion Heumüller; Stefanie Klooß (2020): Kulturerbe unter Wasser. Leitfaden für Baumaßnahmen im Küstenmeer. Schleswig: Landesamt für Kultur und Denkmalpflege Mecklenburg-Vorpommern; Niedersächsisches Landesamt für Denkmalpflege; Archäologisches Landesamt Schleswig-Holstein.

Auer, Jens; Oliver Nakoinz; Christoph Rinne (2016): Archäologie in trübem Wasser – Ein Überblick zur Fundgeschichte und neue Untersuchungen zu einer Holzkonstruktion des 8. Jahrhunderts in der Schlei. Archäologische Nachrichten aus Schleswig-Holstein (22), S. 70–79

Bailey, Geoff; Nena Galanidou; Hans Peeters; Hauke Jöns; Moritz Mennenga, M. (Eds.) (2020): The Archaeology of Europe's Drowned Landscapes. Springer International Publishing, Cham, DOI: 10.1007/978-3-030-37367-2

Förster, Thomas (2000): Schiffswracks, Hafenanlagen, Sperrwerke – Neue archäologische Entdeckungen in der Wismarbucht. Skyllis 1, S. 10–18

Geersen, Jacob; Marcel Bradtmöller; Jens Schneider von Deimling et al. (2024): A submerged Stone Age hunting architecture from the Western Baltic Sea. Proceedings

of the National Academy of Sciences, DOI: 10.1073/pnas.2312008121

Lübke, Harald (2014): Hartz, Jöns, Lübke, Schmölcke, Carnap-Bornheim, Heinrich, Klooss, Lüth, Wolters 2014 – Prehistoric Settlements In The South-Western Baltic Sea Area And Development Of The Regional Stone Age Economy. Final Report Of The Sincos-Ii-Subproject 4. Academia, DOI: 10.5281/ZENODO.260164

Schmölcke, Ulrich; Elisabeth Endtmann; Stefanie Klooß et al. (2006): Changes of sea level, landscape and culture: A review of the south-western Baltic area between 8800 and 4000 BC. Palaeogeography, Palaeoclimatology, Palaeoecology, DOI: 10.1016/j.palaeo.2006.02.009

Supka, Ruth; Jens Schneider von Deimling; Sebastian Krastel; Jacob Geersen (2025): Der ›Blinkerwall‹ in der Mecklenburger Bucht: Von der Entdeckung während einer Ausbildungsfahrt zum Leibniz-Projekt. Christiana Albertina, DOI: 10.38072/2942-2337/p42

Teschendorff, Daniela; Philipp Aumann; Thomas Köhler (2021): Spuren des Zweiten Weltkriegs im Greifswalder Bodden. Kriegsschrott und Kulturgut. In: Florian Huber (Hsg.): Zeitreisen unter Wasser. Theiss, Darmstadt

DOI: 10.23784/HN133-02

Rapid investigation of shallow underwater archaeological sites with parametric multi-transducer sub-bottom profilers

An article by JENS LOWAG, ANDRZEJ PYDYN, MATEUSZ POPEK and JENS WUNDERLICH

Non-invasive remote sensing techniques, such as shallow seismic acoustic imaging methods, are frequently used to explore palaeo-landscapes hidden below seabed, to survey and map underwater archaeological sites. This includes identification of buried archaeological artefacts, such as shipwrecks or artificial constructions from the past. A parametric multi-transducer sub-bottom profiler was applied to image the archaeological site of the medieval harbour of Puck, one of the largest medieval harbours in the Baltic Sea. The acquired high-resolution 3D shallow seismic dataset allowed the identification of a previously unknown and buried wooden shipwreck, to outline the harbour boundary of the medieval port and to trace the palaeo-channel of the local Plutnica River in the Puck Bay. This case study focuses on the results of the sub-bottom profiler survey, but data were fused with results from other remote underwater sensing surveys at the heritage site of Puck during an extensive investigation, such as multibeam and photogrammetric surveys.

parametric acoustics | sub-bottom profiler | medieval harbour | 3D shallow seismic | acoustic imaging
parametrische Akustik | Sedimentecholot | mittelalterlicher Hafen | 3D-Flachseismik | akustische Bildgebung

Nicht-invasive Fernerkundungstechniken, wie z. B. seismische Akustikbildgebungsverfahren, werden häufig eingesetzt, um unter dem Meeresboden verborgene Paläolandschaften zu erforschen und archäologische Unterwasserfundstätten zu vermessen und zu kartieren. Dazu gehört auch die Identifizierung archäologischer Artefakte, wie z. B. Schiffswracks oder künstlicher Konstruktionen aus der Vergangenheit. Ein parametrisches Mehrfachschwinger-Sedimentecholot wurde eingesetzt, um die archäologische Stätte des mittelalterlichen Hafens von Puck, einem der größten mittelalterlichen Häfen der Ostsee, abzubilden. Der erfasste hochauflösende 3D-Datensatz der seismischen Flachortung ermöglichte die Identifizierung eines bisher unbekannten und vergrabenen Holzschiffswracks, die Umrisse der Hafengrenze des mittelalterlichen Hafens zu skizzieren und den Paläokanal des lokalen Flusses Plutnica in der Puck-Bucht nachzuzeichnen. Diese Fallstudie konzentriert sich auf die Ergebnisse der Sedimentecholot-Untersuchung, aber die Daten wurden mit den Ergebnissen anderer Fernerkundungsuntersuchungen am Kulturerbeort Puck während einer umfangreichen Untersuchung, wie z. B. Fächerecholot- und photogrammetrischen Vermessungen, zusammengeführt.

Authors
Jens Lowag and Dr. Jens Wunderlich work for Innomar Technologie GmbH in Rostock. Prof. Andrzej Pydyn and Dr. Mateusz Popek work at the Centre for Underwater Archaeology of the Nicolaus Copernicus University in Toruń, Poland.

jlowag@innomar.com

1 Introduction

Acoustical systems are frequently used for the detection of archaeological objects and structures embedded within the sediments of lakes, rivers and the open sea for many years (Quinn et al. 1997; Wunderlich et al. 2005; Missiaen 2010; Wilken et al. 2022). Typically, 2D reflection seismic systems, also referred to as sub-bottom profilers, are applied to survey archaeological sites line by line to detect signal anomalies within the cross-sectional data records, based on amplitude and phase variations or based on distinct morphological features. Different technologies are used for sound generation, such as linear acoustical transmission of continuous wave pulses (CW) in echo sounders and pingers, transient pulses in boomer and sparker systems and frequency modulated pulses (FM) in Chirp systems. The returning pulses may be either received by the same transducer used for the transmission or by separate receivers and hydrophones. Parametric (i.e. non-linear) sound pulse generation (CW, FM) was also applied for marine archaeological applications (Wunderlich et al. 2005). There is a high potential for this technology

for such investigations due to the high mobility of parametric systems, improved resolution and the capability to work in very shallow waters (Missiaen et al. 2008). The challenges for the acoustical detection of buried archaeological features may be divided into system related technical limitations and environmental constraints. Such technical limitations are:

- The water depth is shallow, ranging from several metres to a few decimetres where low frequency linear sub-bottom profilers encounter issues due to signal ringing and broadening of the transmit pulse, causing high reverberation levels within the first few metres below the transducer and may prohibit the detection of the desired echo signals from shallow archaeological reflectors.
- The broadening of the transmit pulses in low-frequency linear acoustical systems causes a reduced vertical resolution of the acoustical data, particularly close to the water-sediment boundary, where the signal amplitudes are high.
- The acoustical footprint of the sub-bottom profiler is large compared to the spatial dimensions of the archaeological features which firstly reduces the achievable lateral resolution and secondly reduces the detectability of a reflector depending on signal amplitude variations.
- The sound beam pattern of directional linear acoustical sources exhibits side lobes which causes ambiguities in the echo signals.

Typical environmental constraints are:

- The appearance of multiple echo signals, particularly in shallow water, travelling two or more times between the sediment floor and water surface, which are then recorded and may disturb and mask signals of interest from a greater sub-seabed depth than the approximate water depth (also depending on sediment properties and transducer draft).
- The shape and orientation of embedded objects are irregular and may not cause a direct reflection of the sound waves towards the receiver and produce echo signals of low amplitude only.
- The spatial dimensions of archaeological features are typically small compared to the size of the investigation area, hence full coverage cannot be achieved during a line-by-line survey.
- The embedded archaeological objects are often made of materials (e.g. wood) with a low acoustical impedance contrast to adjacent sediments.
- The sediment properties may prohibit the required penetration due to the presence of dense sand, gravel and shells or layers of small gas bubbles caused by the decomposition of organic material

There are few technical approaches to 3D shallow-seismic reflection systems for archaeological applications, like commonly used systems in the oil and gas industry for the large-scale detection and mapping of reservoirs. Typically, a non-directional or wide beam acoustical source is combined with a relatively large focusing receiver array to create a dense dataset and to achieve better site coverage. This enables the generation of a 3D model of the sub-seabed morphology and embedded features, such as wrecks, harbour structures or remains of historical settlements (Plets et al. 2009; Mueller et al. 2013; Wilken et al. 2019). These systems typically require a high effort in data processing and must deal with acoustic diffraction within a complex medium of unknown sound velocities, with irregular morphologies and unresolvable travel paths, causing ambiguities and degrading the resolution. Acoustical beam steering and focussing with increasingly large angular offsets will also cause a broadening of the echo signals and an increase in side lobes with subsequent loss of resolution. These challenges were illustrated by Grøn and Boldreel (2014), where buried wooden posts of a landing pier at an archaeological site in Northern Germany could not be detected with such a 3D system, but clearly imaged with a common single-beam Chirp profiler. The above-mentioned challenges of large acoustical footprints during transmission and high reverberation levels for linear acoustical transmitters in shallow waters are valid for the fusion of multiple 2D seismic sections and the described 3D systems. The fusion of multiple and densely spaced 2D seismic sections into a three-dimensional data representation has been applied as well (Ravnås et al. 2023). Accordingly, the approach within this study was the acquisition of a dense dataset with high vertical and lateral resolution at a relatively small archaeological site by the combination of multiple parametric acoustic sources within a linear array, employing individual narrow sound beams with a small acoustical footprint for each transducer. This technique has successfully been applied to other shallow archaeological sites before, for example at the Roman and medieval site in the intertidal zone of Raversijde (Missiaen et al. 2018).

2 Archaeological site

The archaeological site of the medieval harbour of Puck is located at the inner northwestern part of Puck Bay within the wider basin of the Bay of Gdańsk (Fig. 1). The water depth of the site ranges from about 1 to 3 m. The site was discovered in 1977 by recreational divers (Stępień 1983). During first investigations, early medieval wrecks were discovered, as well as harbour relics and other traces of a settlement. Ultimately, one wreck was recovered and conserved by the Central Maritime Museum

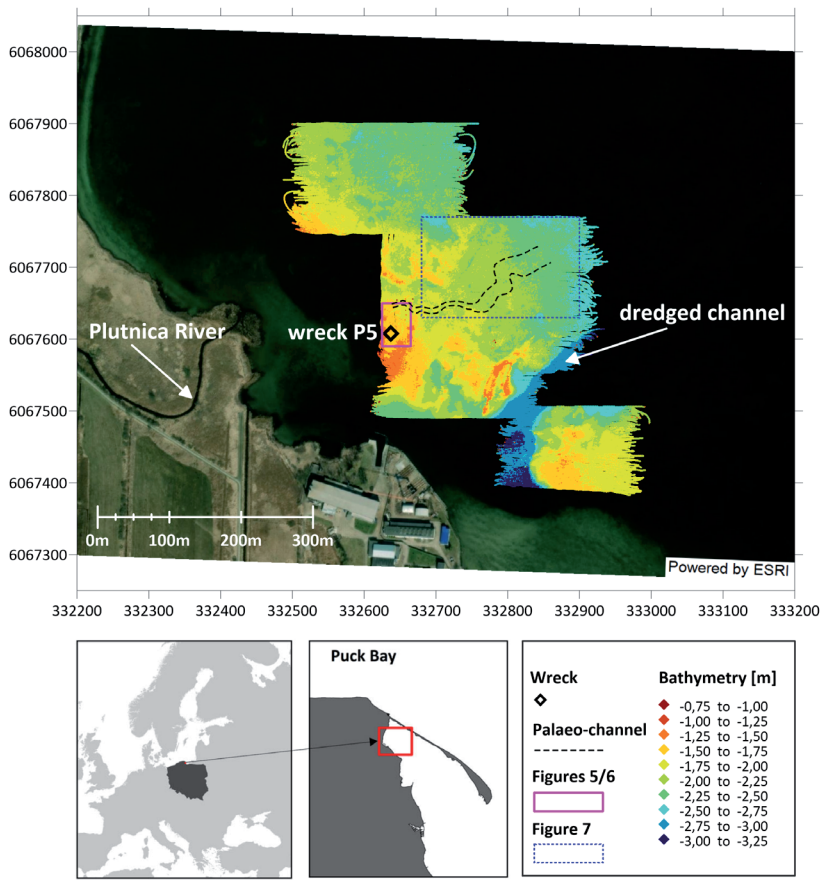

Fig. 1: Overview map of the study area with coloured depth soundings obtained from the 100-kHz high-frequency channel of the parametric system with a sounding density of 50 cm across track (bathymetry data points from two transducers). The location of wreck P5 is marked. The current course of the river Plutnica and the identified palaeo-channel are indicated. Coordinates are given in WGS-84 UTM Zone 34N

in Gdańsk (Szulta 2002). From dating results, three main phases of the harbour development were proposed after the pre-harbour Phase 0 (ranging from the Bronze Age to the 8th century). First, the harbour operational period Phase I (ranging from the 9th to the 10th century), second, the harbour operational period Phase II (occurring in the late 12th century) and finally, the harbour operational Phase III (ranging from the late 13th to the mid-14th century), already showing a significant shrinking in size (Popek 2020). Most of the relics from Phase II were destroyed by the construction and dredging of a channel towards the Puck Mechanical Works. The archaeologically mapped structures of Phase III constituted a jetty, which had a gap in it that formed the entrance to the harbour basin. The two wrecks laying at this entrance (the previously known and excavated wreck P3 and the latest discovered wreck P5) were dated to the 12th and 13th century and the stratigraphic arrangement suggested that both wrecks did not sink later than in the 1340s (Popek 2020). Currently, a vast number of wooden artefacts are visible above seabed (wooden poles, etc.), but others are fully buried below the sediments.

Fig. 2: Line array of four parametric transducers mounted on a small survey vessel. The transducer array has a length of 1 m

3 Methods

3.1 Data acquisition

A parametric sub-bottom profiler dataset was acquired during two surveys, one conducted in December 2018 (two days), the other one in March 2019 (three days), using the Innomar SES-2000 quattro system, bow mounted on a small survey boat (Fig. 2). The parametric acoustical system consisted of a transceiver unit and four transducers, arranged in a linear array. Each transducer had an active size of 155 mm by 155 mm and the distance between two transducer centre-points was 250 mm. Parametric systems produce two slightly different primary frequencies which generate new secondary frequencies (the sum and difference of the primary frequencies), which are received and analysed (Wunderlich et al. 2005). The Innomar system used in this study transmits primary frequencies around a centre frequency of 100 kHz, which generate secondary frequencies between 5 and 15 kHz. The half-power beam width (5 degrees at –3 dB) is very narrow and valid for both, the primary and the secondary frequency of 10 kHz used during acquisition. Due to the narrow sound beam the acoustical footprints of the individual transducers did not overlap significantly at the given water depth range of 1 m to 3 m (Fig. 3). Multiple transducers of the line array were used during reception to focus the energy of the echo signals. The transmitted pulse length was 100 µs and the pulse rate was circa 19 s^{-1} for each transducer. Positioning was realised with a dual-antenna differential GPS receiver utilising cellular network broadcasted correction data for the recording of centimetre accurate sounding positions, water level variations during the survey and true heading

of the transducer array. A motion sensor was used for the recording of heave, roll and pitch motions of the transducer array. The site was divided into several regions of interest and covered by parallel survey lines at 1-m spacing (Fig. 1). Based on the intermittent transmission for the individual transducers, the ping rate and the survey speed, a data density of circa 10 cm per sounding was achieved along track. The average data density across track is 25 cm depending on the navigational offsets from the planned lines but for a single profile the coherent sounding distance is always 25 cm. Every survey line provided four seismic sections with a spacing of 25 cm. A survey speed of around 1.5 m/s to 2 m/s was used and about 700 short lines were acquired during 35 hours of survey with a total coverage of circa 0.13 km^2 (less than three hours per hectare). At the time of writing this case study, the Innomar system has been extended into a version with six transducers which can be arranged into a wider line array with an adjustable transducer spacing and advanced processing for an increased efficiency providing a swath width of up to 250 cm without compromising sounding density along the array.

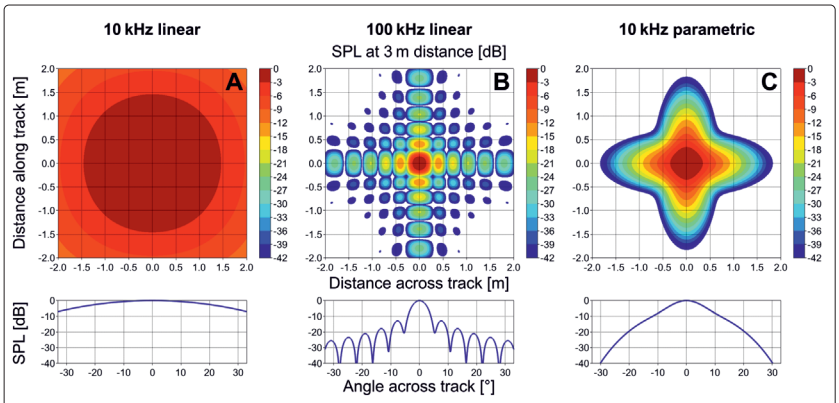

Fig. 3: Comparison of sound pressure levels (SPL) for equally sized transducers at a distance of 3 m, transmitting 10 kHz linear (A), 100 kHz linear (B) and 10 kHz parametric (C). The upper series shows the SPL distribution (acoustical footprint) in dB for an area of 2.0 m by 2.0 m. The lower series shows the SPL level in dB across the transducer centre for an angular range of ±30 degrees. Note the significant difference in footprint size between (A) and (C), as well as the lack of side lobes for (C)

3.2 Data processing

All sub-bottom acoustic records were band pass filtered (5 to 15 kHz) and the seismic sections were depth converted with a constant acoustic velocity of 1500 m/s. Static corrections of the water level variations were applied using the differential GPS data. Sounding positions were corrected for GPS antenna offsets including roll and pitch related deviations from vertical incident angles of the sound beam. Corrections of the heave were applied using the direct heave and roll measurements from the motion sensor. The signal-to-noise ratio was optimised by the application of digital filters in the time domain and a threshold table. An envelope function was applied prior to 3D processing and visualisation. Due to separate soundings per transducer with very narrow sound beams and an almost vertical incident angle towards the seafloor, the amount of diffraction was small and no extensive migration processing was required. Although the system acquires full waveform data, the processing of this dataset did not include processing in the frequency domain, the analysis of phase information or any seismic inversion techniques to determine sediment or material properties.

Due to the navigational constraints of the man-steered boat all combined soundings for a surveyed region resulted in a spatially irregular dataset and needed to be transformed and gridded into uniform lattices. For this, a grid cell size of 12.5 × 12.5 × 1 cm^3 was chosen and the system's resolution enabled the creation of time slices at 1-cm separation. The inverse distance to a power weighted average interpolation method was used as the main gridding method. Some data gaps remained within the seismic cubes even after interpolation due to occasionally significant deviations of the surveyed profiles from the planned lines. The uni-

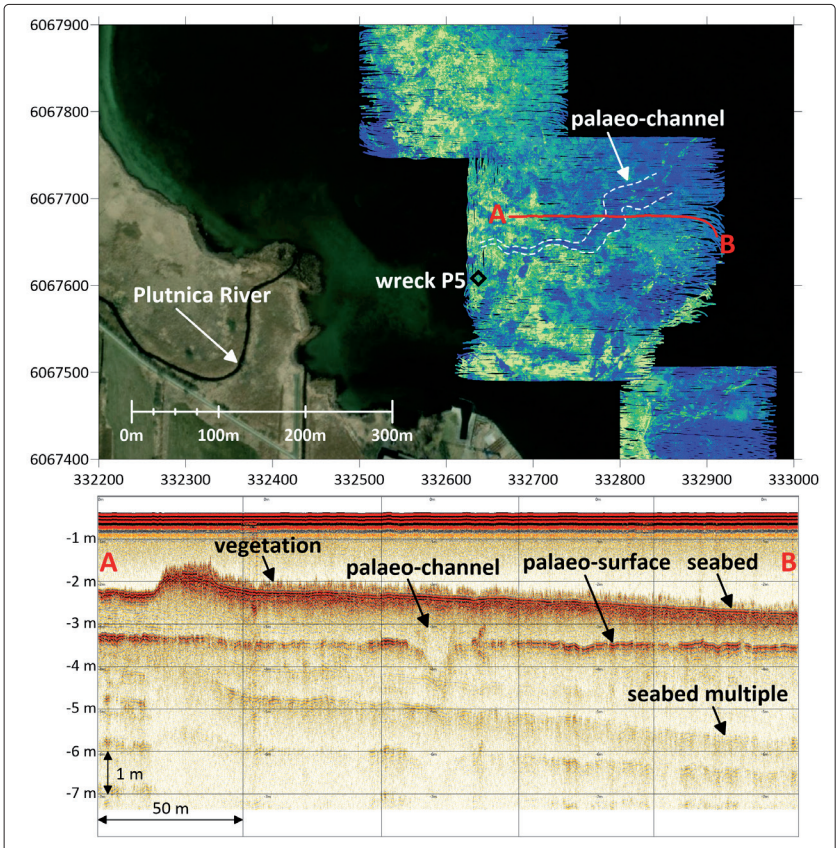

Fig. 4: Time slice from a depth of 330 cm below chart datum obtained from the combined 3D volume of all seismic sections acquired. This depth is the approximate level of a significant palaeo-surface present in the entire survey area. The seismic section (A–B) shows the seabed (with a 20 cm thick vegetation cover) and the palaeo-surface at about 1 m below seabed. The palaeo-channel cutting through the palaeo-surface is about 15 m wide at this location. The interpreted course of the palaeo-channel has been marked on the map

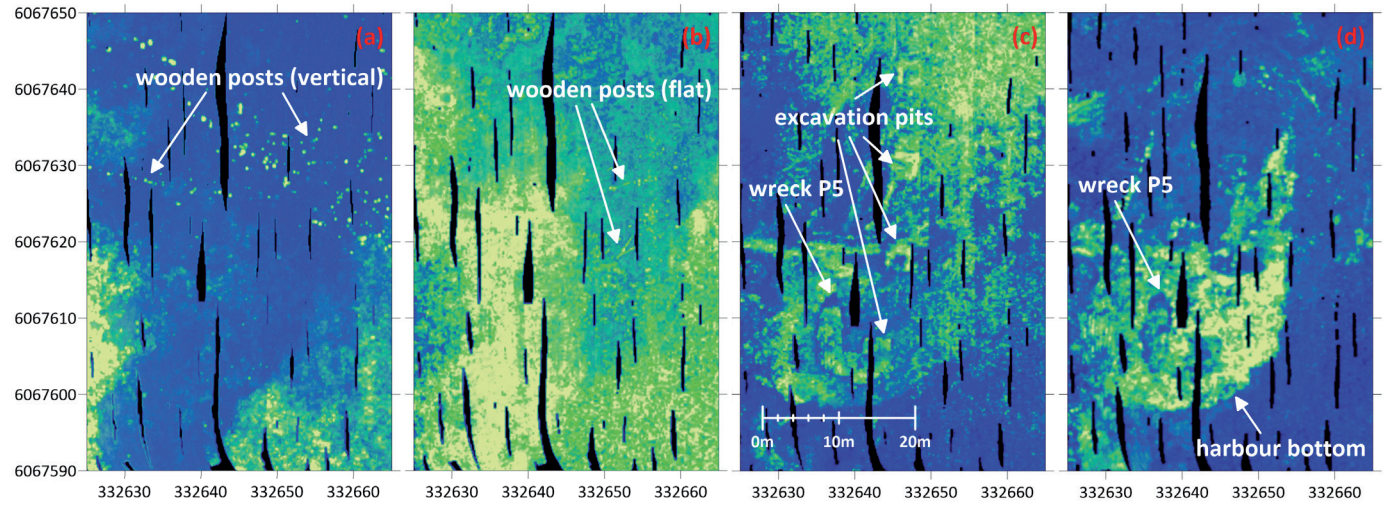

Fig. 5: Series of four time slices around the location of wreck P5 with increasing depths of 140 cm (a), 190 cm (b), 230 cm (c) and 260 cm (d) below chart datum. Subset (a) shows wooden posts standing vertically above seabed, subset (b) shows a few wooden posts laying on the seabed, subset (c) shows the outline of the buried wreck P5 (i.e. shadow from acoustical blanking) and some old excavation pits from the 1990s, subset (d) shows the outline of the buried wreck P5 at the depth level of the top of the harbour sediments

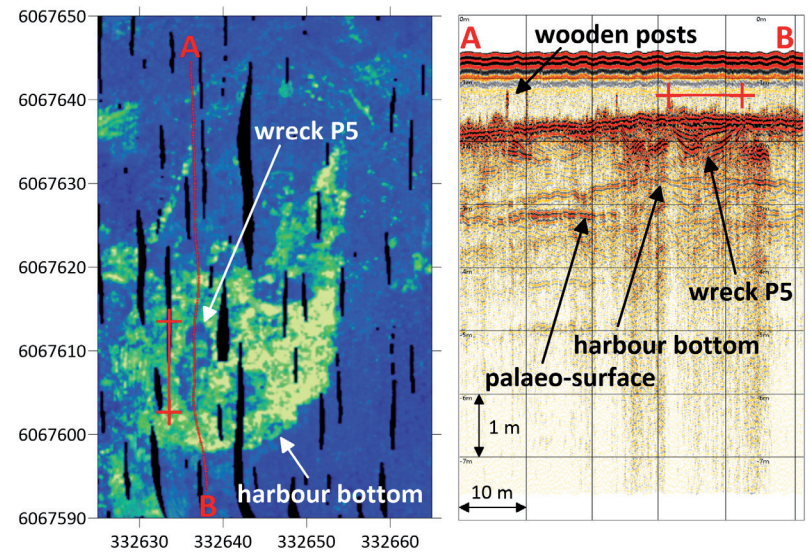

Fig. 6: Time slice around wreck P5 at 260 cm below chart datum at the depth of the top of the harbour sediments and vertical seismic section (A–B) through the wreck location (NS profile). Note the wooden posts, the layered sediment infill at the inner part of the wreck and the circa 50 cm thick harbour sediments deposited on top of the prominent palaeo-surface

form lattices were visualised in 3D with a volume renderer using an opacity and colour map transfer function. Clipping planes were applied to visualise and export time slices below the sediment floor (Fig. 4, Fig. 5 and Fig. 6). Such time slices were easily geo-referenced and imported into GIS packages to pick artefacts and outline structures or to combine them with other geo-spatial datasets, such as multibeam grids or underwater photogrammetry (Pydyn et al. 2021).

4 Results and discussion

The parametric acoustic profiling resulted in sediment penetration of up to 3 m, but typically around 2 m below the seabed. Due to the selected dominant frequency of 10 kHz and a bandwidth of circa 10 kHz, a vertical layer-to-layer resolution of better than 10 cm was achieved.

The bathymetry of the surveyed area showed varying depths between 1.5 and 2.5 m below chart datum, a dredged channel reached a depth of slightly more than 3 m. Some prominent irregularly formed ridges protrude the seabed surface NE of the dredged channel (Fig. 1). These outcropping structures were interpreted as marsh-limnic sediments, consisting of peat and calcareous gyttja (Szymczak et al. 2014). Otherwise, fine sands dominate the bottom sediments of the bay in this area. About one to two metres below seabed a significant high amplitude reflector could be traced throughout the entire survey area and forms a significant palaeo-surface. It is interpreted as the Holocene transgression boundary (Littorina transgression), where the formerly freshwater lake and wetland surface was flooded and transformed into a shallow marine bay (Kramarska et al. 1995). The palaeo-surface reflector is generally flat, occasionally cut by channel features (Fig. 4) with various depths down to one metre below this surface as well as circular and irregular depressions of varying size and depth. Some of the circular depressions can be associated with ground water discharge processes as previously identified in the wider area of the Bay of Puck (Matziak et al. 2024), others may resemble small water filled hollows in the formerly wetland environment (Fig. 7). One prominent channel feature can be traced through the entire survey area in SW to NE direction and forms a meandering palaeo-channel. Some high amplitude reflections are recognisable within the sediments about 30 cm above this approximately

10 m (SW) to 25 m (NE) wide channel feature, following its course. Those two related features can clearly be interpreted as the palaeo-channel of the local Plutnica river (Fig. 4). The sediments above the interpreted palaeo-surface are interpreted as sandy sediments, occasionally silty and gas bearing, which is caused by the decay of organic materials transported into the bay by fluvial processes. Also, numerous and sometimes highly structured and complex features are recognisable within the sediment layer above the palaeo-surface. There is ongoing work to relate those features to their archaeological significance or to geological and depositional sources, such as buried fragments of peat. At the heritage site numerous vertical wooden poles, flat laying wooden poles, stones and other elevated features are recognisable above the seabed (Fig. 5).

On the western side of the survey area where Phase III of the medieval harbour is located, a shipwreck was identified just below the seafloor (Fig. 5). The shape of the wreck with a dimension of circa 10 m × 3 m is clearly seen in the horizontal time slices. A seismic section in NS direction through the wreck location from bow to stern (Fig. 6) indicates that the top of the wreck corpus corresponds with the seabed reflector. Therefore, the wreck shape itself is caused by acoustical blanking from wooden pieces at seabed level where high amplitudes are merged with the strong echoes of the seabed. The inside of the wreck is filled with some layered sediments. The time slice in Fig. 6 is at the same level as a distinct acoustical reflector which is circa 50 cm above the consistent palaeo-surface of the area. This high reflector is interpreted as the top of sediments which fill the previous harbour basin. The distinct outline of the harbour basin is recognisable (Fig. 6).

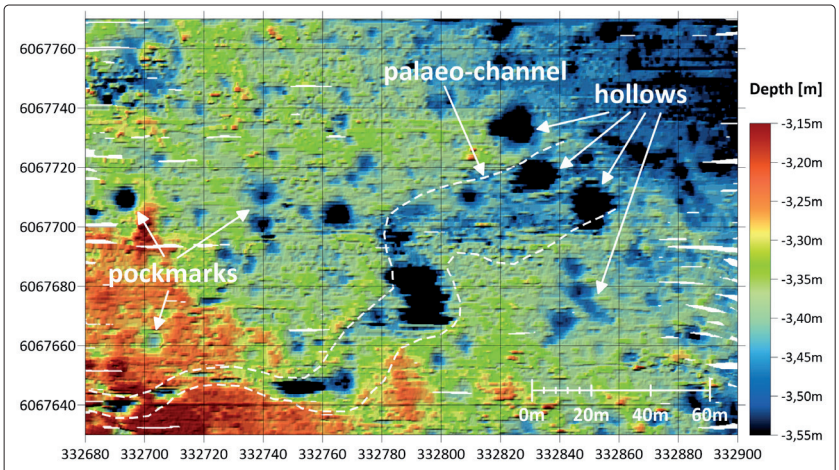

Fig. 7: Regional colour coded height map of the digitised palaeo-surface showing some distinct circular depressions, interpreted as pockmarks caused by groundwater discharge, whereas other irregular depressions are interpreted as formerly water-filled hollows in the pre-transgressional wetland environment. The palaeo-channel of the Plutnica river is clearly recognisable in the palaeo-surface

5 Conclusions

The arrangement of multiple transducers in a fixed linear array resulted in a dense and coherent dataset with good coverage, not achievable by normal line-per-line surveys with single-transducer systems. The use of a parametric sub-bottom profiler allowed to survey in water depths as shallow as one metre and image the sub-seabed morphology in high detail. A buried shipwreck could clearly be identified in the dataset. The lateral extent of the early-medieval harbour of Puck could clearly be outlined from the differences in the acoustical impedance of the sub-seabed sediments. The palaeo-channel of the local Plutnica river was detected and could be traced across the entire survey area covered. Some additional buried features were detected, and further archaeological work is required to assess their relationship to the different phases of the Puck harbour development. The Innomar quattro system with its parametric acoustic technology proved a valuable instrument for the high-resolution 3D imaging of buried archaeological artefacts and mapping palaeo-landscape features. //

Acknowledgements

The development of the multi-transducer sub-bottom profiler system was co-funded by the European Union within the SASMAP project as part of the Seventh Framework Programme.

This study was funded by Grant CE947: Virtual Arch – Visualize to Valorise – For better utilization of hidden archaeological heritage 2017–2020 (Interreg Central Europe).

References

Grøn, Ole; Lars Ole Boldreel (2014): Chirping for Large-Scale Maritime Archaeological Survey: A Strategy Developed from a Practical Experience-Based Approach. Journal of Archaeology, DOI: 10.1155/2014/147390

Kramarska, Regina; Szymon Uścinowicz; Joanna Zachowicz; Maria Kawińska (1995): Origin and evolution of the Puck Lagoon. Journal of Coastal Research, www.jstor.org/stable/25736040

Matciak, Maciej; Marta Małgorzata Misiewicz; Beata Szymczycha et al. (2024): Pockmarks and associated fresh submarine groundwater discharge in the seafloor of Puck Bay, southern Baltic Sea. Science of The Total Environment, DOI: 10.1016/j.scitotenv.2024.173617

Missiaen, Tine; E. Slob; Marinus Eric Donselaar (2008): Comparing different shallow geophysical methods in a tidal estuary, Verdronken Land van Saeftinge, Western Scheldt, The Netherlands. Netherlands Journal of Geosciences, DOI: 10.1017/S0016774600023192

Missiaen, Tine (2010): The potential of seismic imaging in marine archaeological site investigations. Relicta, DOI: 10.55465/EAIE7018

Missiaen, Tine; Dimitris Evangelinos; Chloe Claerhout et al. (2018): Archaeological prospection of the nearshore and intertidal area using ultra-high resolution marine acoustic techniques: Results from a test study on the Belgian coast at Ostend-Raversijde. Geoarchaeology, DOI: 10.1002/gea.21656

Mueller, Christof; Susanne Woelz; Sven Kalmring (2013): High-resolution 3D marine seismic investigation of Hedeby Harbour, Germany. The International Journal of Nautical Archaeology, DOI: 10.1111/1095-9270.12011

Plets, Ruth M. K.; Justin K. Dix; Jon R. Adams et al. (2008): The use of a high-resolution 3D Chirp sub-bottom profiler for the reconstruction of the shallow water archaeological site of the Grace Dieu (1439), River Hamble, UK. Journal of Archaeological Science, DOI: 10.1016/j.jas.2008.09.026

Popek, Mateusz (2020): Średniowieczny port w Zatoce Puckiej w świetle badań archeologicznych (PhD Thesis). Nicolaus Copernicus University in Toruń, DOI: 10.12775/978-83-231-5208-8

Pydyn, Andrzej; Mateusz Popek; Maria Kubacka; Łukasz Janowski (2021): Exploration and reconstruction of a medieval harbour using hydroacoustics, 3-D shallow seismic and underwater photogrammetry: A case study from Puck, southern Baltic Sea. Archaeological Prospection, DOI: 10.1002/arp.1823

Quinn, Rory; Jonathan M. Bull; Justin Dix (1997): Imaging wooden artefacts using Chirp sources. Archaeological Prospection, DOI: 10.1002/(SICI)1099-0763(199703)4:1<25::AID-ARP66>3.0.CO;2-U

Ravnås, Hallgjerd H.; Thomas M. Olsen; Wiktor W. Weibull et al. (2023): Marine Geophysical Survey of a Medieval Shipwreck in Shallow Waters Using an Autonomous Surface Vehicle: A Case Study from Avaldsnes, Norway. Journal of Maritime Archaeology, DOI: 10.1007/s11457-023-09384-1

Stępień, Wiesław (1983): Puck przed Gdańskiem. Z Otchłani Wieków, 49, pp. 49–57

Szymczak, Ewa; Angelika Szmytkiewicz (2014): Sediment deposition in the Puck Lagoon (Southern Baltic Sea, Poland). Baltica, DOI: 10.5200/baltica.2014.27.20

Szulta, Wojciech (2002): Badania podwodnych struktur archeologicznychzalegających w Zatoce Puckiej przeprowadzone w latach 1990 – 1992. Nautologia, Nr 1–2, pp. 76–82

Wilken, Dennis; Tina Wunderlich; Hannes Hollmann et al. (2019): Imaging a medieval shipwreck with the new PingPong 3D marine reflection seismic system. Archaeological Prospection, DOI: 10.1002/arp.1735

Wilken, Dennis; Hanna Hadler; Tina Wunderlich et al. (2022): Lost in the North Sea – Geophysical and geoarchaeological prospection of the Rungholt medieval dyke system (North Frisia, Germany). PLoS ONE, DOI: 10.1371/journal.pone.0265463

Wunderlich, Jens; Gert Wendt; Sabine Müller (2005): High-resolution Echo-sounding and Detection of Embedded Archaeological Objects with Nonlinear Sub-bottom Profilers. Marine Geophysical Researches, DOI: 10.1007/s11001-005-3712-y

Ocean Power & Monitoring

Transform into the cost-efficient and sustainable future

OceanPack™ Underway

Racing

SOCAT ready

pCO_2 optical Analyzer

GHG Monitoring

Modular, easy to use and reliable monitoring incl. pCO_2 and Microplastic

Subsea Li-Ion Batteries

Highly reliable, efficient and safe underwater power solutions for DC + AC

Standard Batteries

API17F Offshore certified

Energy Storage & UPS Systems

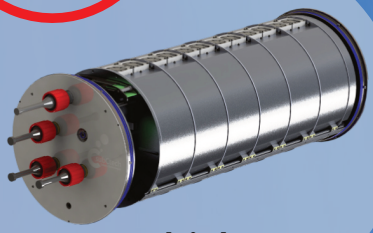

Vehicles

SubCtech GmbH
www.subctech.com
info@subctech.com

ISO 9001 certified by SEC

UN 38.3 Safety tested Transportation Requirements Passed Certified

2021 2030 United Nations Decade of Ocean Science for Sustainable Development

subCtech

DOI: 10.23784/HN133-03

Sub-bottom profiler in underwater archaeology

Study of the palaeolandscape and shipwreck alteration processes at Carthago Nova

An article by FELIPE CEREZO ANDREO, ERWIN HEINE and SEBASTIÁN F. RAMALLO ASENSIO

The application of geophysical methods and underwater photogrammetry for palaeolandscape reconstruction and the determination of shipwreck alteration processes at the bay of Cartagena, Murcia, Spain is presented. Sub-bottom profiler data revealed a chronology of the palaeotopography from the Upper Palaeolithic to the transgressive maximum of the Holocene. Investigations of the site of the wreck *Cartagena 1* show sedimentary processes and dispersion of the remaining ship cargo exacerbated by consequences of extreme climatic events and contemporary garbage dumps. These results underscore the need for comprehensive documentation, with photogrammetry prioritised to achieve a complete and accurate record of the archaeological site.

underwater archaeology | shipwreck | sub-bottom profiler | sedimentation
Unterwasserarchäologie | Wrack | Sedimentecholot | Sedimentation

Die Anwendung geophysikalischer Methoden und der Unterwasserphotogrammetrie zur Rekonstruktion der Paläolandschaft und zur Bestimmung der Änderungsprozesse von Schiffswracks in der Bucht von Cartagena, Murcia, Spanien, wird vorgestellt. Daten des Sedimentecholots enthüllten eine Chronologie der Paläotopographie vom Jungpaläolithikum bis zum transgressiven Maximum des Holozäns. Untersuchungen der Fundstelle des Schiffswracks *Cartagena 1* zeigen Sedimentationsprozesse und eine Ausbreitung der verbliebenen Schiffsladung, die durch die Folgen extremer Klimaereignisse und heutiger Müllablagerungen noch verstärkt wurden. Diese Ergebnisse unterstreichen die Notwendigkeit einer umfassenden Dokumentation, wobei der Photogrammetrie Vorrang eingeräumt werden sollte, um eine vollständige und genaue Erfassung der archäologischen Stätte zu erreichen.

Authors
Dr. Felipe Cerezo Andreo works at the Universidad de Cádiz, Spain.
Prof. Erwin Heine works at the BOKU University, Vienna, Austria.
Dr. Sebastián F. Ramallo Asensio works at the Universidad de Murcia, Spain.

erwin.heine@boku.ac.at

1 Introduction

Underwater archaeology faces the challenge of detecting and analysing cultural remains that remain hidden under the water column and often buried by marine sediments, which limits the effectiveness of conventional visual prospecting methods (Bailey and Flemming 2008). The integration of active acoustic remote sensing techniques, such as sub-bottom profilers (SBP), has established itself as a fundamental tool to overcome these limitations, allowing the characterisation of the geological and sedimentological structure of the seafloor (Rizzo et al. 2024), as well as locating anthropic elements trapped in these sediments (Li et al. 2023). These high-resolution reflection seismic instruments are essential for a less intrusive management approach for the preservation of submerged cultural heritage sites in situ. They provide the non-invasive data needed to understand site formation processes and plan effective protection strategies against accelerated degradation (Winton 2023). The ability of SBPs to penetrate sediments and generate detailed acoustic profiles allows not only the detection of anomalies associated with anthropogenic structures, but also the reconstruction of submerged palaeolandscapes that contextualise human settlements over time (Gusick et al. 2022; Winton 2023). The application of these remote sensing technologies in underwater archaeology encompasses two main approaches: the location and mapping of historic shipwrecks on the seabed or semi-buried, and the study of coastal palaeogeography to identify archaeological sites of submerged interest (Gusick et al. 2022; Plets et al. 2008). This palaeogeographical approach is essential to understand the evolution of coastlines and to locate prehistoric sites that, due to changes in sea level, are now situated underwater (Ghilardi and Pateau 2023). The Holocene maximum transgression, in particular, has

caused the disappearance of large coastal areas that were inhabited during the Pleistocene and Holocene, making the underwater sedimentary record a fundamental archive for the research of regional prehistory (Nieto Prieto 2019). The recent technological evolution of chirp and parametric systems, which incorporate multiple sensors and precision positioning, has made it possible to characterise not only the geometry of the buried materials, but also their state of conservation within the sedimentary column. Thus, based on accurate geophysical evidence, appropriate measures can be implemented to mitigate the aforementioned effects (Souza 2006).

This methodological approach is aligned with the principles of UNESCO's (2001) Convention on the Protection of the Underwater Cultural Heritage, which promotes in-situ preservation and the use of non-destructive techniques for the management of archaeological heritage.

The geoarchaeological study of the Bay of Cartagena (Fig. 1) was conducted within the framework of Cerezo Andreo's (2016) doctoral thesis and was supported by an Innomar student scholarship, which provided access to their sub-bottom profiler.

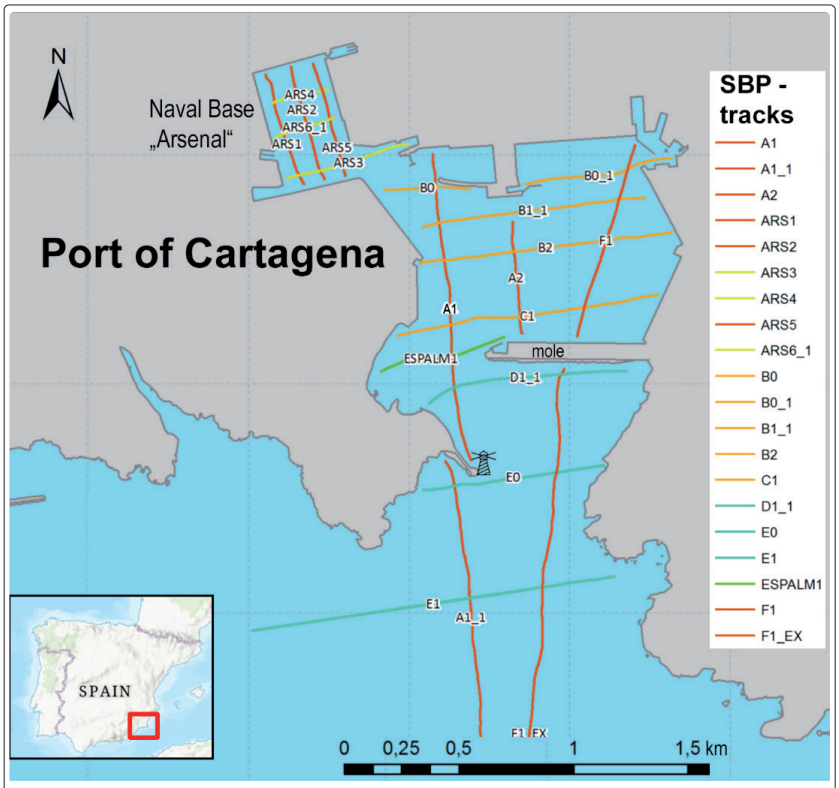

Fig. 1: Map of sub-bottom profiler survey lines from 2015 in the Bay of Cartagena

2 Objectives

The main objectives of the research presented are as follows:

1. To reconstruct the palaeogeographic and sedimentological evolution of the port area of Carthago Nova, to understand its configuration throughout the Holocene transgression.

2. To evaluate the effectiveness of high-resolution geophysical techniques, in particular sub-bottom profiling based on parametric echo sounding, in the detection and characterisation of seismic anomalies associated with potential underwater archaeological sites.

3. To analyse the processes of natural and anthropic alteration on underwater cultural heritage, illustrated by the *Cartagena 1* wreck case study. The focus here is to assess cargo dispersion, its sedimentary covering or uncovering, and the consequences of extreme climatic events such as DANA (»Depresión Aislada en Niveles Altos« – Isolated depression at high levels).

4. Establish a multidisciplinary methodological framework that integrates geophysical prospecting, analysis of past geotechnical data, absolute dating and photogrammetry for the documentation, monitoring and efficient non-intrusive management strategy for the preservation of underwater cultural heritage in dynamic marine environments.

3 Methodology

The methodology used is situated within underwater archaeology as a science of historical research and heritage documentation, with a priority on non-intrusive recording techniques. In 2008, a geophysical survey campaign using a Klein 3900 side-scan sonar was carried out by the National Museum of Underwater Archaeology of Spain and the non-governmental organisation Aurora trust. With these works, it was possible to obtain a sonography of the seabed, which allowed an updated image of the Bay of Cartagena and its accesses (Fernández Matallana 2008; Pinedo Reyes 2012). It was in these works that the *Cartagena 1* wreck was located.

The promising results of this work prompted us to propose a new prospecting campaign within the framework of the Archeotopes project (Ramallo Asension et al. 2015), which was carried out in 2015.

The SES-2000 series are parametric echo sounders that are based on the concept of non-linear generation of acoustic waves. During simultaneous transmission of two signals of slightly different high frequencies at high sound pressure, a new frequency arises, with a frequency equal to the difference between the two primary frequencies. The resulting low-frequency signal allows a better bottom penetration and a high vertical resolution. The SES-2000 device generates a low frequency between 4 kHz and 12 kHz based on primary frequencies of around 100 kHz. Thus, the system is able to achieve a resolution of about 5 cm, an accuracy of ±2 cm + 0.02 % of the water depth for the 100-kHz frequency, and about ±4 cm + 0.02 % of the water depth for the chosen low frequency

Fig. 2: Installation of the sub-bottom profiler on the vessel of the University of Murcia

of 10 kHz (Wunderlich et al. 2005; Heine et al. 2014). Frequencies of 6 kHz and 10 kHz were selected, achieving a penetration up to 15 metres The portable equipment was installed on the research vessel *Betsaida* of the University of Murcia (Fig. 2). 3D positioning and real-time, decimetre-level navigation accuracy were achieved using an Ashtech/Thales DG14 DGPS system. The Eye4Software Hydromagic hydrographic survey package was used to plan survey lines and to map the vessel's position relative to them.

Twenty intersecting profiles were defined (Fig. 1) based on analyses of existing terrestrial geological data. The survey lines were oriented north–south along the bay's main axis and perpendicular to it. The water depth in the bay ranges from 2 m to 78 m. The vessel's speed was maintained at 3.5 knots to optimise sub-bottom profiler performance in the port basin, where water depths ranged from 3 to 18 m (Cerezo Andreo 2016).

The subsequent data processing included filtering and analysis of sub-bottom profiler data and generation of profile section diagrams using Innomar's ISE software, ArcGIS for georeferencing of historic geotechnical boreholes and interpolation of sedimentological profiles and RockWorks for 2D and 3D modeling of the palaeo-seafloor.

To better constrain the area's lithology, the investigation incorporated results from previous analyses of onshore geotechnical borehole samples. Within the framework of the Archeotopes project 457 historical samples carried out between 1999 and 2015 were analysed alongside recent samples. The recent sediment samples were dated by C14 and validated by amino acid racemisation techniques, biomarker studies (gastropods, ostracods, foraminifera and algae) and archaeometric and geomorphological analyses, which allowed a diachronic restitution of the palaeotopography of the environment with a record of more than 12,000 years (Cerezo Andreo 2017; Torres et al. 2018).

Verification actions with an ROV and archaeologist dives were carried out on areas where anomalies in the sub-bottom structures were detected (Cerezo Andreo et al. 2022).

Cartagena 1 wreck and Aladroque project

The study of the *Cartagena 1* wreck began with a 2008 geophysical survey using sub-bottom profiler and side-scan sonar, whose data served as a comparative basis (Fernández Matallana 2008).

The Aladroque project campaigns (2021 to 2022), focused on the impact of DANA-type climate events, incorporated previous data from 2008 and 2015 for specific objectives: to evaluate burial/disinterment processes, sedimentation and anthropic/climatic alterations through repeated geophysics, verification dives and photogrammetry (Cerezo Andreo et al. 2022).

Underwater photogrammetry using photo series obtained by ROVs of the Cartagena Oceanographic Research Institute, has made it possible to generate accurate and original 3D models of the wreck.

The value for the techniques applied in this project became evident in the face of the significant changes observed at the site resulting from time series analysis of the 2008 and 2021/2022 datasets.

4 Results

4.1 The results of the port of Cartagena

The parametric sub-bottom profiler data reconstruct a palaeotopographic chronology from the Upper Palaeolithic to the Holocene transgressive maximum. The analysis of the most representative SBP sections identifies three morpho-stratigraphic units (Fig. 3) The deepest, designated »unit 3« records a glacial palaeotalweg of the last

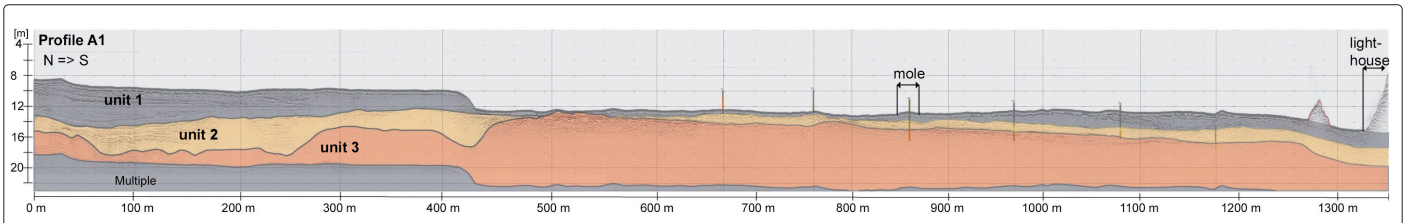

Fig. 3: SBP Profile A1 showing three morpho-stratigraphic units and gently inclined foresets towards the sea (south)

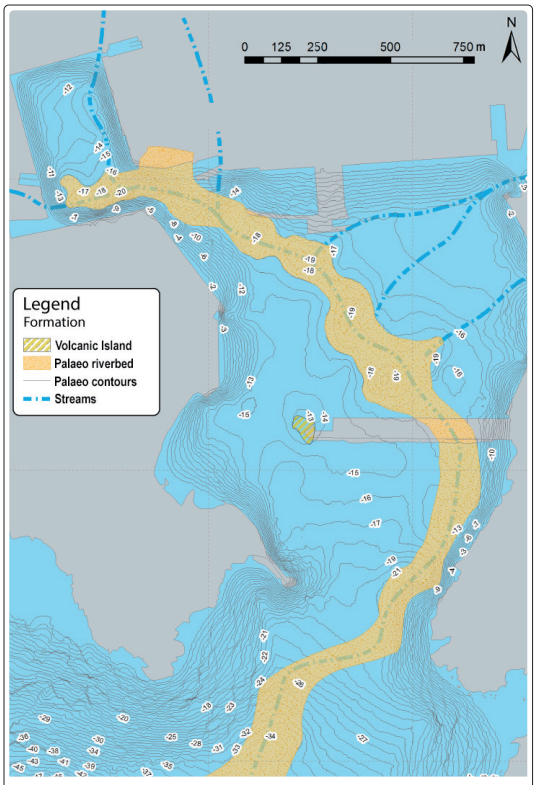

Fig. 4: Interpolation of the pre-transgressive landscape in Cartagena Bay

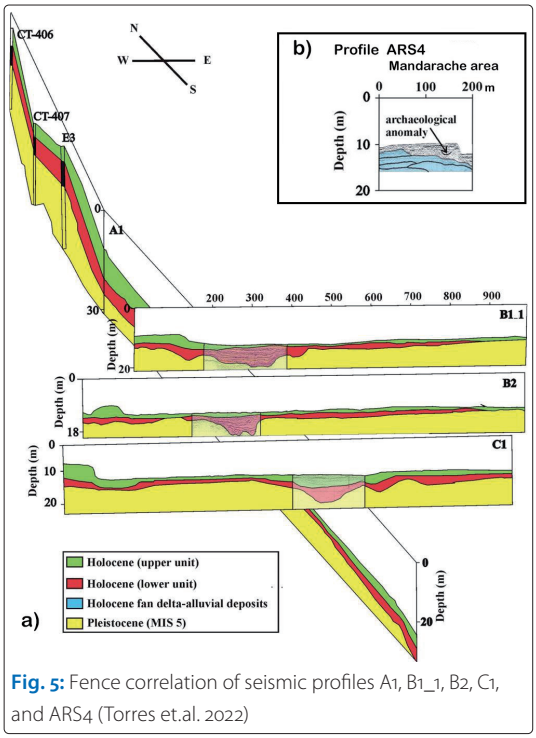

Fig. 5: Fence correlation of seismic profiles A1, B1_1, B2, C1, and ARS4 (Torres et.al. 2022)

glacial period. It crosses the port bay, with foresets gently inclined towards the sea and with morphological differences between the coastal zone and the outer basin, conditioning the configuration of the port during the Holocene transgression (Fig. 3).

This palaeochannel (Fig. 4), associated with the palaeochannel or Benipila wady, showed fan deltaic developments at its northern end (ARS4 profile, Mandarache area), with a stratified lower Holocene seismic unit covered by recent massive mud rich in organic matter and with anthropic influence (Fig. 5a). C14 dating at nearshore »unit 1« (Fig. 3) indicated ~8500 years BP at its base, with contemporary deposits at the top and original thicknesses of up to 12 m in the actual Arsenal area. From an archaeological perspective, the artefacts found in »unit 1« in the Arsenal area indicate a possible 6 × 21 m U-shaped shipwreck at a depth of 12 metres, which is consistent with other shipwrecks found at a similar depth (Fig. 5b).

4.2 Cartagena 1 wreck and Aladroque project

The time series analysis of the 2008 and 2021/2022 datasets of the *Cartagena 1* wreck revealed a removal of sediments covering the wreck of 70 to 80 cm compared to 2008, a dispersion of the cargo that has doubled the original extension. Beyond that, in some areas a doubling of sedimentation could be observed (Fig. 6 and Fig. 7).

Three-dimensional models of the wreck area and its cargo is crucial not only to visualise the reservoir in its current state, but also to facilitate detailed structural analyses and monitoring of changes over time (Fig. 7).

ROV dives at the wreck site documented contemporary trash (plastics, nylon lines, bottles and cans) causing erosion and the rupture of amphorae that protrude from the seabed. This accu-

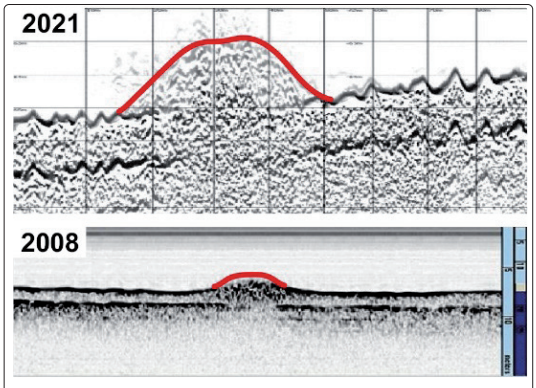

Fig. 6: Comparison of SBP image of the amphorae mound of the *Cartagena 1* shipwreck from 2008 and 2021

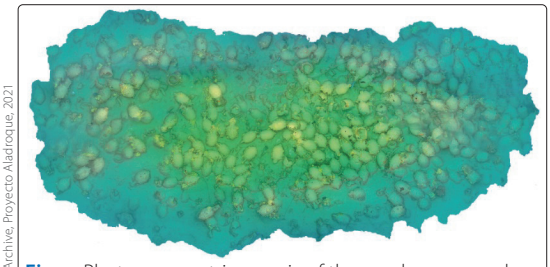

Fig. 7: Photogrammetric mosaic of the amphora mound (*Cartagena 1* shipwreck cargo from 2021)

mulation of harmful anthropogenic debris at the site has increased following high-impact rainfall events in recent years.

Photogrammetric documentation of the impacts of extreme weather events (DANAs), along with graphic records of the resulting damage, has been obtained and is vital for developing conservation proposals and monitoring subsequent alterations.

5 Discussion

The results obtained in this geoarchaeological research projects highlight the ability of high-resolution geophysical techniques, such as the SES-2000 parametric profiler, to reconstruct the palaeotopography of the bay of Cartagena and assess the environmental impact on underwater heritage. The identification of three morpho-stratigraphic units confirms the influence of a glacial palaeotalweg on the configuration of the port during the Holocene transgression, aligning with previous stratigraphic reinterpretations that integrate geophysical and chronological data.

The reinterpretation of previous seismic profiles, such as AR54 in Mandarache, reveals a fan delta at the mouth of the Rambla de Benipila, with a Holocene seismic unit stratified at the bottom and massive at the top, rich in organic matter and with anthropic influence. These units confirm a fluvial palaeotalweg that shaped the port during the Holocene transgression.

These sedimentary dynamics, with variable rates calculated by GIS and C14 dating, allow precise palaeobathymetries to be restored. It reveals underwater sand bars in key areas such as the actual Plaza del Ayuntamiento and Plaza del Rey. These features configure a coastal landscape affected not only by marine transgression initially, but also by a progressive coastal progradation. This progradation is due to high-energy events such as floods or floods that configured and built these sandy bar structures in the deltaic area of what is now the city's military arsenal.

From an archaeological perspective, the seismic anomalies in »unit 1«, such as the possible shipwreck in the Arsenal at 12 m below m.s.l., show the capacity to detect the status of preservation of remains in Holocene sediments and their alteration by anthropic processes. Unfortunately, research on the port of Cartagena is hampered by historical dredging to depths of 13 m, which removed portions of the Holocene seafloor record.

The investigations of the *Cartagena 1* wreck site show sedimentary uncovering and dispersion of the cargo exacerbated by DANA events and contemporary garbage dumps. The combination of photogrammetry with geophysical prospecting and sedimentation monitoring analyses has made it possible to assess the degree of burial and unearthing of the wreck, as well as the interaction between natural processes and human action in the conservation of this important Roman site from the second century BC.

The results of this study underscore the urgency of comprehensive documentation, with photogrammetry prioritised to obtain a complete and accurate record of the archaeological site.

6 Conclusion

The results of this geoarchaeological research in the bay of Cartagena demonstrate the effectiveness of high-resolution geophysical techniques, in particular parametric sub-bottom profilers, to reconstruct underwater palaeotopography and assess environmental impacts on underwater cultural heritage.

Archaeologically, anomalies can be detected preserved in lower Holocene sediments, which is particularly important when the seabed is affected by dredging or construction activities.

The geoarchaeological data, integrated with GIS and geotechnical soundings, allow us to reconstruct palaeolines, bathymetries and variable sedimentation rates. This enriches the understanding of Atlantic-Mediterranean port dynamics, with 14 shipwrecks documented since the eighteenth century.

Underwater photogrammetry using ROVs has proven to be an indispensable tool for assessing the state of conservation of the *Cartagena 1* wreck and accurately documenting the complex alteration processes to which they are subjected. //

Acknowledgements

The results of this work are inserted in the framework of the Archaeotopes I and II projects »Carthago Nova: topography and urban planning of a privileged Mediterranean city« (Mineco-HAR2011-29330 and HAR2014-57672) and Archaeotopes III »Carthago Nova from the coastal environment. Palaeotopography and environmental evolution of the central sector of the Iberian southeast. Population and Productive Dynamics« (HAR2017-85726-C2-1-P) of the Ministry of Science and Innovation (MICINN) (DOI: 10.13039/501100011033) and ERDF funds »A way of making Europe«.

References

Bailey, Geoffrey; Nicholas Flemming (2008): Archaeology of the continental shelf: Marine resources, submerged landscapes and underwater archaeology. Quaternary Science Reviews, DOI: 10.1016/j.quascirev.2008.08.012

Cerezo Andreo, Felipe (2016): Los puertos antiguos de Cartagena: geoarqueología, arqueología portuaria y paisaje marítimo: un estudio desde la arqueología náutica. Universidad de Murcia, http://hdl.handle.net/10201/51041

Cerezo Andreo, Felipe (2017): Los puertos antiguos de Carthago Nova, nuevos datos desde la arqueología marítima y la geoarqueología portuaria. In: Los puertos atlánticos, béticos y lusitanos y su relación comercial con el Mediterráneo. DOI: 10.5281/zenodo.10601730.svg

Cerezo Andreo, Felipe; Soledad Solana Rubio; Francisco López Castejón; Sebastián F. Ramallo Asensio (2022): El impacto de los eventos climáticos tipo DANA en la conservación de los entornos subacuáticos de los accesos al puerto de Cartagena (España). Primeros datos del Proyecto Aladroque. DOI: 10.4995/icomos2022.2022.15403

Fernández Matallana, Francisco (2008): Prospección subacuática en la Marina de Curra (Cartagena). XIX Jornadas de Patrimonio Cultural de la Región de Murcia, pp. 381–383

Ghilardi, Matthieu; Mélanie Pateau (2023): Paléoenvironnements et sociétés humaines. HAL (Le Centre Pour La Communication Scientifique Directe), https://hal.science/hal-04108873

Gusick, Amy E.; Jilian Maloney; Todd J. Braje et al. (2022): Soils and terrestrial sediments on the seafloor: Refining archaeological paleoshoreline estimates and paleoenvironmental reconstruction off the California coast. Frontiers in Earth Science, DOI: 10.3389/feart.2022.941911

Heine, Erwin; Ilse Kogelbauer; Andreas Prokoph; Willi Loiskandl (2014): Hydrographic Surveying of the Steppe Lake Neusiedl. Mapping the Lake Bed Topography and the Mud Layer. Photogrammetrie – Fernerkundung – Geoinformation (PFG), DOI: 10.1127/1432-8364/2014/0228

Li, Tianguang; Zhiqing Huang; Xiaobo Zhang et al. (2023): Application of pseudo-3D sub-bottom profile imaging technology in small submarine target detection. Research Square, DOI: 10.21203/rs.3.rs-3261014/v1

Nieto Prieto, Xavier (2019): La evolución conceptual de la arqueología subacuática. Pyrenae, DOI: 10.1344/pyrenae2019.vol50num1.1

Plets, Ruth M. K.; Justin K. Dix; Jon R. Adams et al. (2008): The use of a high-resolution 3D Chirp sub-bottom profiler for the reconstruction of the shallow water archaeological site of the Grace Dieu (1439), River Hamble, UK. Journal of Archaeological Science, DOI: 10.1016/j.jas.2008.09.026

Pinedo Reyes, Juan (2012): Actuaciones arqueológicas submarinas en nueva dársena deportiva »Marina de Curra«, Cartagena. Actas de las Jornadas de ARQUA 2011, pp. 47–51

Ramallo Asensio, Sebastián; María Milagrosa Ros-Sala; Francisca Navarro-Hervás et al. (2015): ARQUEOTOPOS Project. Harbour of Cartagena an approach from the Paleotopography and Geoarcheology. DOI: 10.13125/mgw-1572

Rizzo, Angela; Giovanni Scicchitano; Giuseppe Mastronuzzi (2024): A set of guidelines as support for the integrated geo-environmental characterization of highly contaminated coastal sites. Scientific Reports, DOI: 10.1038/s41598-024-58686-4

Souza, Luiz Antonio Pereira de (2006): Revisão crítica da aplicabilidade dos métodos geofísicos na investigação de áreas submersas rasas. DOI: 10.11606/t.21.2006.tde-30102006-171206

Torres, Trinidad; Sebastián Ramallo; Yolanda Sánchez-Palencia et al. (2018): Reconstructing human-landscape interactions in the ancient Mediterranean harbour of Cartagena (Spain). The Holocene, DOI: 10.1177/0959683617752838

Torres, Trinidad; José E. Ortíz; Sebastián Ramallo et al. (2022): Development of the marine Holocene environment in a drowned paleovalley with final anthropic influence in the Cartagena Bay (Murcia, SE Spain). The Holocene, DOI: 10.1177/09596836221080759

UNESCO (2001): Convention on the Protection of the Underwater Cultural Heritage. www.unesco.org/en/legal-affairs/convention-protection-underwater-cultural-heritage?hub=412

Winton, Trevor (2023): Application of Parametric Sub-Bottom Profilers for Responsible in Situ Management of Underwater Shallow-Buried Archaeological Materials. Historical Archaeology, DOI: 10.1007/s41636-023-00391-6

Wunderlich, Jens; Gert Wendt; Sabine Müller (2005): High-resolution Echo-sounding and Detection of Embedded Archaeological Objects with Nonlinear Sub-bottom Profilers. Marine Geophysical Researches, DOI: 10.1007/s11001-005-3712-y

DOI: 10.23784/HN133-04

Discovering wrecks while mapping for infrastructure

An article by STEFFEN WIERS

Discovering wrecks is a common occurrence while surveying for infrastructure projects. In most cases the wrecks are known and only a confirmation of their positions is required. Sometimes things get more interesting, because there is a story to be told about the wreck or due to obvious damages that led to the accident. In some rare instances we discover a previous unknown wreck or a wreck is excavated. This article showcases three examples of wrecks surveyed by Fugro Germany Marine. The *DS Norge,* a steamer that sank in 1871 and was previously unknown. The *MV Høegh Aigrette* that sank close to Dover, UK, with a V-shaped incision in its hull. And the wrecks of the Swedish ship blockade, a deliberate line of wrecks offshore Rügen in the Baltic Sea.

wreck discoveries | underwater archaeology | cable survey | excavation | magnetometer | UNCLOS
Wrackfunde | Unterwasserarchäologie | Kabelvermessung | Ausgrabung | Magnetometer | UNCLOS

Bei Vermessungsarbeiten für Infrastrukturprojekte werden häufig Wracks entdeckt. In den meisten Fällen sind die Wracks bekannt und es ist nur eine Bestätigung ihrer Positionen notwendig. Manchmal wird es jedoch interessanter, weil es eine Geschichte über das Wrack zu erzählen gibt oder weil offensichtliche Schäden zu erkennen sind, die zu dem Unfall geführt haben. In seltenen Fällen entdecken wir ein bisher unbekanntes Wrack oder ein Wrack wird ausgegraben. Dieser Artikel zeigt drei Beispiele für Wracks, die von Fugro Germany Marine vermessen wurden. Die *DS Norge,* ein Dampfer, der 1871 sank und zuvor unbekannt war. Die *MV Høegh Aigrette,* die in der Nähe von Dover, Großbritannien, mit einem V-förmigen Einschnitt im Rumpf sank. Und die Wracks der schwedischen Schiffsblockade, einer absichtlich angelegten Reihe von Wracks vor der Küste Rügens in der Ostsee.

Author
Dr. Steffen Wiers is Senior Geophysicist at Fugro in Bremen.

s.wiers@fugro.com

Introduction

During survey work interesting discoveries are regularly made along the way. For the clients of Fugro Germany Marine (hereafter referred to as Fugro), these discoveries often mean additional work, as wrecks or other archaeological finds need to be avoided or cleared before any infrastructure project can take place. In the case of cables or pipelines a simple rerouting is often sufficient and that's the end of the story. A wreck report is written and is usually submitted to country agencies, like the respective hydrographic services, in case a finding is located inside territorial waters or the exclusive economic zone, and at a minimum reported in a relevant wreck database.

It must be mentioned that there are guidelines and rules in the United Nations Convention on the Law of the Sea (UNCLOS) regarding archaeological and historical finds outside of countries jurisdictions. But while these rules may protect any finds, it is not a mandate for further investigation or salvage.

In any case, wrecks are part of history and often tell interesting stories or even lead to further investigations by archaeologists. Here we present some examples from Fugro's work that instigated further research: the discovery of the wreck of the *DS Norge* in Østergapet offshore Kristiansand, Norway, the wreck of the *MV Høegh Aigrette* in the Strait of Dover, UK/Netherlands, and the discovery of the several wrecks of the Swedish ship blockade offshore Rügen, Germany.

Methodology

During cable route surveys Fugro routinely deploys multibeam echo sounder (MBES), side-scan sonar (SSS), sub-bottom profiler (SBP) and single magnetometer (MAG), all of which can be used to find wrecks. Wrecks exposed on the seafloor are easily mapped using MBES and SSS, producing highly detailed images. SBP and MAG on the other hand mostly indirectly identify wrecks.

MBES is used on all surveys and mounted to the hull of the ship, provides the best position fix. Resolution is dependent on water depth and usually gridding is performed at ~10 % of the water depth. In shallow water, even smaller debris and containers are easily identified and details can be resolved, while in deep water, larger objects are still visible, but details are obscured.

SSS is usually deployed during cable route and marine infrastructure surveys, towed behind the

ship at a constant altitude above the seafloor. On hydrographic surveys SSS may be deployed to acquire more data on wrecks. Resolution is dependent on the swath range, speed of tow and sonar frequency, but for typical projects it is between 0.1 and 0.5 m. Since the system is towed close to the seabed, it does not depend on water depth. Positioning accuracy is highly dependent on the towing distance of the SSS fish, with deeper waters needing longer cables and towing distances. Generally, an accuracy of ±2 m is considered acceptable. Correlation with MBES can lead to improved positioning while retaining the SSS's detailed resolution.

SBP is much more limited in finding and identifying wrecks. The system is usually hull-mounted and only a direct path over an object can give a response in the data. Nevertheless, objects can be identified by refraction hyperbolas. Association is more difficult but usually possible if any objects are recorded in relevant databases.

MAG can be a great tool to locate metallic objects and wrecks usually give a very strong response. Positioning is similar to SSS, in the case of magnetometer arrays and close line spacing. Single magnetometers impose an additional restriction since no direct pass over an object is necessary for detection. A wreck can be tens of metres away from the line and still be detected.

In general, a combination of all sensors yields the best results. But in practise MBES and SSS are the sensors most used.

DS Norge

The *DS Norge* was a paddle steamer of the newly founded Bergen Steamship Company, Det Bergenske Dampskibsselskab (DBD). It was built in 1854 by Thomas Wingate & Co in Glasgow and an early acquisition into the growing company. It served the company's Bergen–Hamburg route via Stavanger and Kristiansand.

In early September 1855, the *DS Norge* (Fig. 1), leaving Kristiansand on route to Hamburg, collided with the *DS Bergen,* another steamer of DBD. According to a newspaper article (Fig. 2), visibility was low when the two ships collided near the Oxhoe Lighthouse, although, other sources mention good visibility (Skipet 1988).

Only 15 minutes after the collision, the *DS Norge* sank. The incident is considered to be the first major Norwegian maritime disaster in the age of steamships, in which more than half of the 70 passengers lost their lives. Blame was laid on the captain of the *DS Norge,* who was sentenced to 160 days in prison.

Despite the known location of the collision, the wreck of the *DS Norge* was not located until more than a century later. The *MV Fugro Helmert* was conducting survey operations for a cable across the Skagerrak in 2018 when an unknown wreck

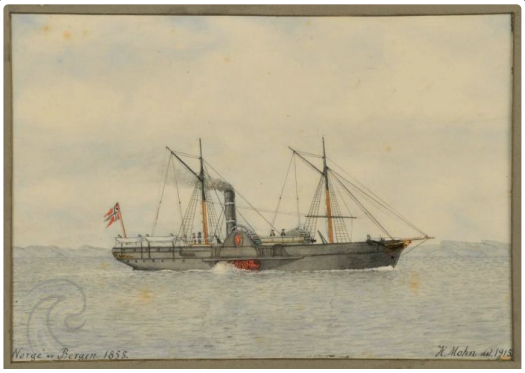

Photo: Norsk maritimt museum

Fig. 1: *DS Norge*

COLLISIONS, AND UPWARDS OF SEVENTY LIVES LOST, AT SEA.—Information reached Lloyd's on Saturday, confirming the loss of the Norwegian steam-ship Norge, with 70 of her passengers and crew, by a collision with the Bergen steamer on the 11th, about a mile and a-half from Christiana, near Oxhoe Light-house. The weather was at the time hazy, and the Bergen struck the Norge with such force as to cut her nearly in two amidships, and she foundered in deep water immediately. About 30 passengers and crew saved themselves by scrambling on board the other steamer. Another collision was reported yesterday by telegraph from Marseilles, between the Mongibello steamer and the barque Santa Annunziata, near Hyeres Islands. The latter sunk instantly. The crew were saved, but two passengers who were asleep in the cabin perished.

Fig. 2: Newspaper article, reporting on the collision of the *DS Norge* and the *DS Bergen*

was discovered. As per usual procedure, a wreck report was issued and forwarded to the Norwegian authorities.

The wreck was found to be in pristine condition, resting in an upright position on the seabed in a water depth of 165 m (Fig. 3). The multibeam

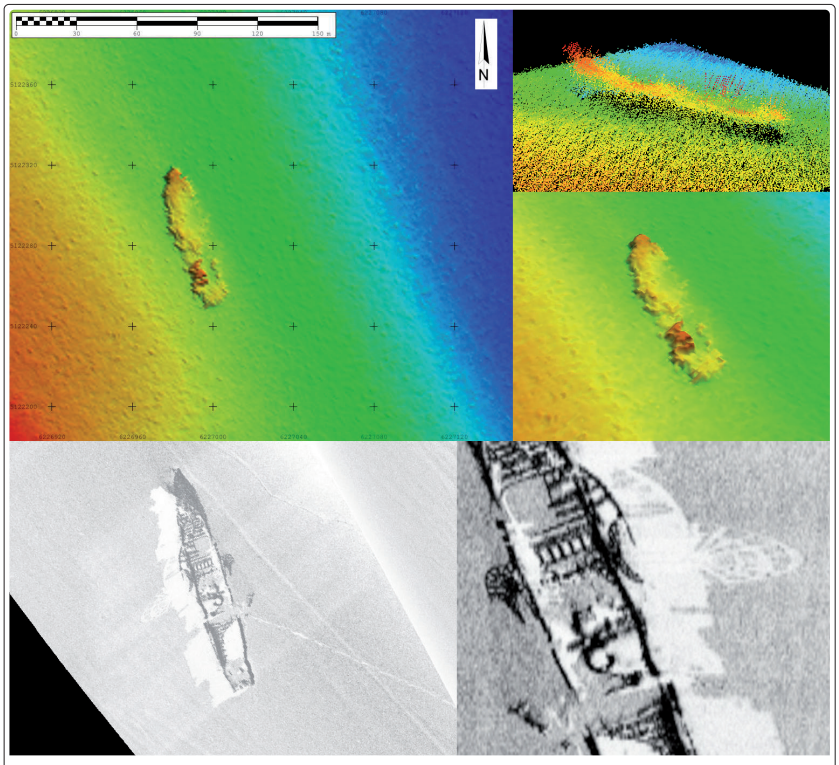

Fugro data

Fig. 3: Multibeam echo sounder and side-scan sonar images of the *DS Norge*

echo sounder shows a clear outline and allowed for a very accurate position fix (Fig. 3). More details can be seen in the multiple side-scan sonar passes (Fig. 3). Parts of the superstructure and paddles are clearly visible, while no obvious signs of the collision itself can be seen.

The Norwegian Maritime Museum concluded that it could be the *DS Norge,* after studying the data provided. In 2019, the museum conducted an ROV dive in cooperation with SubseaX and Saastad ROV, which was live streamed on YouTube, to inspect the wreck (Norwegian Maritime Museum 2020).

MV Høegh Aigrette

Another wreck surveyed by Fugro is that of the *MV Høegh Aigrette* in the English Channel approximately 12 nautical miles east of Ramsgate, UK, near the Goodwin Sands. It sank after a collision with another cargo vessel, the Norwegian freighter *Sunriver* on 25th of November 1967. The general cargo ship was en route from Duala (Cameroon) to Svendborg (Denmark), loading timber and general cargo.

The two ships collided in thick fog and the *MV Høegh Aigrette* sank after about three hours. The loaded logs spread across the English Channel, impeding traffic on the important shipping lane. All crew of the *MV Høegh Aigrette* were rescued and brought ashore at Dover, captured in a short film by Reuters. The *Sunriver* only sustained slight damage.

Fugro surveyed the wreck of the *MV Høegh Aigrette* during an Maritime & Coastguard Agency (MCA) campaign in 2007. The wreck was routinely surveyed with additional lines from all sides, producing high quality data. The maps show a mainly intact wreck lying on its port side (Fig. 4). On the starboard side a V-shaped incision is visible, believed to be the result of the collision with the *Sunriver.*

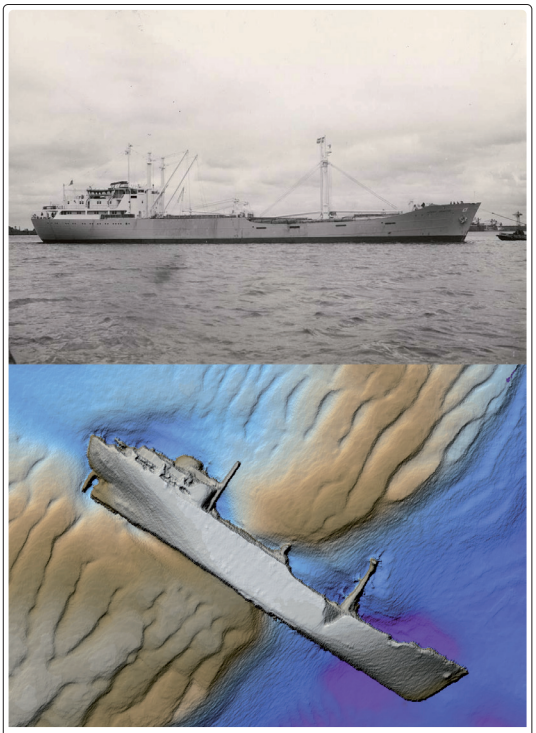

Photo: Hansen Pedersen (Cargo Ship Fo7120A).
MBES data: Courtesy of UK Maritime and Coastguard Agency. Data acquisition, processing and visualisation by Fugro

Fig. 4: Photo (top) and multibeam echo sounder data from the wreck of the *MV Høegh Aigrette*

The wreck lies in a water depth of 35 m with the highest point of the wreck at 23.6 m. The data shows that the wreck lies directly on the sediment with no visible freespan and well defined scours around the wreck, the survey further revealed a debris field around the wreck and scattered remains of fishing nets.

Swedish ship blockade

One of the more spectacular wreck sites was surveyed by Fugro for the Nord Stream 1 pipeline project in the Baltic Sea (Nord Stream 2008). Several wrecks line the eastern entrance of the Greifswalder Bodden (Fig. 5). They are the result from a deliberate barrier that was put in place by Swedish marine forces in 1715 during the Great Northern War (Belasus 2013; Auer 2021).

From 1700 to 1721 a Russian-led coalition contested Swedish supremacy in Northern, Central and Eastern Europe. In 1715, a naval battle took place near the island of Rügen in the Baltic Sea (Fig. 6). A Swedish flotilla tried to defend the island, and with it the access to Swedish Pomerania, against two Danish flotillas. Stralsund, in particular, stood in the way of a full-scale invasion, but the Russian coalition had to conquer the island of Rügen first, to deploy their artillery. And in turn, they had to establish naval supremacy around the island.

In 1715, two fairways existed to enter the Greifswald Bodden from the Baltic Sea. One was between the islands of Ruden and Usedom, the ›Osttief‹, and the other was between Rügen and Ruden, the ›Westtief‹. The Swedish forces, hoping to force the Danish flotillas in reach of their land-based artillery batteries on Rügen, sank 20 smaller ships and fishing boats in both fairways. They loaded the vessels with stones to sink them at a distance of 40 to 60 m (Belasus 2013). Despite the great effort, the Swedish forces lost the battle due to a disgruntled local pilot who showed the Danes a way through the barrier (Belasus 2013).

Forgotten for a long time, the barrier was rediscovered in 1996, allowing archaeologists to investigate 18th century ship-building techniques (Belasus 2013; Auer 2021).

During both Nord Stream pipeline projects, no suitable passage was found to satisfy distance requirements to any of the wrecks. The only option left was to excavate some of the wrecks, lay the pipeline and afterwards putting the wrecks back (Nord Stream 2008; Belasus 2013; Auer 2021).

The excavations for Nord Stream 2 were conducted by Trident Archäologie and some impressive un-

derwater photogrammetry was collected (Sketchfab 2020a, 2020b). The remains of the ship timber can be seen through the ballast stones, used to sink the ship (Trident 2023). Excavation was done in several phases, starting with removal of all stones that cover the wreck, followed by careful disassembly of the remains of the ship (Trident 2023).

Fugro conducted several more surveys in the area for diverse projects, such as power cables and liquefied natural gas (LNG) pipelines over the years where the initial findings from Nord Stream 1 have repeatedly assisted interpretation.

Final remarks

Discovering wrecks is always an exciting event during survey. Even more so, if the wreck is not listed in any database. Although this is rare, Fugro did discover some over the years. If wrecks are listed, commonly more information is available. However, the primary goal is usually to assess the relevance for the (infrastructure) project and not its historical or archaeological value. But while less interesting for infrastructure companies, wrecks can be of high importance for historians and archaeologists. During some projects archaeological assessments are a requirement that can lead to successful cooperations, for example during Nord Stream 1 (Thadeusz 2010). //

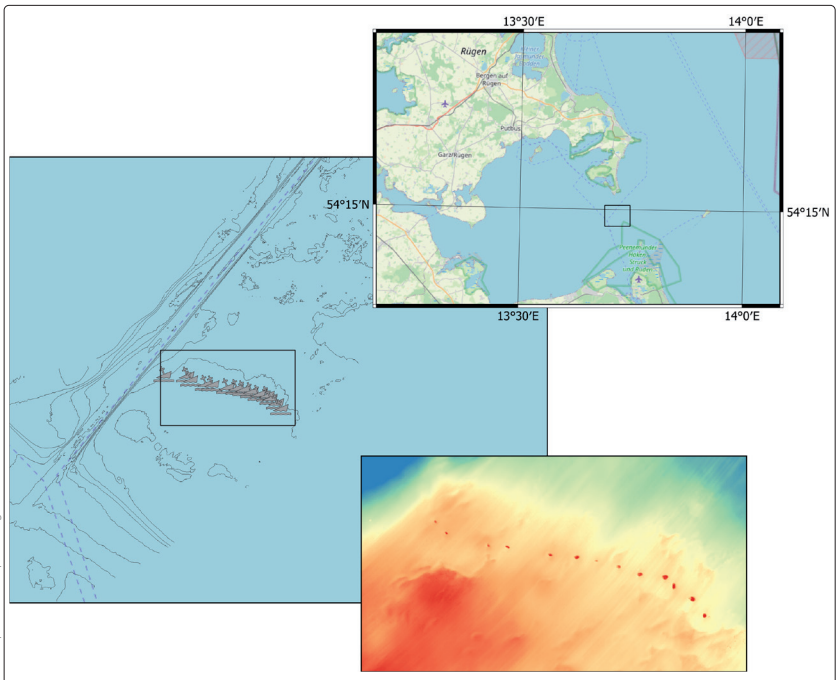

Fig. 5: The Swedish blockade between Rügen and Ruden. Contours are at 1 m interval


Abbildung
Der
See Battaille
Derer
Königl. Dänisch- und Schwedischen Flottillen
Welche im Monat Sept. 1715. zwischen Rüden und Rügen vorgangen, benebst der auffbesagter Insul Rügen zwischen den 15. und 16. Nov. geschehenen glücklichen Landung.
Rügen
Ost See
Westen Tieffe
Schär von vielen Triebsande
Oester Tieffe
Versenckung
Pommern
Usedom
Erklärung der Buchstaben.
Gedruckt 1715. den 23. Novembr.

Fig. 6: Newspaper article from 1715, reporting on the naval battle that took place between Sweden and Denmark

References

Auer, Jens (2021): Two ships under rocks: a glimpse into rural shipbuilding in western Pomerania. Archaeonautica, DOI: 10.4000/archaeonautica.1534

Belasus, Mike (2013): The Great Northern War Underwater: A Swedish Ship Barrier of 1715 in Northeast Germany. In: Natascha Mehler (ed.): Historical Archaeology in Central Europe. Society of Historical Archaeology, Special Publication No. 10, pp. 231–239

Nord Stream (2008): Nord Stream plant Bergung von Überresten eines historischen Schiffswracks vor Rügen. www.nord-stream.com/de/presse-info/pressemitteilungen/nord-stream-plant-bergung-von-ueberresten-eines-historischen-schiffswracks-vor-ruegen-183/

Norwegian Maritime Museum (2020): Følg arkeologene på direktesendt søk etter vraket av D/S Norge forlist 1855. YouTube, www.youtube.com/watch?v=GtAxHqRoWVk

Sketchfab (2020a): Wreck Fpl. 64 - Ship Barrier, Bay of Greifswald. https://skfb.ly/6TsRT

Sketchfab (2020b): Wreck Fpl. 63 - Ship Barrier, Bay of Greifswald. https://skfb.ly/6TsRV

Skipet (1988): Norsk Skipfartshistorisk Selskap, Nr. 1. www.nb.no/items/URN:NBN:no-nb_digitidsskrift_2018050281015_001?page=3

Thadeusz, Frank (2010): Truhe voller Kostbarkeiten. Der Spiegel, Archiv, www.spiegel.de/spiegel/a-706429.html

Trident (2023): Bergung eines Schiffswracks von 1715 im Greifswalder Bodden. https://trident.eu.com/de/news/fpl46-1-de

DOI: 10.23784/HN133-05

From Structure from Motion and Multi-view Stereo to Gaussian Splatting

Advanced digital documentation of underwater archaeological sites

An article by DIMITRIOS SKARLATOS, MARINOS VLACHOS and STELLA DEMESTICHA

Underwater photogrammetry is widely recognised as the gold standard for documenting underwater cultural heritage (UCH), providing a non-intrusive method to generate high-resolution geometric documentation for underwater sites. Despite its utility, the medium's inherent optical challenges – notably, refraction at the air-water interface and spectral attenuation – continue to impede the achievement of survey-grade accuracy and radiometric fidelity. This feature paper examines the evolution from traditional photogrammetry to modern structure-from-motion and multi-view stereo (SfM-MVS) techniques and beyond. Critically, it highlights the transformative potential of machine learning (ML) in mitigating these physical constraints, using underwater archaeological sites from the eastern Mediterranean as case studies. To demonstrate the transformation of methodologies, several test cases are mentioned; how the SfM methodology affected the network setup, coordinates' calculation and monitoring, the use of ML to restore colour information and to correct water refraction in coastal sites, and finally the potential of underwater 3D Gaussian splatting (3DGS) to bridge remaining challenges.

underwater photogrammetry | Structure from Motion | machine learning | underwater network
Unterwasserphotogrammetrie | Structure from Motion | maschinelles Lernen | Unterwassernetzwerk

Die Unterwasserphotogrammetrie gilt weithin als Goldstandard für die Dokumentation des Kulturerbes unter Wasser und bietet eine nicht-invasive Methode zur Erstellung hochauflösender geometrischer Dokumentationen von Unterwasserstätten. Die medienbedingten optischen Herausforderungen – insbesondere die Brechung an der Luft-Wasser-Grenzfläche und die spektrale Dämpfung – behindern weiterhin das Erreichen einer in der Vermessung üblichen Genauigkeit und radiometrischen Wiedergabetreue. Dieser Fachartikel untersucht die Entwicklung von der traditionellen Photogrammetrie zu modernen Structure-from-Motion- und Multi-View-Stereo-Techniken (SfM-MVS) und darüber hinaus. Er verdeutlicht insbesondere das transformative Potenzial des maschinellen Lernens (ML) zur Minderung dieser physikalischen Einschränkungen und verwendet dabei Unterwasserarchäologiestätten im östlichen Mittelmeerraum als Fallstudien. Um die Weiterentwicklung der Methoden zu veranschaulichen, werden mehrere Testfälle aufgeführt: wie sich die SfM-Methode auf die Netzwerkeinrichtung, die Berechnung und Überwachung von Koordinaten, die Verwendung von ML zur Wiedergabe von Farben und zur Korrektur der Wasserbrechung an Küstenstandorten ausgewirkt hat; und schließlich das Potenzial von Unterwasser-3D-Gaussian-Splatting (3DGS) aufgezeigt, um die verbleibenden Herausforderungen zu überwinden.

Authors
Prof. Dimitrios Skarlatos and Dr. Marinos Vlachos work at the Cyprus University of Technology.
Prof. Stella Demesticha teaches at University of Cyprus.

dimitrios.skarlatos@cut.ac.cy

1 Introduction

Photogrammetry has been widely accepted as a 3D documentation technique and method for underwater heritage sites. Still, from early implementations using PhotoModeler (Green et al. 2002), to modern structure-from-motion (SfM) and multi-view stereo (MVS) approaches (Skarlatos et al. 2012), underwater photogrammetry has undergone a significant evolution. Currently, MVS algorithms can generate dense point clouds that describe complex surfaces with unprecedented detail. This has been used on a wide scope of archaeological fieldwork procedures, including daily mapping in excavation projects, or documentation of sites during surveys and extended reality applications (Bruno et al. 2019). This integration of SfM and MVS has effectively democratised underwater photogrammetry, transforming it from a specialised, rigorous methodology into a widely accessible tool utilised by non-specialists in several

small-scale expeditions or rapid monitoring visits, by research teams or student groups.

Nonetheless, several key challenges persist, among which the most critical ones are the establishment and long-term stability of underwater control networks, the accurate colour restoration and effective visual representation, as well as the correction of water refraction during airborne mapping of shallow coastal heritage sites. While alternative 3D acquisition technologies exist, such as acoustic methods (Benetatos et al. 2024; Janowski et al. 2024) and LiDAR (Janowski et al. 2024; Agrafiotis et al. 2020), they are excluded from this discussion on archaeological documentation, as they are typically deemed either insufficiently precise, dense or prohibitively expensive.

Regarding data acquisition platforms, small and cost-effective remotely operated vehicles (ROVs) present a potential alternative to diver-based surveys, when project budget allows for their deployment. However, for an ROV to reliably deliver high-quality image data, it must be stable, integrated with positioning systems such as ultra-short baseline (USBL) and capable of carrying adequate camera payloads with lights. This requirement necessitates a complex and costly system, often unaffordable for small-scale expeditions. Consequently, ROV deployment is primarily reserved for deep-water operations (Alexandrou et al. 2024) or cases where bottom-time limitations prevent divers from adequately recording a site.

This paper examines the evolution from traditional photogrammetry to modern SfM-MVS techniques, drawing from lessons learned over more than 15 years of interdisciplinary collaborative work between the Department of Civil Engineering and Geomatics of the Cyprus University of Technology and the Archaeological Research Unit of the University of Cyprus.

2 Underwater network

In terrestrial surveying, the establishment of a geodetic network is a standard process, necessary in complex sites, where obstacles and terrain morphology block direct lines of sight, or in sites where the landscape undergoes constant change. Both scenarios resemble the operational reality of underwater archaeological sites, where visibility is restricted and excavation activities can alter the seabed topography daily. However, the underwater environment further exacerbates these challenges; Global Navigation Satellite System (GNSS) and standard optical instruments cannot be used, hence surveyors are deprived of the absolute positioning tools taken for granted on land. Consequently, the establishment of a stable underwater control network is not a trivial task but a challenge. The network serves as the rigid skeleton to spatially and temporally relate measurements and 3D reconstructions. Without fixed reference points, it is impossible to maintain metric integrity for long-term monitoring or to accurately co-register the progress of an excavation spanning multiple years.

It should be noted that the best way for establishing an underwater network is the use of ultra short baseline acoustic positioning systems (USBL) or short baseline acoustic positioning systems (SBL). Although their recent drop in price presents an opportunity, however, the use of such systems in underwater archaeology tends to be very rare.

2.1 Network materialisation

The reference points of a network need to serve two purposes: recognisability and stability. In terrestrial surveying, identifying stable ground and fixing reference points is a trivial process with a variety of possible fixations, varying from concrete landmarks to nails and spikes. The most common solution involves drilling holes in which special surveying marks are fixed with epoxy resin. In the underwater environment, however, none of these processes are straightforward. While fixing points on a rocky seabed might be achieved using drills and screws, securing stable reference points on sandy bottoms or seagrass meadows presents a challenge. A solution that can be adopted (Alexandrou et al. 2024) on rocky seabed or in seagrass meadows is hammering a metal rod, with a 16-mm PVC end pile cap and a retroreflective target on top (Fig. 1). The cap on the rod can be attached using a two-material plaster like epoxy, which can be hand-mixed and placed underwater.

For a more robust solution, adopted and validated across multiple sites in Cyprus, 2-inch PVC tubes

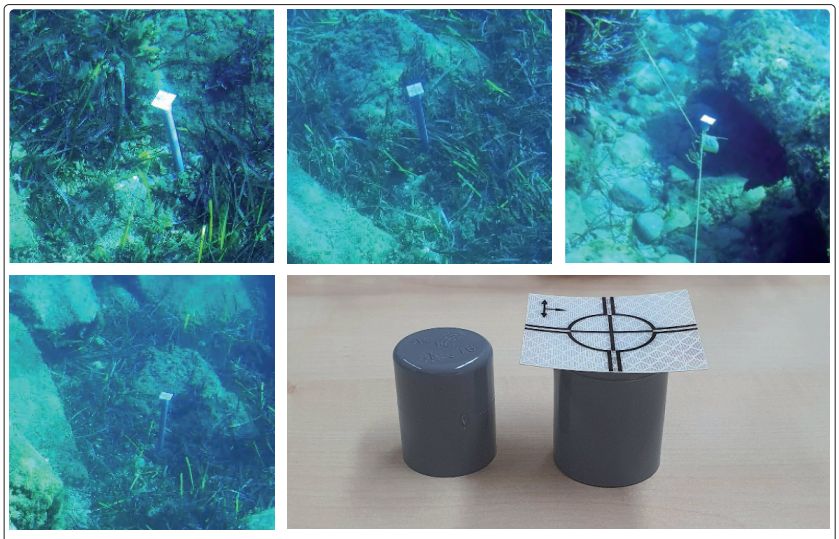

Fig. 1: Rods and 16-mm PVC pipe end cap, with retroreflective target. Reference points placed at Amathous harbour, 3 m depth

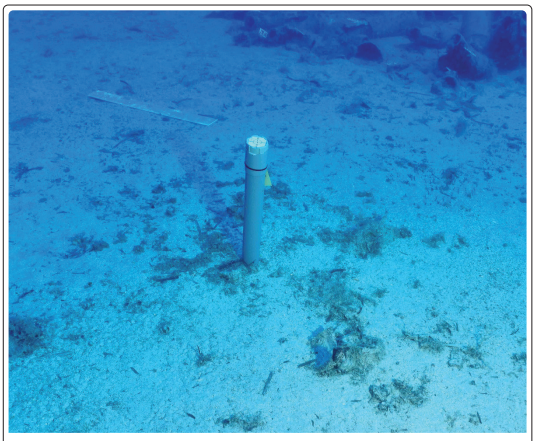

Fig. 2: Example of a 2-inch PVC tube, used as reference points (Mazotos shipwreck site, 45 m depth)

can be used for stable points (Fig. 2). These tubes are pushed deep into sand at selected positions around the site that must be mapped. A threaded cap with a retroreflective target attached is then screwed onto the top of each pole. The friction of the sediment along with the water pressure ensure that the tube remains fixed and cannot be removed accidentally. This modular design is crucial for long-term monitoring. If targets require cleaning or replacement after several years, the caps can be easily unscrewed, brought to the surface, and subsequently re-installed without disturbing the deep-seated pole. However, as this methodology does not protect the poles from external disturbances (e.g., fishing gear, anchors, accidental hits with divers' fins), their stability must be verified in the beginning of every new excavation season, preferably on an annual basis.

2.2 Coordinate estimation using trilateration or photogrammetry

Geodetic theory dictates that a network should ideally consist of equilateral triangles to maximise geometric strength. In the context of a shipwreck, this is rarely feasible, because placing control points in the middle of cargo concentration may damage the artefacts. Consequently, the only viable solution is to establish the network at the periphery, typically leaving empty a buffer zone of 1 to 2 metres off the main concentration, so that to avoid the risk of disturbing buried archaeological material.

Such a layout forces the network into a configuration with large open voids in the middle (Fig. 3). In shallow waters up to 4 m deep, use of long poles with GNSS sensors on top or retroreflective and total stations on shore (Alexandrou et al. 2024) can provide coordinates with approximately 5-cm accuracy (Balletti et al. 2016). However, when the site is deeper, measuring long baselines with traditional tape and processing them with trilateration is not only tedious, but also prone to significant gross errors due to tape sag, currents or divers' nitrogen narcosis. Furthermore, in flat sites where the network lacks significant height variation, trilateration suffers from inherent geometric weakness, leading to unacceptably high uncertainty in the Z-axis (depth).

Using photogrammetric measurements (x,y coordinates on the surface of the photo) to estimate coordinates for the network reference points has three distinct benefits:

- Creation of a true 3D network, with increased vertical precision. The camera projection cen-

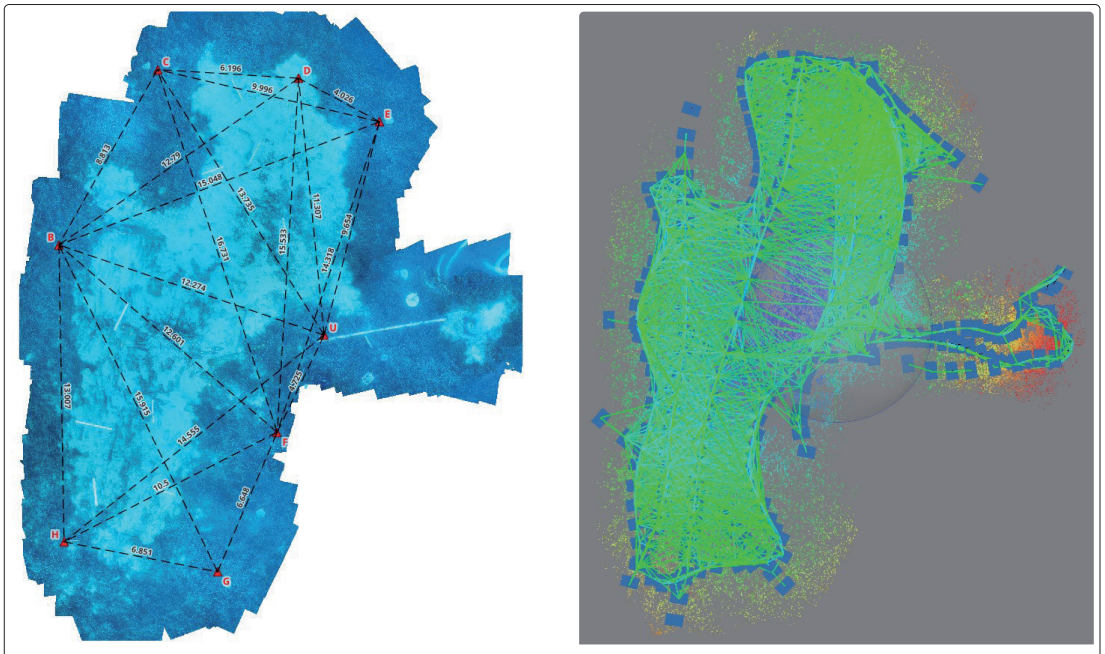

Fig. 3: The network at the *Nissia* shipwreck site. Left: with artificial trilateration. Right: actual photogrammetry

tres are acting as additional network points, on a different depth. Three-dimensional precision may be further enhanced using oblique photos if necessary.
- Increased redundancy of observations, which translates into more stable geometry, better detection of outliers and ultimately increased precision.
- Increased precision due to photographs resolution; depending on the camera-to-object distance, this can be at the order of 1 mm per pixel, or better.

There are two main disadvantages of photogrammetry, however: scale recovery and visibility. Scale recovery may be overcome using several scale bars spread around the site (see Fig. 3), to avoid long baselines, which suffer from the tape measurement problems. Poor visibility affects marking accuracy of the retroreflective targets in the photos and reduces the camera-to-object distance, resulting in an increased number of photos. For example, in a Monte Carlo simulated trilateration scenario (Skarlatos et al. 2019) applied on the *Nissia* shipwreck site in Cyprus (see Fig. 3), with rather optimistic uncertainties applied to tape measurements, it was possible to achieve uncertainties of ±6 cm in horizontal accuracy and ±64 cm in vertical accuracy. When measured using a geometrically moderate photogrammetric network, with 1 mm average ground pixel size, the same network, may achieve ±0.2 cm in horizontal accuracy and ±0.2 cm in vertical accuracy. The simulation of using tape measurements and trilateration on a real site verifies the theoretical assumption that photogrammetry is superior for network's coordinate estimation in underwater environment.

2.3 The vertical reference challenge

While in terrestrial networks, vertical reference can be easily determined via GNSS or bullseye spirit levels, underwater depth measurement relies on pressure sensors. To establish vertical reference, depth measurements are acquired next to each landmark, using the same dive computer, in a single dive. It is important to note that dive computers have readings of ±0.1 m and cannot attain the necessary precision for such network. However, these measurements should be used to define the vertical axis of the network rather than the shape. When distributed across a network of 20 m in length, i.e. approximately the length of the *Nissia* (Fig. 3), the relative levelling error can be reduced to ±2 cm (Skarlatos et al. 2019). The internal geometry of the network remains defined by the rigid photogrammetric block, while the pressure readings merely orient this block to the gravity vector.

2.4 Monitoring network's stability

The main benefit of a surveying network comes from its guaranteed stability, which in constantly changing underwater environment is not a given. In the underwater environment main risks come from trawlers' fishing nets, divers with fins, airlift anchors, etc. Therefore, established networks should be thoroughly checked in the beginning of each excavation period. The ability to detect and identify movement is based on Least Square theory, which provides extensive statistics for blunder detection (data snooping).

As a rule, a dedicated photographic data acquisition is performed prior archaeological work, covering the reference points and the site, with emphasis on the geometry of the photogrammetric block rather than on covering the archaeological remains. When coordinates on the reference points are considered stable, the coordinates from field seasons are used with ±0.02 m accuracy. Tie points and reference points are assigned one pixel accuracy in image level. The internal sigma estimation of the solution and the residuals (error) from the coordinates are checked against each other. In case any landmark demonstrates error, which is three times larger (equivalent to 99.7 % confidence level) than the estimated sigma (Table 1). There isn't any strict protocol for checking suspicious points. Usually, they are first double-checked for image residuals, then they are individually checked for error

GCP	X	Y	Z	X error	Y error	Z error	XYZ error	X sigma	Y sigma	Z sigma	XYZ sigma
B	18.213 m	28.805 m	−26.360 m	0.001 m	−0.001 m	−0.003 m	0.003 m	0.001 m	0.001 m	0.002 m	0.002 m
C	22.531 m	36.488 m	−27.129 m	0.005 m	0.000 m	0.000 m	0.005 m	0.001 m	0.001 m	0.002 m	0.002 m
D	28.715 m	36.106 m	−27.484 m	−0.004 m	0.000 m	0.002 m	0.005 m	0.001 m	0.001 m	0.001 m	0.002 m
E	32.261 m	34.199 m	−27.415 m	0.001 m	0.006 m	−0.001 m	0.006 m	0.001 m	0.001 m	0.001 m	0.002 m
F	27.777 m	20.601 m	−26.328 m	−0.006 m	−0.003 m	0.000 m	**0.007 m**	0.001 m	0.001 m	0.002 m	0.002 m
G	25.163 m	14.488 m	−25.757 m	−0.002 m	−0.004 m	−0.002 m	0.005 m	0.001 m	0.001 m	0.002 m	0.002 m
H	18.439 m	15.800 m	−25.534 m	0.005 m	0.002 m	0.003 m	**0.007 m**	0.001 m	0.001 m	0.002 m	0.002 m

Table 1: Typical Least Square bundle adjustment results. This represents the *Nissia* network checking during the beginning of 2017 excavation period, three years after the initial excavation. Values marked blue represent points' movement exceeding triple the equivalent sigma

magnitude on the neighbouring reference points, if the point under investigation is treated as check point. Finally, if the point is assumed displaced, then new coordinates are assigned. It should be mentioned that only rarely have we identified movements across different field seasons, which validates the stability of the chosen tubes to act as reference points. Nevertheless, the same verification approach is used when there is a suspicion for accidental displacement of a reference point. While the collaboration and proper reporting of all divers is necessary to maintain a stable network, it must also be pointed out that for a sound estimation of precision, measurements must be accompanied with realistic and not overoptimistic accuracy.

2.5 Summary

To establish a stable control network in challenging underwater environments, several factors need to be taken into consideration, starting from the use of reference points. Photogrammetry is far more accurate than traditional trilateration, as it demonstrates significantly higher precision. Therefore, it has widely been adopted in free network solutions for initial estimation of the network's coordinates. Vertical reference is defined by averaging dive computer readings to orient the photogrammetric block to the gravity vector as a trade-off between simplicity and accuracy. Long-term integrity must be ensured through annual Least Square bundle adjustment, which statistically validates the network's stability and isolates any reference points displaced by external disturbances.

3 Colour restoration

3.1 Motivation

Optical underwater imaging is central to underwater archaeology and marine sciences. Wavelength-dependent absorption and scattering distort recorded colour, cause chromatic shifts, contrast loss and spatially inconsistent radiometry. As a result, raw imagery does not reliably represent true object or habitat reflectance, making colour restoration essential for meaningful interpretation. In underwater archaeology, colour is a critical cue for material identification, assessment of the state of preservation and temporal comparison in photogrammetric documentation. Without correction, variations induced by imaging geometry or water properties may be misinterpreted as archaeological features or markers of change, whereas inconsistencies propagate into mosaics and textured models, thus limiting scientific reliability (Rossi et al. 2021). In marine sciences, colour serves as a proxy for biological composition and condition, supporting habitat mapping and coral reef monitoring, yet attenuation reduces sensitivity to ecological variability. In structurally complex habitats, visualization is often prioritised over radiometric reliability, hindering quantitative evaluation, as emphasised by Rossi et al. (2021). Moreover, restoration approaches demonstrate that visually appealing results do not necessarily correspond to accurate colour recovery when the underlying image formation is not properly addressed (Vlachos et al. 2025a). Consequently, underwater colour restoration is required for the transition from visually convincing representations to scientifically robust and quantitatively interpretable optical data across disciplines (Rossi et al. 2021).

3.2 Problems and limitations

Underwater colour restoration is constrained by environmental, optical and operational factors that vary between shallow and deep-water environment, requiring different approaches.

In shallow waters, variable natural illumination and mixed lighting conditions produce strong radiometric inconsistencies, while wavelength-dependent colour loss and contrast degradation persist despite reduced attenuation. In deep water, imaging relies entirely on artificial illumination, with strong distance-dependent attenuation, limited illumination footprint and dominant backscatter tightly coupling colour degradation to camera-to-object distance (CoD), often resulting in severe spatial colour variability even within single images. In both contexts, enhancement-based methods improve visual appearance but do not recover physically meaningful colour, limiting their suitability for evaluative applications (Rossi et al. 2021). In deep-water datasets, operational constraints typically preclude radiometric calibration, and colour degradation has been shown to affect photogrammetric performance, including feature matching and dense reconstruction (Vlachos et al. 2025a; Vlachos et al. 2022a).

Physically based approaches model absorption and backscatter to invert the underwater image formation process. Geometry-aware methods have demonstrated improved colour consistency in large-scale surveys (Bryson et al. 2016) and revised physical models that separate direct signal attenuation from backscatter address fundamental limitations of atmospheric formulations (Akkaynak and Treibitz 2019). However, such methods generally require accurate range data, assumptions about water properties, stable illumination or controlled acquisition protocols, which are rarely available in diver-based surveys and legacy archaeological datasets (Vlachos and Skarlatos 2021).

Learning-based approaches estimate colour correction mappings directly from data but are constrained by the lack of reliable underwater ground truth and frequent reliance on synthetic training datasets. Many operate purely in image space, neglecting the strong dependence of col-

our degradation on depth and scene geometry, which can result in visually plausible but radiometrically inconsistent corrections that negatively affect photogrammetric processing (Vlachos et al. 2025b).

Mapping of the *Mazotos* and *Nissia* shipwrecks (Vlachos and Skarlatos 2024; Vlachos et al. 2025a; Skarlatos et al. 2019; Vlachos et al. 2025b; Bruno et al. 2019) exemplifies datasets acquired under realistic archaeological constraints, lacking dedicated radiometric calibration and exhibiting strong depth- and geometry-dependent colour degradation. These conditions have motivated restoration strategies that exploit information already available in SfM–MVS pipelines, adapt to scene geometry and support both visual interpretation and photogrammetric robustness. Building on evidence that colour correction influences reconstruction quality (Vlachos et al. 2022b), the Self-Adaptive Colour Calibration framework integrates SfM–MVS-derived CoDs with learning-based correction, addressing key gaps between fully physical and purely data-driven approaches (Vlachos et al. 2025b).

Colour restoration approach using DL

To overcome the limitations of physically based and traditional image-driven approaches under realistic underwater documentation constraints, a deep learning (DL)-based colour restoration framework, termed the Self-Adaptive Colour Calibration (SACC) pipeline, was developed for underwater photogrammetric datasets, where controlled calibration, environmental optical measurements and dedicated colour targets are typically unavailable.

The SACC pipeline restores colour by learning the relationship between image radiometry and scene geometry using a Feedforward Neural Network (FNN) (Vlachos and Skarlatos 2024). Rather than explicitly modelling underwater light propagation, the method learns a data-driven correction that accounts for distance-dependent colour degradation. A central assumption is that datasets acquired with artificial illumination include observations captured under favourable lighting conditions with minimal attenuation; these are treated as relative reference colours, enabling supervised learning without external ground truth. As a result, the pipeline is self-adaptive and trained on a per-dataset basis, adjusting to local water conditions and acquisition geometry (Vlachos and Skarlatos 2024; Vlachos et al. 2025a) (Fig. 4).

The pipeline is integrated within a standard SfM–MVS workflow and relies exclusively on data products routinely generated during 3D reconstruction, including multi-view imagery, sparse point correspondences and depth or camera-to-object distance (CoD) estimates. By exploiting this information, the network learns to map degraded colour observations to corrected values while remaining fully compatible with photogrammetric processing (Vlachos et al. 2025a).

Compared to fully physical models, the SACC pipeline does not require explicit estimation of absorption or backscatter coefficients, water optical properties or controlled acquisition protocols. By incorporating CoD information, it also overcomes the limitations of purely image-space DL approaches. Importantly, the correction is applied in a controlled manner that preserves image texture and avoids artefacts known to affect feature detection, feature matching and dense reconstruction quality in SfM–MVS workflows (Vlachos et al. 2022b; Vlachos et al. 2025b).

3.3 Applications to the Mazotos and Nissia shipwreck sites

The SACC pipeline was evaluated on underwater archaeological datasets from the *Mazotos* and *Nissia* shipwrecks, that represent realistic documentation scenarios with limited calibration opportunities. At *Mazotos* (–44 m), imagery was acquired at depths exceeding 40 m under exclusively artificial illumination, exhibiting strong distance-dependent colour attenuation. The SACC pipeline enabled dataset-wide colour restoration without physical colour charts, improving radiometric consistency and supporting more stable textured 3D recon-

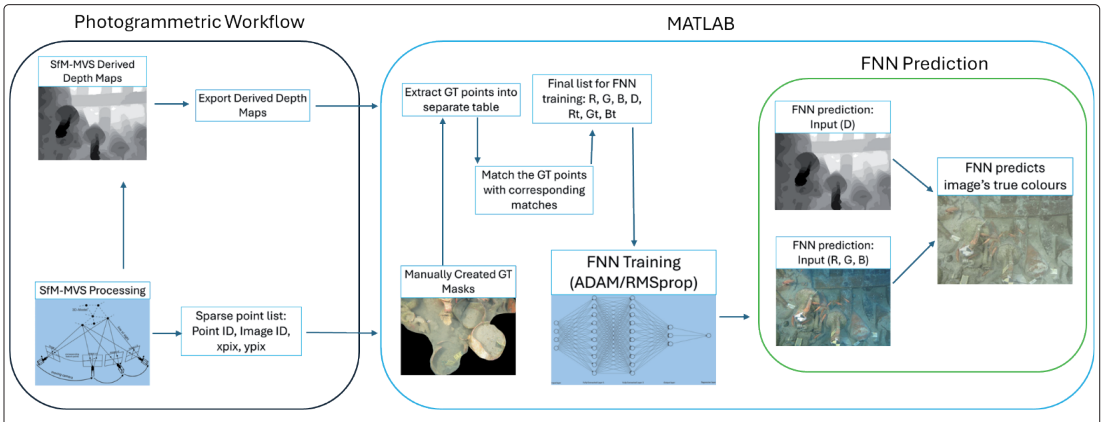

Fig. 4: Summary of the Self-Adaptive Colour Calibration pipeline (image from Vlachos et al. (2025b))

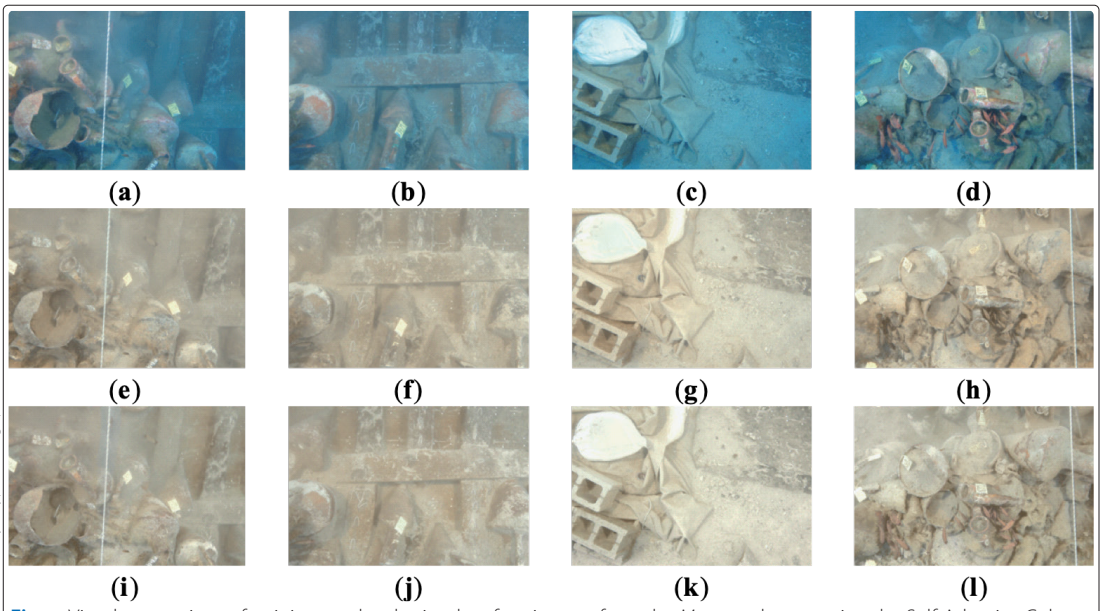

Credits: MA-RELab, © University of Cyprus, Photographer: Massimiliano Secci

Fig. 5: Visual comparison of training results obtained on four images from the *Mazotos* dataset using the Self-Adaptive Colour Calibration pipeline (a to d: original images; e to h: Adam optimiser-based prediction results; i to l: RMSprop optimiser-based prediction results). Camera: Sony SLT-A57. Images acquired at the *Mazotos* shipwreck site

structions in a complex excavation environment (Vlachos and Skarlatos 2024). Fig. 5 presents four images from the 2019 field season at *Mazotos,* together with their colour-corrected counterparts produced using predictors trained with different optimisers.

At *Nissia* (–27 m), a more controlled evaluation scenario was available, with the inclusion of colour reference targets, which enable quantitative assessment of restoration accuracy. Results showed improved agreement between restored and reference colours, particularly in the red and green channels, while highlighting remaining challenges in blue channel recovery. The *Nissia* case study also enabled systematic evaluation of the pipeline's impact on feature matching and reconstruction robustness (Vlachos et al. 2025b). Fig. 6 presents five images from the dataset acquired during the 2024 field season at *Nissia,* alongside their colour-corrected counterparts produced using predictors trained with the Adam and RMSprop optimisers.

3.4 Summary

The Self-Adaptive Colour Calibration (SACC) pipeline is a deep learning–based, geometry-aware colour restoration strategy for underwater photogrammetric documentation. By exploiting SfM–MVS-derived depth information and dataset-internal reference colours, it bridges the gap between physically grounded and purely image-based methods. Its application to the *Mazotos* and *Nissia* shipwrecks demonstrates its suitability for

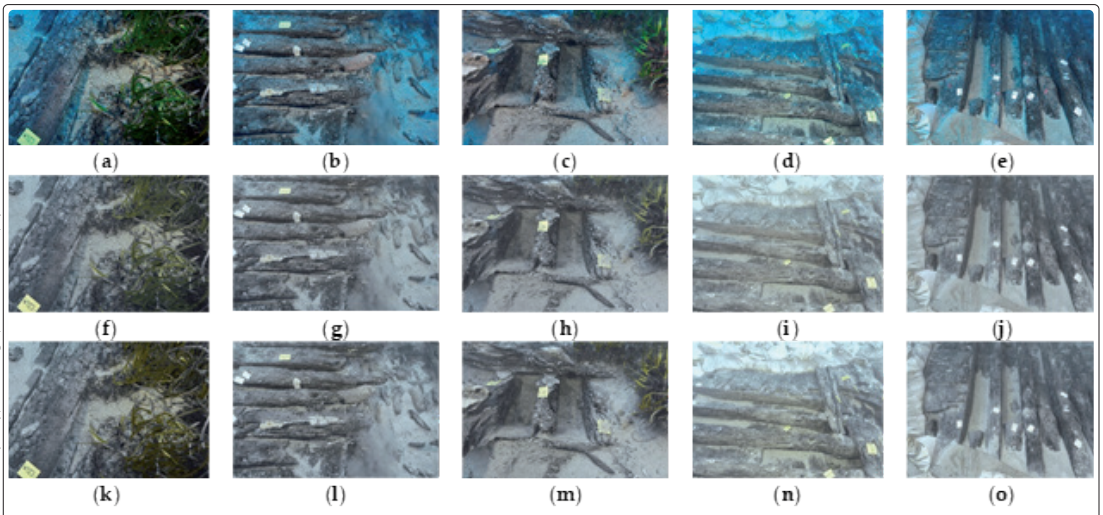

Credits: MARELab, © University of Cyprus, Photographer: Andonis Neophytou

Fig. 6: Visual comparison of training results obtained on five images from the *Nissia* dataset using the Self-Adaptive Colour Calibration pipeline (a to e: original images; f to j: Adam optimiser-based prediction results; k to o: RMSprop optimiser-based prediction results). Camera: Nikon D510. Images acquired at the *Nissia* shipwreck site

underwater archaeological datasets, supporting the use of colour as evaluative information rather than purely visual enhancement.

4 Coastal sites and drone mapping

4.1 Motivation

Mapping coastal sites is essential for a range of engineering and archaeological applications. While established methodologies exist for terrestrial zones (e.g., drones, LiDAR) and the seabed (e.g. echo sounders), achieving a seamless, unified model across the land-sea boundary remains a significant challenge.

While echo sounders typically generate point clouds lacking visual colour information, which is critical for identifying specific archaeological features, unmanned surface vehicles (USVs) equipped with multibeam echo sounders (MBES) and underwater nadiral cameras allow for detailed 3D and visual documentation. The use of underwater cameras facilitates direct application of SfM and MVS photogrammetry, as water refraction effects can be effectively absorbed during camera self-calibration.

Aerial drones equipped with bathymetric LiDAR offer another potential solution for seamless surface modelling, but generating seamless orthophotomosaics from such data requires specific water refraction corrections. Aerial drone photogrammetry represents an affordable and effective solution in regions with high water clarity, such as the Eastern Mediterranean. This approach is particularly valuable in very shallow waters, where unmanned surface vehicles (USV) or swimmers cannot operate safely. The application of through-water aerial photogrammetry, however, is currently limited because standard commercial software fails to account for air-water refraction, a phenomenon that introduces significant geometric errors regardless of water depth or flight altitude (Skarlatos and Agrafiotis 2018). Applying unified mapping techniques was critical for mapping numerous coastal sites, including the Amathus harbour, Cyprus (Empereur and Verlinden 1987), Pavlopetri (Harding et al. 1969) and Epidaurus (Davidde Petriaggi et al. 2020), Greece, and Caesarea, Israel (Hohlfelder et al. 1983). These sites require a holistic approach that seamlessly connects underwater and terrestrial remains.

For example, the late 4th century BC harbour of Amathus, Cyprus, is a very good example of a shallow site, with extensive architectural remains on land and under the sea, that can only be studied through accurate mapping and documentation within a unified, seamless spatial reference system. Firstly, close examination of the moles and breakwaters is hindered by the very shallow depth and the rich marine flora, so aerial photography is the only way to understand the architectural layout. Moreover, the Amathus harbour works are organically connected with coastal monuments of the ancient city, from which they are now detached, due to coastal erosion; and at the same time, submerged terrestrial structures within its basin should be recorded with accuracy, so that other phenomena of coastal changes can be documented.

4.2 Through-water photogrammetric documentation

There are three primary justifications for employing through-water aerial surveys: 1) the extensive size of the survey area, 2) the requirement for a seamless visual survey encompassing both terrestrial and underwater structures, and 3) extremely shallow water depths (Alexandrou et al. 2024) that preclude the use of underwater photography. It is important to note that while a combined approach utilising an aerial drone for land and a USV equipped with MBES and a hull-mounted camera yields superior image resolution, it invariably results in a data void within the surf zone. In cases of underwater or harbour structures, this zone can contain critical information.

The principal impediment to aerial photogrammetric mapping in this context is water refraction, which violates the fundamental collinearity assumption (straight visual line) of photogrammetry. Accurate geometric results require two-media photogrammetry, a capability currently absent in standard commercial software, thereby limiting the widespread adoption of this methodology.

To address this, a solution employing ML to correct the erroneous bathymetric point clouds generated by standard SfM–MVS processes that neglect refraction has been proposed in Agrafiotis et al. (2024) and in Agrafiotis et al. (2021). The Support Vector Machine (SVM) model was trained using reference LiDAR bathymetric data (Agrafiotis et al. 2024) and synthetic bathymetric and imagery datasets (Agrafiotis et al. 2021). Following the depth correction of underwater points, all corresponding images undergo differential rectification based on the corrected depths to ensure accurate orthorectification and mosaicking. This method has been successfully validated at several sites, including the ancient harbour of Amathus, Paphos harbour and Agia Napa marina (Fig. 7).

Despite the high bathymetric accuracy achieved, the methodology is subject to specific limitations. Flight altitudes must generally exceed 30 metres to mitigate the impact of dynamic wave patterns on SfM feature matching. Additionally, caustic patterns in very shallow water and turbidity can hinder the process. Furthermore, the use of an RTK-enabled drone is strongly recommended to ensure geometric stability. Perhaps the most

Fig. 7: This aerial orthophotomosaic of Amathounta harbour has a resolution of 2.5 cm and has been produced by drone aerial photos, after water refraction correction. For scale reference, visible south jetty is approximately 170 m long

significant constraint is the assumption of a planar water surface. This simplification affects both LiDAR and photogrammetric approaches, as the scientific community continues to seek viable solutions for real-time wave modelling to accurately define surface normals for the rigorous application of Snell's law.

5 The way forward

The adoption of machine learning is primarily justified in cases where the precise physical formulas governing a phenomenon are unknown or too complicated to estimate; the model cannot be calibrated due to missing information; not all variables can be determined due to equipment limitations. Given the complex physical formulae of light propagation, the constantly changing underwater environmental parameters affecting light propagation and the limited environmental data, machine learning offers a significant potential. As mentioned above, ML has been utilised in underwater colour restoration and bathymetric evaluation, bypassing the full physical models.

The use of 3D Gaussian splatting (3DGS) in underwater 3D reconstruction, seems to offer distinct advantages over traditional structure-from-motion (SfM) and multi-view stereo (MVS) pipelines. Where MVS approaches struggle in aquatic environments due to featureless textures, light flickering and significant scattering, 3DGS leverages differentiable rasterisation to achieve near real-time rendering in speeds that far exceed those of MVS. At the same time 3DGS represents scenes as explicit point clouds with Gaussians splatted onto the image plane, providing a balance between the explicit geometry of MVS and the photorealistic rendering.

A critical advantage of most recent 3DGS frameworks (Li et al. 2025; Yang et al. 2025; Liu et al. 2024), is their capacity to integrate the physical Image Formation Models (IFMs). In MVS, the water medium's effects such as wavelength attenuation and backscatter are baked into the texture, resulting in colour cast models. Conversely, physics-aware 3DGS manage to model these optical interactions, allowing the disentanglement of the scene's true albedo from the participating medium. This capability facilitates simultaneous 3D reconstruction and colour restoration, effectively »removing« the water to present the scene as it would appear in air.

Regarding the later, the promise of 3DGS as a tool to merge 3D reconstruction, 3D representation and colour restoration, becomes an attractive potential. Being able to combine, in a single solution water refraction correction, geometry recovery and colour restoration into a fast holistic tool, seems like the holy grail of underwater photogrammetry.

Such tool would ultimately be able to utilise aerial photos for correct geometric reconstruction of sea bottom and land removing the effect of water altogether, creating a seamless true colour orthophoto mosaic and corresponding digital surface model over the mapping area.

However, the application of 3DGS in underwater domains is not without limitations. The framework relies on SfM algorithms for camera pose estimation and point cloud initialisation. This creates a significant dependency on photogrammetry, with all current limitations in turbid or texture-poor underwater scenes where point operators fails to identify sufficient feature matches. Problems with suspended particles and floaters in the photos, degrading the geometric fidelity of the resulting reconstruction and representation, seems to have been dealt successfully (Li et al. 2025; Yang et al. 2025; Liu et al. 2024; Wang et al. 2025), but issues with marine life and moving seaweeds, still remain. In terms of point density and detail in geometric accuracy, 3DGS are still behind traditional SfM–MVS, without any tangible signs of how they could bridge the gap.

Consequently, while 3DGS provides superior visual presentation and restoration capabilities, the resulting point density and geometric connectivity may require further refinement to match the metrological precision of dense MVS meshes. Nevertheless, the potential of ML in underwater applications for archaeology and marine and ocean sciences is undoubtable. //

References

Agrafiotis, Panagiotis; Konstantinos Karantzalos; Andreas Georgopoulos; Dimitrios Skarlatos (2020): Correcting Image Refraction: Towards Accurate Aerial Image-Based Bathymetry Mapping in Shallow Waters. Remote Sensing, DOI: 10.3390/rs12020322

Agrafiotis, Panagiotis; Konstantinos Karantzalos; Andreas Georgopoulos; Dimitrios Skarlatos (2021): Learning from Synthetic Data: Enhancing Refraction Correction Accuracy for Airborne Image-Based Bathymetric Mapping of Shallow Coastal Waters. Journal of Photogrammetry, Remote Sensing and Geoinformation Science (PFG), DOI: 10.1007/s41064-021-00144-1

Akkaynak, Derya; Tali Treibitz (2019): Sea-Thru: A Method for Removing Water From Underwater Images. Proceedings of the IEEE/CVF Conference on Computer Vision and Pattern Recognition (CVPR), DOI: 10.1109/CVPR.2019.00178

Alexandrou, Antreas; Filip Škola; Dimitrios Skarlatos et al. (2024): Underwater Virtual Exploration of the Ancient Port of Amathus. Journal of Cultural Heritage, DOI: 10.1016/j.culher.2024.09.006

Balletti, Caterina; Carlo Beltrame; Eleonora Costa et al. (2016): 3D Reconstruction of Marble Shipwreck Cargoes Based on Underwater Multi-Image Photogrammetry. Digital Applications in Archaeology and Cultural Heritage, DOI: 10.1016/j.daach.2015.11.003

Benetatos, Christoforos; Stefano Costa; Giorgio Giglio et al. (2024): Exploring the Mediterranean: AUV High-Resolution Mapping of the Roman Wreck Offshore of Santo Stefano al Mare (Italy). Journal of Marine Science and Engineering, DOI: 10.3390/jmse13101921

Bruno, Fabio; Alessandro Lagudi; Loris Barbieri et al. (2019): Virtual Tour in the Sunken »Villa con Ingresso a Protiro« Within the Underwater Archaeological Park of Baiae. International Archives of the Photogrammetry, Remote Sensing and Spatial Information Sciences, DOI: 10.5194/isprs-archives-XLII-2-W10-45-2019

Bryson, Mitch; Matthew Johnson-Roberson; Oscar Pizarro; Stefan B. Williams (2016): True Color Correction of Autonomous Underwater Vehicle Imagery. Journal of Field Robotics, DOI: 10.1002/rob.21638

Davidde Petriaggi, Barbara; Panagiota Galiatsatou; Salvatore Medaglia et al. (2020): The Submerged »Villa of the Dolia« Near Ancient Epidaurus: The Preliminary Results of the First Excavation and Conservation Campaign. Proceedings of the Honor Frost Foundation Conference

Empereur, Jean-Yves; Colette Verlinden (1987): The Underwater Excavation at the Ancient Port of Amathus in Cyprus. The International Journal of Nautical Archaeology and Underwater Exploration, No. 16.1, pp. 7–11

Green, Jeremy; Sheila Matthews; Tufan Turanli (2002): Underwater Archaeological Surveying Using PhotoModeler, VirtualMapper: Different Applications for Different Problems. International Journal of Nautical Archaeology, DOI: 10.1006/ijna.2002.1041

Harding, Anthony; Gerald Cadogan; Roger Howell (1969): Pavlopetri: An Underwater Bronze Age Town in Laconia. The Annual of the British School at Athens, No. 64, pp. 113–42

Hohlfelder, Robert L.; John Peter Oleson; Avner Raban; Robert L. Vann (1983): Sebastos, Herod's Harbor at Caesarea Maritima. The Biblical Archaeologist, DOI: 10.2307/3209823

Janowski, Łukasz; Dimitrios Skarlatos; Panagiotis Agrafiotis et al. (2024): High Resolution Optical and Acoustic Remote Sensing Datasets of the Puck Lagoon. Scientific Data, DOI: 10.1038/s41597-024-03199-y

Li, Jiachen; Guangzhi Han; Jin Wan; Yuan Gao; Delong Han (2025): DualPhys-GS: Dual Physically-Guided 3D Gaussian Splatting for Underwater Scene Reconstruction. Graphics, DOI: 10.48550/arXiv.2508.09610

Liu, Shaohua; Junzhe Lu; Zuoya Gu; Jiajun Li; Yue Deng (2024): Aquatic-GS: A Hybrid 3D Representation for Underwater Scenes. Computer Vision and Pattern Recognition, DOI: 10.48550/arXiv.2411.00239

Rossi, Paolo; Massimo Ponti; Sara Righi et al. (2021): Needs and Gaps in Optical Underwater Technologies and Methods for the Investigation of Marine Animal Forest 3D-Structural Complexity. Frontiers in Marine Science, DOI: 10.3389/fmars.2021.591292

Skarlatos, Dimitrios; Stella Demesticha; Stavroula Kiparissi (2012): An ›Open‹ Method for 3D Modelling and Mapping in Underwater Archaeological Sites. International Journal of Heritage in the Digital Era, DOI: 10.1260/2047-4970.1.1.1

Skarlatos, Dimitrios; Panagiotis Agrafiotis (2018): A Novel Iterative Water Refraction Correction Algorithm for Use in Structure from Motion Photogrammetric Pipeline. Journal of Marine Science and Engineering, DOI: 10.3390/jmse6030077

Skarlatos, Dimitrios; Fabio Menna; Erica Nocerino; Panagiotis Agrafiotis (2019): Precision Potential of Underwater Networks for Archaeological Excavation Through Trilateration and Photogrammetry. International Archives of the Photogrammetry, Remote Sensing and Spatial Information Sciences, DOI: 10.5194/isprs-archives-XLII-2-W10-175-2019

Vlachos, Marinos; Dimitrios Skarlatos (2021): An Extensive Literature Review on Underwater Image Colour Correction. Sensors, DOI: 10.3390/s21175690

Vlachos, Marinos; Dimitrios Skarlatos (2024): Self-Adaptive Colour Calibration of Deep Underwater Images Using FNN and SfM-MVS-Generated Depth Maps. Remote Sensing, DOI: 10.3390/rs16071279

Vlachos, Marinos; Alessio Calantropio; Dimitrios Skarlatos; Filiberto Chiabrando (2022a): Modelling Colour Absorption of Underwater Images Using SfM-MVS Generated Depth Maps. International Archives of the Photogrammetry, Remote Sensing and Spatial Information Sciences, DOI: 10.5194/isprs-archives-XLIII-B2-2022-959-2022

Vlachos, Marinos; Dimitrios Skarlatos; Alessio Calantropio; Filiberto Chiabrando (2022b): An Adhoc UW Image Colour Correction Method and the Impact on Image Feature Matching & SfM-MVS 3D Reconstruction. 2022 International Conference on Interactive Media, Smart Systems and Emerging Technologies (IMET), DOI: 10.1109/IMET54801.2022.9929653

Vlachos, Marinos; Dimitrios Skarlatos; Stella Demesticha (2025a): Self-Adaptive Colour Calibration Pipeline for Deep Underwater Image Restoration: A Reference-Based Evaluation. Virtual Archaeology Review, DOI: 10.4995/var.2024.24170

Vlachos, Marinos; Dimitrios Skarlatos; Stella Demesticha (2025b): The Impact of a Deep Learning Self-Adaptive Colour Restoration Pipeline for Deep Underwater Images in 3D Reconstruction. International Archives of the Photogrammetry, Remote Sensing and Spatial Information Sciences. DOI: 10.5194/isprs-archives-XLVIII-2-W10-2025-309-2025

Wang, Haoran; Nantheera Anantrasirichai; Fan Zhang; David Bull (2025): UW-GS: Distractor-Aware 3D Gaussian Splatting for Enhanced Underwater Scene Reconstruction. Computer Vision and Pattern Recognition, DOI: 10.48550/arXiv.2410.01517

Yang, Daniel; John J. Leonard; Yogesh Girdhar (2025): SeaSplat: Representing Underwater Scenes with 3D Gaussian Splatting and a Physically Grounded Image Formation Model. Computer Vision and Pattern Recognition, DOI: 10.48550/arXiv.2409.17345

KONGSBERG

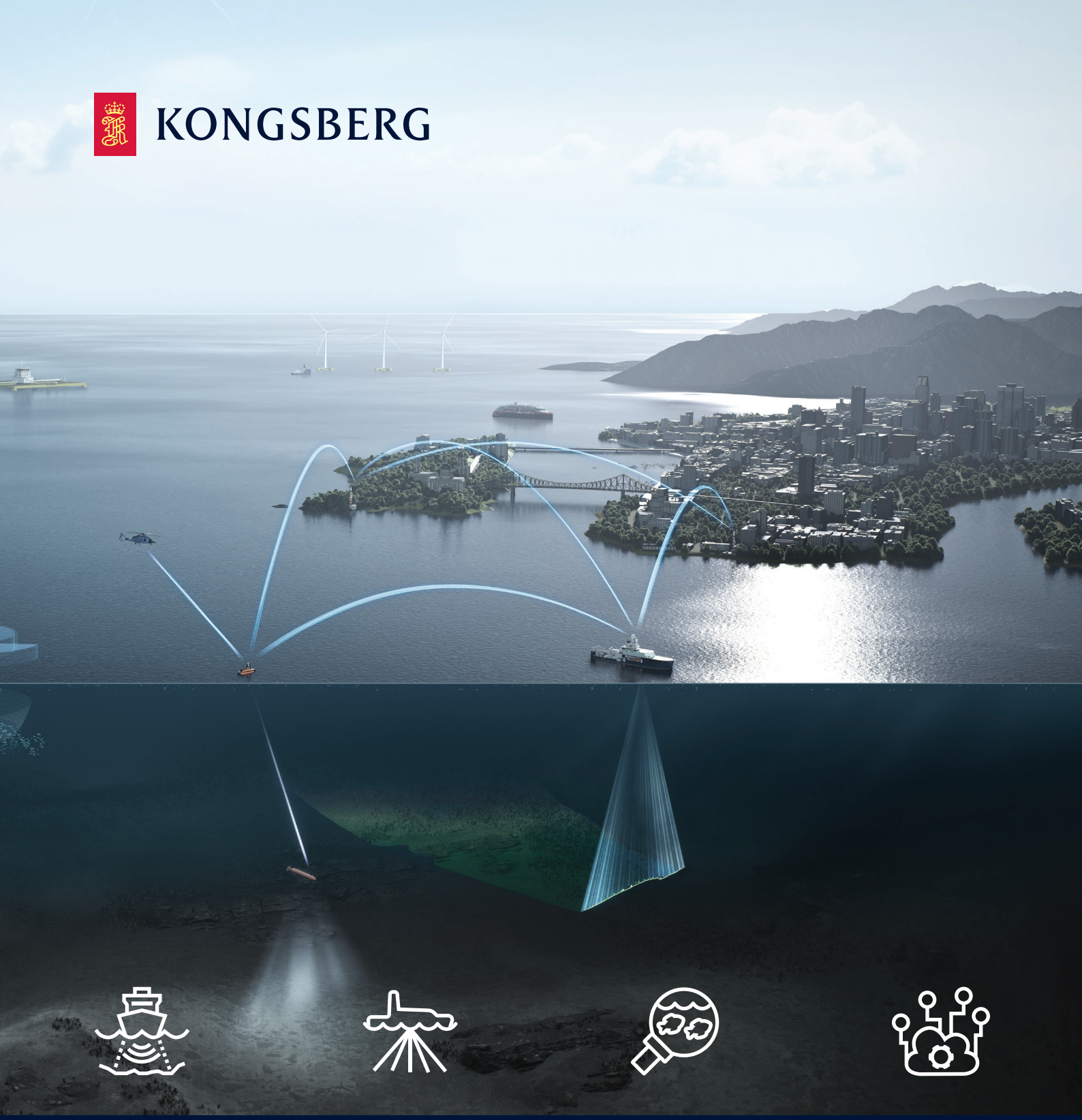

Discovering the secrets of the ocean

kongsberg.com/discovery

DOI: 10.23784/HN133-06

Lückenschluss im »Weißen Band« vor Helgoland

Fusion von Mikrobathymetrie, Snippet-Backscatter und parametrischer Echolotung für die hydrographische und geoökologische Prospektion

Ein Beitrag von JENS SCHNEIDER VON DEIMLING und MERVE JENSEN

Die Vermessung der Helgoländer Flachwasserzone (bis 10 m Tiefe) ist aufgrund starker Gezeiten, Untiefen und dichten Kelpbewuchses äußerst anspruchsvoll. Um diese Kartierungslücke zu schließen, setzt die Arbeitsgruppe der CAU Kiel das Forschungsboot *FB Zostera* ein. Durch die Fusion von hochauflösender Fächerecholot-Bathymetrie, Snippet-Backscatter und parametrischer Sedimentecholotung wird ein digitales Geländemodell mit einer Auflösung von 0,5 Metern erstellt. Die Methodik ermöglicht es, rein akustisch sowohl die Vegetationsoberkante als auch die Morphologie des wahren Meeresbodens zu differenzieren. Diese Daten bilden die Basis für präzise Habitatmodellierungen, geologische Analysen des Helgoländer Unterwassersockels sowie die Detektion unterwasserarchäologischer Funde.

Helgoländer Felssockel | Mikrobathymetrie | Habitatmodellierung | Weißes Band | Rückstreustärke
Heligoland rocky reef | micro-bathymetry | Benthic habitat mapping | White ribbon | backscattering strength

Surveying the Heligoland shallow water zone (down to 10 m depth) is highly demanding due to strong tidal currents, shoals and dense kelp forests. To bridge this mapping gap, the research group at CAU Kiel utilises the research vessel *FB Zostera*. By fusing high-resolution multibeam echo sounder (MBES) bathymetric data, snippet backscatter and parametric sub-bottom profiling, a digital terrain model with a 0.5-metre resolution is generated. This methodology enables a purely acoustic differentiation between the vegetation canopy and the true seafloor morphology. These data provide the foundation for precise habitat modelling, geological analysis of the mesozoic basement and the detection of underwater archaeological finds.

Autoren
Dr. Jens Schneider von Deimling lehrt und forscht an der Christian-Albrechts-Universität zu Kiel (CAU) zum Thema experimentelle Hydroakustik und Habitatkartierung.
Merve Jensen ist Doktorandin an der CAU mit Schwerpunkt auf experimenteller Hydroakustik und der Kartierung von Braunalgen um Helgoland.

jens.schneider@ifg.uni-kiel.de

Helgoland ist aus vielerlei Perspektiven ein ganz besonderer Ort. Aus geologischer Sicht erheben sich hier Schichten aus der Erdmittelzeit (Mesozoikum), deren prominenteste Ausprägung die »Lange Anna« aus rotem Buntsandstein bildet. Im Norddeutschen Becken liegt dieser Buntsandstein normalerweise in Tiefen von rund 3000 Metern, wurde hier jedoch infolge salztektonischer Prozesse an die Oberfläche gehoben. Diese geologische Anomalie setzt sich unter Wasser fort und bildet eine in der Nordsee einmalige Unterwasserlandschaft aus Felsriffen, welche zur artenreichsten Region in deutschen Gewässern führte und unter anderem ein wertvolles Habitat für Großalgen und Hummer darstellt.

Aus hydrographischer Sicht stellt Deutschlands einzige Hochseeinsel eine wahre Herausforderung dar: flaches Wasser, unbekannte Untiefen und Felsvorsprünge, starke Gezeitenströme und ein raues, sich ständig wechselndes Wellenbild machen Vermessungsarbeiten außerordentlich anspruchsvoll. Besonders kritisch ist hierbei das sogenannte »Weiße Band« der Küstenkartierung – eine ultraflache Übergangszone (ca. 1 bis 6 Meter Wassertiefe). Dieser Bereich ist für die meisten Vermessungs- und Forschungsschiffe nicht sicher befahrbar und bleibt optischen Fernerkundungsmethoden aufgrund der Trübung und des Bewuchses vor Helgoland weitgehend verborgen. Um die Kartierungslücken innerhalb dieses Bereiches zu schließen, führte unsere Arbeitsgruppe »Marine Geophysik und Hydroakustik« an der Christian-Albrechts-Universität zu Kiel (CAU) in den vergangenen Jahren intensive Kartierungen mit *FK Littorina* und *FB Zostera* durch. Diese Arbeiten wurden unlängst durch die Initiative des Aktionsprogramms Natürlicher Klimaschutz (ANK) weiter gefördert. Unser Ziel ist ein lückenloses, nahtloses Modell des Meeresbodens des gesamten Helgoländer Felssockels. Dafür kooperieren wir eng mit dem Bundesamt

für Seeschifffahrt und Hydrographie (BSH), das die tieferen Bereiche mit dem Vermessungsschiff *Wega* abdeckt, sowie mit dem Landesbetrieb für Küstenschutz, Nationalpark und Meeresschutz Schleswig-Holstein (LKN.SH), der topobathymetrische LiDAR-Daten beisteuert (Abb. 1).

Methodik und nautische Herausforderungen im Ultraflachwasser

Für die Vermessung der extrem flachen Bereiche setzen wir unser spezialisiertes Küstenforschungsboot *FB Zostera* ein. Das Boot ist mit einem Norbit iWBMS-Fächerecholot (MBES) sowie dem Applanix-INS Wavemaster II ausgestattet. Die Positionierung und Höhenbestimmung erfolgen mit Zentimetergenauigkeit mittels RTK-Korrekturdaten (dank der Unterstützung durch die AXIO-NET GmbH). Parallel betreiben wir ein parametrisches Sedimentecholot (Innomar smart), welches über eine eigens entwickelte Trigger-Box mit dem MBES synchronisiert im Master-Slave-Betrieb arbeitet, um akustische Interferenzen zu vermeiden.

Die Vermessung verlangt dem Team (Abb. 2) und dem Material alles ab: Die exponierte Lage in der Deutschen Bucht führt zu teils erheblichem Wellengang, der unser kleines, nur 7 Meter langes Flachwasserboot (Abb. 2) mitunter an seine nautischen Grenzen bringt. Aufgrund der komplexen Bathymetrie navigieren wir bei der Datenerfassung mit einer schlanken Echtzeit-Visualisierung (Norbits DCT) auf hellen, großen Monitoren – dies ist für die Sicherheit in den teils unkartierten Gebieten überaus wichtig.

Hinzu kommt eine äußerst komplexe Ozeanografie, welche die Datenqualität maßgeblich beeinflusst: rund um Helgoland treffen drei verschiedene Wasserkörper aufeinander, die mit den Gezeiten stark verlagert werden. In den morphologischen Senken zwischen den aufragenden Felsrücken bilden sich oftmals abgeschlossene, stagnierende Wassermassen mit abweichender Dichte. Dies führt zu erheblichen räumlichen und zeitlichen Schwankungen der Schallgeschwindigkeit in der Wassersäule. Zur Minimierung der daraus resultierenden Refraktionsfehler erfassen wir jede Stunde mehrere Schallgeschwindigkeitsprofile mit einer AML Minos-X-Sonde. Die MBES-Auswertung einschließlich Raytracing-Korrektur, Patch-Test, automatischer und manueller Filterung und Tiefenbeschickung mittels RTK auf das Mean Sea Level (MSL) unter Verwendung des GCG2016-Modells erfolgte in QPS Qimera. Die bereinigten MBES-Daten passen sich gut in die umgebenden LiDAR-Daten des LKN.SH ein (Abb. 3). Um die Backscatter-Signale bestmöglich auswerten zu können, wurden die Daten gemäß den Empfehlungen der Backscattering Working Group (BSWG) mit konstanter Sendeleistung aufgenommen (Lamarche und Lurton 2018).

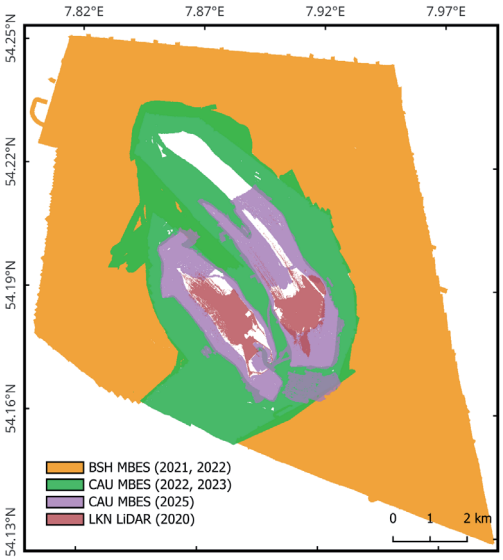

Abb. 1: Übersichtskarte der Datenfusion am Helgoländer Felssockel. Dargestellt ist die räumliche Abdeckung der verschiedenen Vermessungskampagnen. Die nahtlose Karte setzt sich aus hochauflösenden Fächerecholotdaten der CAU Kiel für das Flachwasser, den tieferen Messungen des BSH *(Wega)* sowie den topobathymetrischen LiDAR-Daten des LKN.SH zusammen

Geologische Strukturen in neuer Dimension

Während sich die großräumige Geologie des Helgoländer Felssockels mittels der vom BSH erstellten Rasterauflösung von 10 Metern erahnen lässt, bleibt die feinskalige Morphologie im Meter- und

Abb. 2: Im Einsatz auf Helgoland. Das Team der Arbeitsgruppe Marine Geophysik und Hydroakustik (CAU Kiel) und des AWI Sylt im Hafenbecken. Das wendige und nur 7 Meter lange Forschungsboot *FB Zostera* wurde speziell für die hydroakustische Vermessung von extremen Flachwasserzonen umgebaut und ausgerüstet

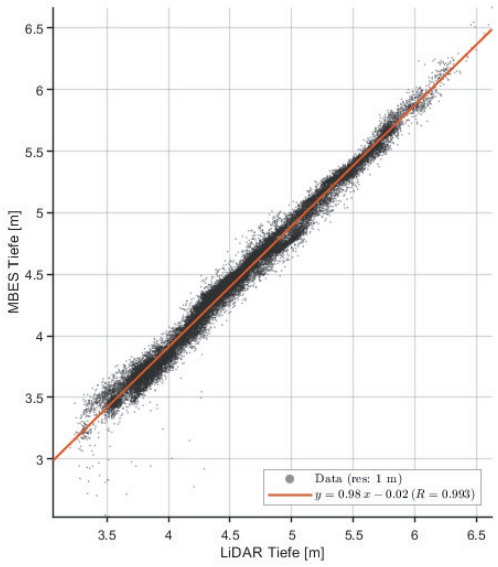

Abb. 3: Datenvalidierung durch Korrelationsplot. Gezeigt ist der direkte statistische Vergleich der im ultraflachen Bereich durch das *FB Zostera* erhobenen bathymetrischen Daten mit den überlappenden LiDAR-Daten. Der Plot demonstriert die exakte Einpassung und die hohe Konsistenz der unterschiedlichen Messverfahren in der Übergangszone, was durch eine hervorragende statistische Korrelation von R = 0,993 bestätigt wird

Dezimeterbereich nur unzureichend abgebildet. Mit unseren neuen Daten können wir Grids mit einer Auflösung von 0,5 × 0,5 Metern generieren, erst hierdurch werden wahre geologische und tektonische Vorgänge sichtbar.

Wie in Abb. 4 zu erkennen ist, lassen sich an den anstehenden Felsformationen tektonische Verwerfungen, geologisches Schichteinfallen und Streichen, oder verschiede Erosionsmuster quantitativ messen. Dies ist ein fundamentaler Schritt für die zukünftige geologische 3D-Rekonstruktion des gesamten Helgoländer Komplexes.

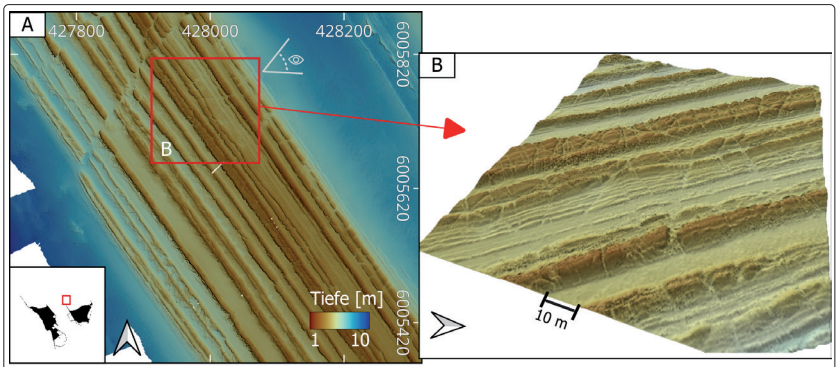

Abb. 4: Bathymetrische Darstellung des geologischen Muschelkalk-Aufschlusses. Das extrem feine Raster macht komplexe Bruchzonen sichtbar. Hier lässt sich das geologische Schichteinfallen und Streichen tatsächlich exakt messen. Dies ist ein fundamentaler Schritt für die zukünftige geologische 3D-Rekonstruktion des gesamten Untergrunds

Vom Tiefenwert zum Prädiktor: Mikrobathymetrie als Basis der Habitatmodellierung

Für viele Hydrographen und Geowissenschaftler stellt das bathymetrische Raster das klassische Endprodukt dar. In der modernen marinen Ökologie ist es jedoch eher der Anfang, und in den letzten 15 Jahren wurde das große Potenzial hydrographischer Messungen für die benthische Lebensraumuntersuchung und Modellierung erkannt (Brown et al. 2011). Fächerecholote setzen sich hier immer mehr durch als das Mittel der Wahl gegenüber herkömmlichen Seitensichtsonaraufnahmen (Misiuk und Brown 2024). Allerdings, wenn das Basis-Grid zu grob ist (wie bei den historischen 10-Meter-Rastern), liefern auch die daraus abgeleiteten morphometrischen Parameter – die sogenannten Prädiktoren – falsifizierte oder unbrauchbare Werte für die Habitatmodellierung.

Mit unseren neuen, ultrahochauflösenden Datensätzen können wir diese essenziellen Prädiktoren nun quantitativ exakt berechnen. Zu den wichtigsten aus der Bathymetrie abgeleiteten Parametern für maschinelle Lernverfahren zählen die Hangneigung (Slope), die Exponierung (Aspect) sowie die Rauigkeit (Terrain Ruggedness Index – TRI). Die Exponierung steuert maßgeblich den Einfluss von Strömungs- und Wellenenergie. Wo exakt die verschiedenen benthischen Lebensformen bevorzugt siedeln, ist Gegenstand aktueller Untersuchungen, und wir erachten die Ergebnisse als überaus zielfördernd für eine verbesserte Modellierung der benthischen Arten (Schubert et al. 2016). Die Rauigkeit (TRI) quantifiziert die lokale topografische Heterogenität und ist bei Helgoland ein exzellenter Indikator für freiliegendes Felsgestein (Jensen 2024). Gleichzeitig liefert sie entscheidende Hinweise auf Mikronischen, auf die beispielsweise juvenile Hummer angewiesen sind, und kann hiermit hilfreich sein für optimierte Wiederansiedlungsmaßnahmen für den Hummer. Ergänzt wird dies durch den Benthischen Lageindex (BPI), der Kuppen und Senken identifiziert. Neben der akustischen Rückstreustärke gehören gerade diese bathymetrischen Ableitungen zu den stärksten Prädiktoren überhaupt, um benthische Habitate verlässlich vorherzusagen.

Snippet Backscatter: Ein neuer Blick auf den Meeresboden

Für eine detaillierte geologische und biologische Habitatkartierung ist das Rückstreusignal (Backscatter) von unschätzbarem Wert, da wir auf eine Differenzierung von Hartsubstrat und Weichsediment angewiesen sind. Hierzu wurden die Daten in QPS FMGT radiometrisch und geometrisch korrigiert; eine sogenannte Beam-Pattern-Korrektur und Harmonisierung des Backscatter zwischen dem vom BSH aufgezeichneten

(Kongsberg) und den unsrigen (Norbit) Backscatter-Werten steht noch aus. Im Gegensatz zur reinen bathymetrischen Aufnahme mit einem Wert des Bodenfinders pro Beam, liefert die Snippet-Technologie eine Zeitreihe des Echos für jeden einzelnen Beam, wodurch sich side-scan-ähnliche Mosaike mit einer räumlichen Auflösung von nur 0,1 × 0,1 Metern erzeugen lassen (Abb. 5).

Für eine physikalisch korrekte Klassifizierung muss der Backscatter vor Helgoland zwingend hinsichtlich des wahren Einfallswinkels unter Einbezug des detailreichen digitalen Geländemodells (DEM) korrigiert werden. Andernfalls wird die Rückstreustärke fälschlicherweise durch die Hangneigung und nicht durch die substratspezifischen Eigenschaften dominiert.

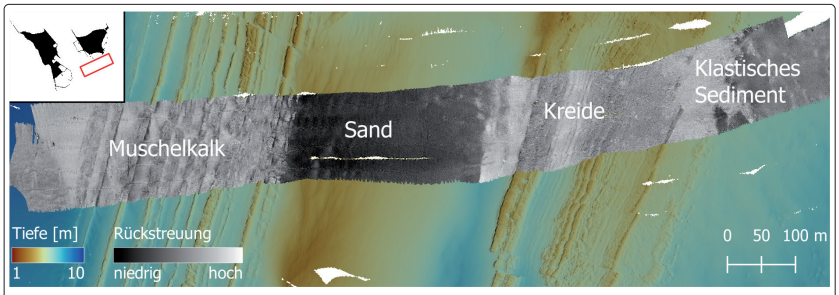

Abb. 5: Hochauflösender MBES-Snippet-Backscatter (0,1 × 0,1 Meter), aufliegend auf der Bathymetrie südlich der Helgoländer Düne. Anhand der Rückstreustärke lassen sich die unterschiedlichen geologischen Formationen (Muschelkalk, Kreide, Sedimente), die Späth (1990) nach intensiven Taucharbeiten und nach Luftbildauswertung identifizierte, rein akustisch klar erkennen und zentimetergenau auskartieren. Erwähnenswert ist hierbei, dass das massive Festgestein oft eine geringere Rückstreuung zeigt im Vergleich zum umliegenden klastischen Sediment, welches im Verhältnis zur akustischen Wellenlänge bei 400 kHz eine höhere Mikrorauigkeit aufweist

Die Herausforderung: Optische Limits, Kelpwälder und direkter Nachweis

Helgoland ist berühmt für seine dichten Unterwasserwälder aus Großalgen (Kelp), insbesondere dem Palmentang *(Laminaria hyperborea)*. Was ökologisch von hohem Wert ist, erschwert die hydrographische Vermessung ungemein. Besonders deutlich wird dies bei dem Versuch, das Flachwasser mittels flugzeuggestützter optischer Methoden zu erfassen. Die Auswertung der topobathymetrischen LiDAR-Daten (Riegl VQ 820) des LKN.SH offenbarte eine maximale Eindringtiefe von wenigen Metern unter dem mittleren Meeresspiegel. Während über hellen, sandigen Sedimenten (vereinzelt bis zu maximal 6 Metern) noch optische Bodenechos registriert wurden, versagte das System über den bewachsenen Felsriffen nahezu vollständig. Da Großalgen in dichten, mehrstöckigen »Wäldern« wachsen, ist die kumulative Lichtabsorption entsprechend groß; inwieweit eine Full-Waveform-Analyse Abhilfe schaffen kann, soll zukünftig untersucht werden. Insgesamt wachsen vor Helgoland über 250 verschiedene Algenarten, optische Verfahren stoßen vor Helgoland hierdurch an physikalische Grenzen, weshalb wir das Gebiet mühsam akustisch mit der *Zostera* abfahren und vermessen mussten.

Das dichte Blätterdach des Palmentangs *(Laminaria hyperborea)* in der Wassersäule erzeugt auch bei Fächerecholotaufnahmen erhebliche akustische Störsignale, was die hydrographische Bestimmung des wahren Meeresbodens in hohem Maße erschwert: das resultierende Problem ist, dass der Bodenfindungsalgorithmus des Fächerecholots oft fälschlicherweise Missdetektionen an der Oberkante des Kelpwaldes durchführt, was eine manuelle Bereinigung der Echos erfordert (Abb. 6).

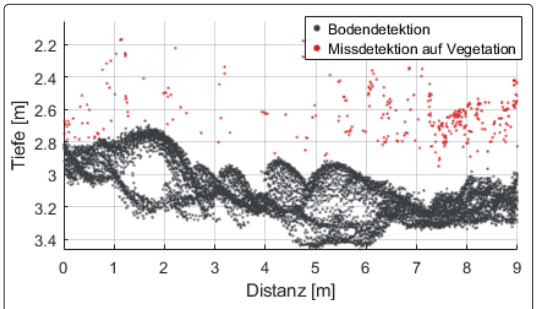

Abb. 6: Detektionen des Bodenfindungsalgorithmus des Fächerecholots (MBES) in Wassertiefen <4 Metern, aggregiert über 30 Pings. In vegetationsbedeckten Bereichen kommt es systematisch zu Fehlidentifikationen des Vegetationsdachs als Meeresboden

Diese Problematik lässt sich jedoch durch die Einbindung unserer synchronisierten Innomar-Messungen wirkungsvoll adressieren. Das parametrische Sub-Bottom-Profiler-System emittiert hochfrequente Primärsignale (100 kHz), aus denen im Wasserkörper eine niederfrequente Differenzfrequenz (10 kHz) mit sehr schmalem Abstrahlwinkel erzeugt wird. Der resultierende Schallstrahl durchdringt das Blätterdach: im Echogramm zeichnet sich der wahre, harte Meeresboden als klarer Reflektor deutlich unterhalb der diffusen Vegetationsschicht ab (Abb. 7). Auf diese Weise wird nicht nur die zuverlässige Bodendetektion im dicht bewachsenen Flachwasser gewährleistet, aus der Differenz zwischen Boden und Oberkante der Vegetation lässt sich zudem die Bewuchshöhe der Pflanzen präzise bestimmen. Der direkte Nachweis dieser Volumenstrukturen in der Wassersäule mit Unterwasserkameraaufnahmen des Kelp durch das Landesamt für Landwirtschaft, Umwelt und ländliche Räume (LLUR) und der Tauchfirma Submaris dient fortan als hervorragende, flächendeckende Ground-Truthing-Grundlage für unsere Vorhersagemodelle im Rahmen des ANK-Projekts LABLUC, um die gesamte Biomasse und das CO_2-Einlagerungspotenzial bewerten zu können.

Darüber hinaus deuten unsere akustischen Untersuchungen darauf hin, dass sich bisher kartierte Großalgenarten wie *Laminaria hyperborea, Saccharina latissima* und *Desmarestia aculeata* künftig

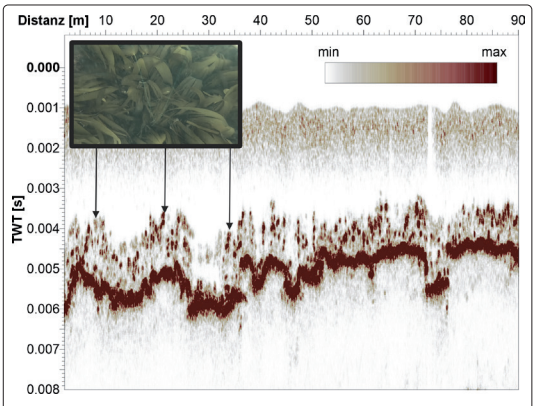

Abb. 7: Echogramm der hochfrequenten Komponente des Innomar-Systems (Darstellung des Amplitudenbetrags). Der harte Buntsandstein tritt als klar definierter, kontinuierlicher Reflektor deutlich unterhalb der diffusen Vegetationsschicht hervor. Die eindeutige Trennung beider Signalanteile ermöglicht eine zuverlässige Bodendetektion im dicht bewachsenen Flachwasser sowie die präzise Bestimmung der Bewuchshöhe aus der Differenz zwischen Bodenreflektor und Vegetationsoberkante

möglicherweise rein akustisch voneinander differenzieren lassen. Um dieses enorme Potenzial für die Habitatkartierung zu erschließen, wird zukünftig im Rahmen einer Doktorarbeit eine detaillierte Full-Waveform-Analyse der akustischen Rückstreudaten durchgeführt. Hierbei werden charakteristische Parameter der Echo-Einhüllenden und der gesamten Wellenform untersucht, um verlässliche, artspezifische akustische Signaturen abzuleiten.

Schnittstelle zur Unterwasserarchäologie: Zufallsfunde im Sonar

Die hohe räumliche Auflösung unserer Kartierungen schlägt eine direkte Brücke zum Schwerpunktthema dieser HN-Ausgabe: der Unterwasserarchäologie. Wenn der Meeresboden mit Auflösungen im Dezimeterbereich vermessen wird, treten unweigerlich Strukturen zutage, die nicht-geologischen Ursprungs sind. Im Rahmen unserer Arbeiten kooperieren wir eng mit der Forschungstaucher-Firma Submaris. Das Team von Submaris betaucht Helgoland seit über zehn Jahren, primär im Kontext des optischen Monitorings der Algenwälder. Dabei gelangen bereits spektakuläre Funde, darunter historische englische Kanonen (Abb. 8) sowie die Bergung einer U-Boot-Netzsäge aus dem Ersten Weltkrieg (Huber 2020).

Diese Funde zeigen das enorme Potenzial moderner Hydrographie für den Denkmalschutz auf. Solche archäologischen Verdachtsstellen und die Methodik zu ihrer Detektion in komplexen geologischen Umgebungen sind mittlerweile Gegenstand aktueller Forschungen, unter anderem im Rahmen des laufenden SEASCAPE-Projekts.

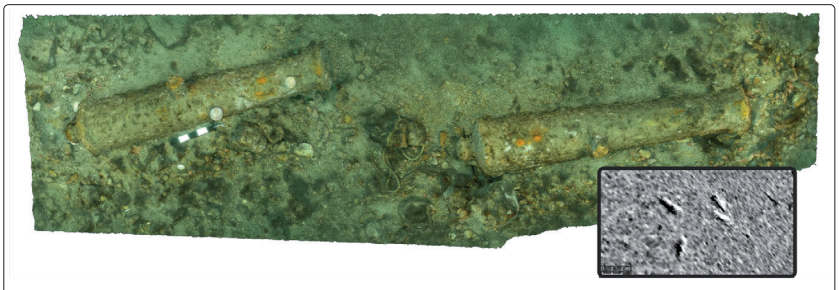

Dr. Florian Huber (Submaris)

Abb. 8: Photogrammetrische Aufnahme einer englischen Kanone am Meeresboden. Der Referenzstab misst 0,5 Meter Länge. Die visuelle Dokumentation solcher Funde erfolgte durch die Forschungstaucher. Mit Hilfe unserer neuen hochauflösenden MBES-Snippet-Backscatter- und Bathymetriedaten (Inlet) konnten solche morphologischen Anomalien identifiziert werden, was bei gezielten Tauchgängen zur Entdeckung von sechs weiteren, bisher völlig unbekannten Kanonen führte.

Fazit

Die Bündelung moderner hochauflösender hydroakustischer Technologie auf kleinen, flexibel einsetzbaren Plattformen wie dem *FB Zostera,* ergänzt durch Datensätze staatlicher Institutionen (BSH, LKN.SH, LLUR), ermöglicht es uns heute, das bislang nur fragmentarisch erfasste »Weiße Band« der Küste hochauflösend zu schließen – nicht nur aus hydrographischer, sondern auch aus der geoökologischen Perspektive. Die daraus abgeleiteten Datenprodukte (von präziser Bathymetrie, über Wassersäulenanalysen bis hin zu Snippet-Backscatter und Meeresbodenklassifikation) sind nicht nur der Schlüssel für ein modernes geologisches Verständnis und den Schutz mariner Ökosysteme, sondern eröffnen uns auch völlig neue Einblicke in unser maritimes kulturelles Erbe. //

Literatur

Brown, Craig J.; Stephen J. Smith; Peter Lawton; John T. Anderson (2011): Benthic Habitat Mapping: A Review of Progress Towards Improved Understanding of the Spatial Ecology of the Seafloor Using Acoustic Techniques. Estuarine, Coastal and Shelf Science, DOI:m10.1016/j.ecss.2011.02.007

Huber, Florian (2020): UC 71 – Archäologie und Geschichte eines deutschen U-Boots, Historische Archäologie, Sonderband 2020, S. 161–178

Jensen, Merve (2024): Acoustic multibeam and topo bathymetric LiDAR analyses of Germany's complex underwater landscape around Heligoland (North Sea). Master thesis, CAU

Lamarche, Geoffroy; Xavier Lurton (2018): Recommendations for improved and coherent acquisition and processing of backscatter data from seafloor-mapping sonars. Marine Geophysical Research, DOI: 10.1007/s11001-017-9315-6

Misiuk, Ben; Craig Brown (2024): Benthic habitat mapping: A review of three decades of mapping biological patterns on the seafloor. Estuarine, Coastal and Shelf Science, DOI: 10.1016/j.ecss.2023.108599

Schubert, Philipp; Jens Wein; Inka Bartsch (2016): Kartierung und Modellierung der Braunalgenbestände um Helgoland im Sommer 2015. Endbericht SUBMARIS (im Auftrag des LLUR

Späth, Christian (1990): Zur Geologie der Insel Helgoland. Die Küste, Nr. 49, S. 1–32

KI-generiertes Bild

38. Hydrographentag
DVW-Seminar

»Hydrographie im Kontext der Nachhaltigkeit«

23. bis 25. Juni 2026
in Lübeck-Travemünde

Anmeldung unter:

www.dhyg.de/index.php/de/hydrographentag/registrierung

Frühbucherrabatt bis 30. April

DOI: 10.23784/HN133-07

»Ohne hydrographische Vermessungsmethoden wären wir in der Archäologie aufgeschmissen«

Ein Wissenschaftsgespräch mit JENS AUER

Dr. Jens Auer ist Landesarchäologe beim Landesamt für Kultur und Denkmalpflege in Mecklenburg-Vorpommern. Im HN-Interview berichtet er, was sich an archäologisch Wertvollem unter der Wasseroberfläche der Ostsee verbirgt, zum Beispiel Wracks, versunkene Siedlungen und Raketenreste. Er weist darauf hin, dass Archäologen keine Schätze suchen, sondern Zusammenhänge. Die Funde aus der Geschichte können uns mehr lehren, als wir gemeinhin glauben, weswegen es so wichtig ist, sie zu erhalten.

Unterwasserarchäologie | Fundstellen | Wracks | steinzeitliche Siedlungsreste
underwater archaeology | archaeological sites | wrecks | Stone Age settlement remains

Dr. Jens Auer is the state archaeologist at the State Office for Culture and Monument Preservation in Mecklenburg-West Pomerania. In this interview, he talks about the archaeological treasures hidden beneath the surface of the Baltic Sea, such as shipwrecks, sunken settlements and rocket debris. He points out that archaeologists are not looking for treasures, but for connections. Historical finds can teach us more than we generally believe, which is why it is so important to preserve them.

Interviewer
Lars Schiller und Dr. Jens Schneider von Deimling führten das Interview mit Dr. Jens Auer per E-Mail im Februar.

j.auer@lakd-mv.de

Sie kümmern sich um das archäologische Kulturerbe. Das heißt, Sie erfassen ein Bodendenkmal, Sie pflegen es, Sie bergen es zum Teil auch und Sie erhalten es. Was ist eigentlich die in der Archäologie gebräuchliche Pluralform – Bodendenkmäler oder Bodendenkmale?

Wir sagen normalerweise Bodendenkmale – aber an sich sind beide Formen gebräuchlich.

Bodendenkmale können auch unter Wasser liegen. Was darf man sich alles unter Unterwasserdenkmalen vorstellen? Wracks, klar, aber was noch?

Ja, die meisten Menschen denken vor allem an Schiffswracks. Das Spektrum an Fundstellen ist aber deutlich breiter. Wenn wir chronologisch vorgehen, dann müssen wir eigentlich in der Steinzeit beginnen. Bis vor circa 10 000 Jahren waren große Teile der heutigen Ostsee noch nicht überflutet. In diesen Bereichen haben Menschen gelebt und gejagt – und natürlich auch Spuren hinterlassen. Diese finden wir in den gesamten Küstenbereichen. Ein spektakuläres Beispiel ist der 2022 in über 20 Meter Tiefe entdeckte Blinkerwall, der wahrscheinlich von frühen Rentierjägern errichtet wurde.

Dann haben wir natürlich auch die Überreste von Wasserbauten und Hafenanlagen, Einzelfunde wie zum Beispiel Anker oder Teile von Schiffsladungen, und schließlich auch Flugzeugwracks und gerade in Mecklenburg-Vorpommern vor Peenemünde auch Teile von Raketen und Lenkwaffen, die dort während des Zweiten Weltkriegs erprobt wurden und in die Ostsee gestürzt sind.

Wie viele Bodendenkmale gibt es in der Nordsee und in der Ostsee?

Das ist eine schwierige Frage – denn wir kennen lediglich einen Bruchteil der wirklich vorhandenen Fundstellen. In Mecklenburg-Vorpommern sind uns inzwischen über 4000 Unterwasserfundstellen bekannt, aber es kommen ständig neue Fundmeldungen dazu. Gerade durch die intensiven geophysikalischen Untersuchungen im Vorlauf zu Offshore-Baumaßnahmen werden viele neue archäologische Fundstellen entdeckt.

Was liegt an archäologisch Wertvollem im Meer?

Eigentlich genau das, was ich gerade genannt habe. Archäologen suchen ja keine Schätze im klassischen Sinn, sondern sie versuchen, das Leben in der Vergangenheit zu entschlüsseln.

Auch auf den ersten Blick unbedeutende Wracks oder Funde können einen hohen archäologischen Wert haben, wenn sie uns zum Beispiel Einblicke in Schiffbau, Handelsbeziehungen oder aber auch das Leben von Seefahrern geben.

Was finden Sie in Binnengewässern?

Das Fundspektrum in Binnengewässern ist sogar fast noch breiter als das im Meer. Flüsse und Seen waren nicht nur Transportwege, sondern konnten auch Kultorte sein. So finden wir in Binnengewässern neben Brücken, Siedlungsresten und Wasserfahrzeugen manchmal auch Opfergaben aus ver-

schiedenen Zeiten. In Mecklenburg-Vorpommern werden jedes Jahr unzählige archäologische Funde aus den Flüssen und Seen geborgen.

Wie funktioniert die Prospektion und die Dokumentation unter Wasser?

Im Prinzip ganz ähnlich wie an Land. Bei der Prospektion kommen allerdings meist geophysikalische Methoden zum Einsatz, um effektiv große Wasserbereiche absuchen zu können. Gefundene Anomalien werden dann durch Taucher oder ROVs untersucht. Bei der Dokumentation zeichnet man heutzutage nicht mehr unter Wasser wie früher, sondern nutzt, wo immer möglich, die Photogrammetrie, das heißt man erstellt dreidimensionale Modelle aus Bilddaten. Bei sehr schlechter Sicht kann es allerdings auch sein, dass man auf traditionelle Vermessungsmethoden mit Maßband und Zollstock zurückgreifen muss!

An Land hat die LiDAR-Vermessung in den letzten Jahren zu bahnbrechenden archäologischen Entdeckungen geführt. Sehen Sie unter Wasser ähnlich potente technologische Fortschritte in der Prospektion?

Ich sehe, gerade für die häufig archäologisch relevanten Flachwasserbereiche, enormes Potenzial in der LiDAR-Vermessung. Hier ist ein Einsatz der traditionellen geophysikalischen Methoden oft schwierig und ein flächendeckender Einsatz von Grünlicht-Laser würde uns sicher sehr wertvolle Informationen liefern – an den Küsten und sicher auch in Binnengewässern.

Wie oft müssen Trassen im Meer anders verlegt werden, weil bei der Prospektion ein Bodendenkmal gefunden wurde? Wie lange dauert ein Verfahren zur Überprüfung?

Das passiert wirklich relativ häufig, vor allem aber in Küstennähe, wo die Anzahl an archäologischen Fundstellen relativ hoch ist und der Spielraum nur gering. Wir versuchen allerdings, immer so früh wie möglich an der Planung beteiligt zu werden, um frühzeitig den Umgang mit bekannten Bodendenkmalen zu besprechen und bisher unbekannte Bodendenkmale im Wirkbereich des geplanten Vorhabens aufzufinden. Ganz wichtig ist dabei unter anderem die archäologische Auswertung der im Projekt erhobenen geophysikalischen Daten – und bei Eingriffen in den Boden auch die archäologische Baubegleitung. In einem guten Abstimmungsprozess gibt es keine langen Wartezeiten, vor allem dann nicht, wenn die archäologischen Arbeiten direkt in die Bauvorbereitung integriert werden. Wir haben einen Leitfaden erstellt, um gerade diesen Prozess noch einmal zu erläutern (www.kulturwerte-mv.de/static/LAKD/LA/Dateien/Leitfaden_Unterwasserkulturerbe.pdf).

Wann ist Tauchen denkmalgerecht?

Tauchen ist dann denkmalgerecht, wenn man, wie es immer so schön heißt, nichts als Blasen hinterlässt. Man kann sich jedes Wrack gerne anschauen,

Dr. Jens Auer

sollte aber nichts anfassen, bewegen oder gar mitnehmen! Bei archäologischen Fundstellen ist der Kontext oder Fundzusammenhang ungeheuer wichtig, um den Fund zu verstehen. Sobald man den verändert, verändert man auch das Verständnis und die Interpretation der Fundstelle.

Was ist Schiffsarchäologie?

In der Schiffsarchäologie beschäftigen wir uns spezifisch mit Schiffswracks. Häufig steht dabei die Konstruktion der Wracks im Vordergrund. Diese ist besonders spannend, wenn man bedenkt, dass Schiffe ja lange Zeit die fortschrittlichsten Verkehrsmittel waren. Schiffbau spiegelt daher das technische Know-how einer Gesellschaft wider.

»Eine aktive archäologische Erfassung zu Wasser gibt es bisher nicht«

Dr. Jens Auer

Wenn ein Hydrograph in seinen Daten ein Wrack entdeckt, was muss er dann tun?

Dann sollte der Hydrograph das Wrack immer den zuständigen Denkmalfachbehörden melden. In Mecklenburg-Vorpommern ist das das Landesamt für Kultur und Denkmalpflege (www.kulturwerte-mv.de/Landesarchaeologie). In den Denkmalschutzgesetzen der Bundesländer ist diese Meldepflicht auch festgeschrieben.

Gibt es eine Karte, in der alle Wracks verzeichnet sind? Oder sind die Koordinaten geheim? Wie oft werden die Liegeplätze kontrolliert?

Ja, die gibt es. Eine der wichtigsten Aufgaben unserer Behörde ist die Inventarisierung von Bodendenkmalen. Wir überprüfen, ob es sich bei Funden um Bodendenkmale nach unserem Denkmalschutzgesetz handelt, und kartieren diese dann in unserem hauseigenen Geografischen Informationssystem. Unser Verzeichnis ist allerdings nicht öffentlich, da viele sensitive Daten enthalten sind. Die Kontrolle von Fundplätzen ist eine enorme Aufgabe. Dabei bekommen wir zum Beispiel Hilfe von ehrenamtlichen Bodendenkmalpflegern. Eine ungeheuer wichtige Informationsquelle sind für uns auch die vom Bundesamt für Seeschifffahrt und Hydrographie erhobenen Daten.

Wer entscheidet, ob ein Wrack erhaltenswert ist? Wann wird es geborgen? Was spricht dagegen?

Das entscheidet eigentlich das Denkmalschutzgesetz. Nur wenn ein Wrack auch die dort genannten Kriterien erfüllt, wird es zum Bodendenkmal – und ist damit aus archäologischen Gründen erhaltenswert. Wir versuchen immer, so viele Informationen zu einem Wrack zu sammeln wie möglich, um fundierte Entscheidungen treffen zu können. Generell gilt bei Bodendenkmalen dann immer das Prinzip der Erhaltung in situ. Wir versuchen, die Fundstelle in ihrem ursprünglichen Zustand an Ort und Stelle zu erhalten. Denn jeder Eingriff bedeutet gleichzeitig eine Zerstörung des Fundzusammenhangs. Geborgen wird ein Wrack nur, wenn sich dies absolut nicht vermeiden lässt. Da der Fundzusammenhang nach der Grabung unwiederbringlich verloren ist, ist eine sorgfältige Dokumentation der Fundstelle und der geborgenen Funde von äußerster Wichtigkeit. Auch der Verbleib des geborgenen Materials muss klar geregelt sein, denn die Konservierung von Nasshölzern und anderen Funden aus dem Meer ist zeitaufwendig und mit hohen Kosten verbunden.

Wird nach dem Entdecken einer magnetischen Anomalie gezielt nach einem Wrack gesucht?

Nein. Allerdings werden Munitionsbergungen durch Taucher oder ROVs immer von Archäologen begleitet. Hier wird ja gezielt nach magnetischen Anomalien von bestimmter Größe gesucht, und in vielen Fällen werden dabei auch archäologische Hinterlassenschaften, nicht selten auch Schiffswracks, entdeckt.

Werden noch alte Akten ausgewertet, um anhand eines konkreten Verdachts auf Wracksuche zu gehen?

Das passiert ganz selten – und wenn, dann meistens in einem Forschungszusammenhang. Wir arbeiten in 99 Prozent aller Fälle genau anders herum und versuchen eher, ein gefundenes Wrack anhand von Archivmaterialien zu identifizieren.

Das BSH sucht nach Unterwasserhindernissen. Wie oft entpuppt sich ein lästiges Unterwasserhindernis als wertvolles Bodendenkmal?

Das ist ehrlich gesagt recht häufig der Fall! Glücklicherweise funktioniert der Informationsaustausch mit dem BSH hervorragend, sodass wir immer schnell über Neufunde informiert werden.

Auch Hobbyarchäologen machen sich auf die Suche, meist illegal. Warum ist Magnetangeln gefährlich?

Magnetangeln ist nicht nur gefährlich, sondern bei uns im Bundesland auch genehmigungspflichtig. Allerdings macht das hohe Aufkommen von Kriegsmunition in unseren Gewässern Magnetangeln zu einem wahrlich riskanten Hobby. Wer wirklich Interesse an der Archäologie hat, sollte stattdessen erwägen, sich als ehrenamtlicher Bodendenkmalpfleger zu betätigen.

Was verstehen Sie unter einem Unterwasserkulturerbe?

In unserem Bundesland ist die Definition von Bodendenkmalen bzw. Kulturerbe – darunter natürlich auch das Unterwasserkulturerbe – im Denkmalschutzgesetz festgeschrieben. Im Unterschied zur Definition in der UNESCO-Konvention zum Schutz des Unterwasserkulturerbes von 2001 kennen wir allerdings keine Zeitbeschränkung. Bei uns müssen Spuren menschlicher Existenz am Seegrund nicht mindestens 100 Jahre unter Wasser liegen, um Kulturerbe zu werden, sondern wir können auch jüngere Fundstellen, zum Beispiel

aus dem Zweiten Weltkrieg, als Bodendenkmale schützen.

Wo gibt es steinzeitliche Siedlungsplätze in Gewässern? Was wurde da entdeckt? Und wie wurden sie entdeckt, etwa mit den Methoden der Hydrographie?

Steinzeitliche Siedlungsplätze gibt es überall entlang unserer Küsten. Den Blinkerwall hatte ich ja schon erwähnt. Zur Auffindung ist es vor allem wichtig, die Landschaft und ihre Veränderung zu verstehen. Jäger und Sammler waren dort aktiv, wo genügend Nahrung als Lebensgrundlage vorhanden war. Wenn man die steinzeitliche Landschaft rekonstruieren kann, ist es auch möglich, gezielt nach genau solchen Orten zu suchen. Dabei helfen sowohl geophysikalische Methoden und Geräte wie Sub-Bottom-Profiler als auch geotechnische Untersuchungen zum Beispiel von Bohrkernen, mit denen einzelne geologische Schichten charakterisiert und datiert werden können. Aber auch Side-Scan-Sonare können eingesetzt werden, um zum Beispiel Torfkanten in Küstennähe zu finden, in deren Umgebung Teile urzeitlicher Landschaften erhalten sind.

Hydrographen verwenden verschiedene Sensoren – Fächerecholot, Sedimentecholot, Seitensichtsonar, Magnetometer. Wahrscheinlich wollen Sie immer möglichst alle Daten in Kombination haben, oder?

Das liefert auf jeden Fall immer die besten Ergebnisse, da man so ein möglichst vollständiges Bild des Untersuchungsgebiets bekommt und zusätzlich bereits erste Aussagen zum Charakter von Anomalien treffen kann. Man weiß dann gleich, ob eine in den Side-Scan-Daten sichtbare Anomalie magnetisch ist oder nicht.

Für die Überwachung von Bodendenkmalen werden vor allem flächendeckende Fächerecholotaufnahmen verwendet. Wer führt diese Messungen durch? Wer beauftragt sie?

Leider fehlen uns die Möglichkeiten, solche Aufnahmen zu beauftragen oder selbst zu sammeln. Wir nutzen daher ausschließlich Daten anderer Behörden, wie zum Beispiel dem BSH, oder aber

Daten, die im Verlauf von Bauprojekten gewonnen werden. Eine aktive archäologische Erfassung zu Wasser gibt es bisher nicht.

Nutzen Sie auch Laserscanningaufnahmen unter Wasser?

Nein, bisher nicht. Das ist aber sicher auch ein spannendes Thema für die Zukunft.

»Hydrographische Daten sind die Arbeitsgrundlage jedes Unterwasserarchäologen«

Dr. Jens Auer

Welche Methoden spielen bei der Positionierung unter Wasser eine Rolle?

Hier nutzen wir nach Möglichkeit RTK-GPS. Im Flachwasser am Vermessungsstab oder, wenn es tiefer wird, auch an Bojen, die vom Taucher geschleppt werden. In der Ostsee werden häufig akustische Positionierungssysteme (USBL) genutzt, um Funde einzumessen.

Gibt es genau spezifizierte Anforderungen an die Vermessung?

Das hängt ein bisschen vom Verwendungszweck ab. Generell gilt: je genauer, desto besser. Wir haben die Grundanforderungen an geophysikalische Vermessung und archäologische Dokumentation in verschiedenen Richtlinien festgeschrieben. In den meisten Fällen sind die für die Baugrunderkundung erhobenen geophysikalischen Daten auch gut für die archäologische Auswertung geeignet, zumindest wenn es um Wracks oder Wrackteile geht. Für die Auffindung oder Eingrenzung von steinzeitlichen Siedlungsplätzen sind aber deutlich detailliertere Informationen notwendig.

Braucht die Archäologie die Hydrographie?

Absolut! Ohne hydrographische Vermessungsmethoden wären wir aufgeschmissen. Hydrographische Daten sind die Arbeitsgrundlage jedes Unterwasserarchäologen!

Was würden Sie gerne besser können?

Wir nutzen inzwischen fast ausschließlich 3D-Modelle zur archäologischen Dokumentation. Was ich allerdings wirklich spannend finde – und gerne besser können würde –, ist die Nutzung dieser Modelle zur publikumswirksamen Vermittlung. Ich denke, hier gibt es enormes Potenzial, was allerdings ganz andere Kenntnisse in 3D-Modellierung voraussetzt.

Was wissen Sie, ohne es beweisen zu können?

Dass Menschen leider niemals aus ihrer eigenen Geschichte lernen. //

DOI: 10.23784/HN133-08

Analysis of seafloor sediment distribution in the Port of Hamburg using backscatter data from dual-head multibeam systems for the optimisation of a sedimentological model

An article by MUHAMMAD FAIZAN KAYANI

This article presents the analysis and classification of seafloor surface sediments in the Port of Hamburg using normalised backscatter data from dual-head multibeam echo sounder systems to optimise the existing sedimentological model of the Hamburg Port Authority (HPA). Seven locations within the port were selected for detailed backscatter analysis. Ground-truth sediment samples and corresponding median grain size (D50) values were used to develop a machine learning-based sediment classification. A Random Forest regressor was trained on backscatter intensity data and D50 values to predict continuous grain size distributions at the pixel level of backscatter mosaics. Re-substitution and K-fold cross-validation results demonstrate that combining mean backscatter intensities from 200 kHz and 400 kHz significantly improves predictive performance compared to single-frequency inputs. Comparison with the existing HPA sedimentological model shows that the machine learning approach more accurately captures spatial variations in seafloor sediment grain size, particularly in coarse and mixed sediment environments, and provides closer agreement with ground-truth data, whereas the current HPA model tends to oversimplify local sediment dynamics.

multibeam backscatter | sediment classification | machine learning | Port of Hamburg
Fächerecholot-Rückstreuung | Sedimentklassifizierung | maschinelles Lernen | Hafen Hamburg

Dieser Artikel präsentiert die Analyse und Klassifizierung von Sedimenten auf dem Gewässerboden im Hamburger Hafen unter Verwendung normalisierter Rückstreudaten von Dual-Head-Fächerecholotsystemen zur Optimierung des bestehenden sedimentologischen Modells der Hamburg Port Authority (HPA). Sieben Bereiche innerhalb des Hafens wurden für eine detaillierte Rückstreuanalyse ausgewählt. Anhand von Sedimentproben und den entsprechenden mittleren Korngrößenwerten (D50) wurde eine auf maschinellem Lernen basierende Sedimentklassifizierung entwickelt. Ein Random-Forest-Regressor wurde anhand von Rückstreuintensitätsdaten und D50-Werten trainiert, um kontinuierliche Korngrößenverteilungen auf Pixelebene von Rückstreumosaiken vorherzusagen. Die Ergebnisse der Resubstitution und der K-fachen Kreuzvalidierung zeigen, dass die Kombination der mittleren Rückstreuintensitäten von 200 kHz und 400 kHz die Vorhersageleistung im Vergleich zu Einfrequenz-Daten deutlich verbessert. Ein Vergleich mit dem bestehenden sedimentologischen HPA-Modell zeigt, dass der maschinelle Lernansatz räumliche Schwankungen der Korngröße von Bodensedimenten, insbesondere in groben und gemischten Sedimentumgebungen, genauer erfasst und eine bessere Übereinstimmung mit den Bodenproben liefert, während das aktuelle HPA-Modell dazu neigt, die lokale Sedimentdynamik zu stark zu vereinfachen.

Author
Muhammad Faizan Kayani
studied Hydrography at HCU.

mfaizankayanios@gmail.com

Background

The Port of Hamburg, which is situated on the River Elbe, is a very significant part of the German economy, and it is the destination of hundreds of ships every year. The port area of Hamburg receives large marine traffic, ranging from small ships to large container ships. It is essential to ensure navigation safety. To ensure this, it is essential to understand the sedimentation behaviour of this area.

Sedimentation in the Port of Hamburg shows a clear dependence on river discharge conditions. During periods of low discharge, tidal processes predominate, leading to increased sediment transport from the North Sea towards the port. In contrast, during periods of high discharge, sediment input is primarily controlled by river transport and enhanced upstream erosion within the catchment area (Ohle et al. 2024).

Nowadays, MBES backscatter is widely used to classify seafloor surface sediments better, define marine habitats and support the development of efficient maritime spatial planning. More recent advancements in technology have enabled the acquisition and analysis of backscatter at different sonar operating frequencies (Menandro et al. 2025).

The Hamburg Port Authority (HPA) currently uses the Stratigraphic Morphodynamic Modeling System (SMMS) as its main sedimentological model to describe the spatial distribution of seafloor surface sediments within the port area. This model provides a continuous overview of sediment accumulation over time (Sievers 2021). To test the accuracy of this sedimentology model, advanced backscatter results needed to be compared with this model to improve its accuracy and provide a better classification approach by reducing the need for large sediment sampling campaigns.

Area overview: Port of Hamburg

The Port of Hamburg is located in the tidal-influenced bifurcation zone of the lower River Elbe in northern Germany. The port area is affected by both the river flow and the tidal influence from the North Sea, which together determine the movement, deposition and erosion of sediments (Ohle et al. 2024).

Seven key areas were selected based on their sediment behaviour, hydrodynamic conditions (ebb and flood currents), vessel traffic intensity and the presence of major container terminals. In addition, these areas were chosen because the sedimentological model shows anomalous behaviour in these regions, which requires further investigation within the scope of this research. The selected research areas are: Köhlbrand, Strandhafen, Köhlfleet, Waltershofer Hafen, Vorhafen, Norderelbe 7 and Reiherstieg.

Survey planning and data acquisition

Surveys were planned for all seven mentioned areas. Fig. 1 shows an overview of the boundary polygons of the selected areas over the Port of Hamburg. Surveys for each area were planned to ensure complete coverage and sufficient overlap between the survey lines. The number of track lines varied across areas due to differences in spatial extent.

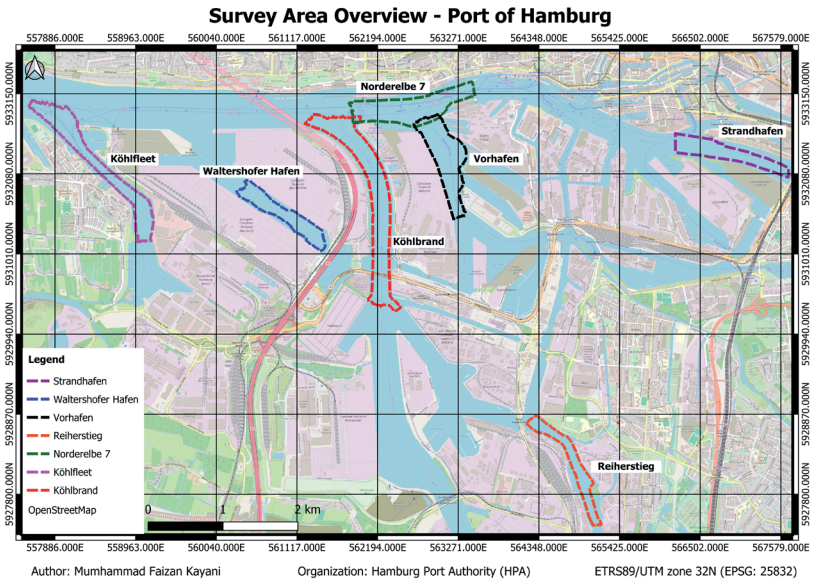

Fig. 1: Survey area overview of all the selected regions in the Port of Hamburg

A total of 14 datasets were acquired using the *Deepenschriewer 1* vessel equipped with a Teledyne Reson SeaBat T20-R dual-head multibeam echo sounder. Frequency-modulated (FM) waveforms were recorded at 200 kHz and 400 kHz, with survey lines designed for 100 % overlap and run in opposite, parallel directions using a 70° swath angle. The automated tracker was enabled throughout to ensure stable and continuous data acquisition. Additionally, one dataset was acquired using multispectral functionality at 200, 300 and 400 kHz. Bathymetric and normalised backscatter data were recorded in S7K format using Teledyne Reson's Sonar UI, while Qinsy served as a navigation display for real-time vessel positioning and tracking.

In this article, the Köhlbrand area is discussed in detail and serves as the primary example to show the entire workflow. The same steps were applied to all the other areas.

Data processing

All the final bathymetric surfaces and backscatter mosaics were generated in Teledyne Geospatial CARIS HIPS and SIPS under ETRS89/UTM Zone 32N (EPSG: 25832) coordinate system. The bathymetric data processing workflow included creating a new vessel file with updated offsets, lever arms and TPU settings and importing the S7K files into CARIS HIPS and SIPS. Navigation and sound velocity profiles were validated and bathymetric data were georeferenced using GNSS and the local geoid (GCG2016). An appropriate grid resolution of 0.5 m was selected based on footprint calculations. Data were cleaned using quality filters, followed by manual swath editing. A CUBE surface was then generated and validated.

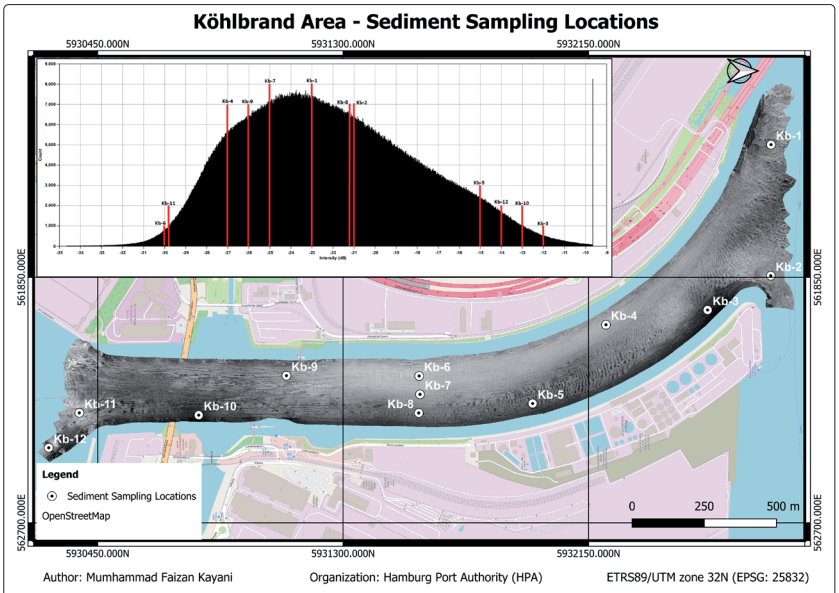

Fig. 2: Köhlbrand area 200-kHz backscatter mosaic and histogram showing the intensity (dB) distribution, with sampling points marked according to their respective dB values and visual contrast

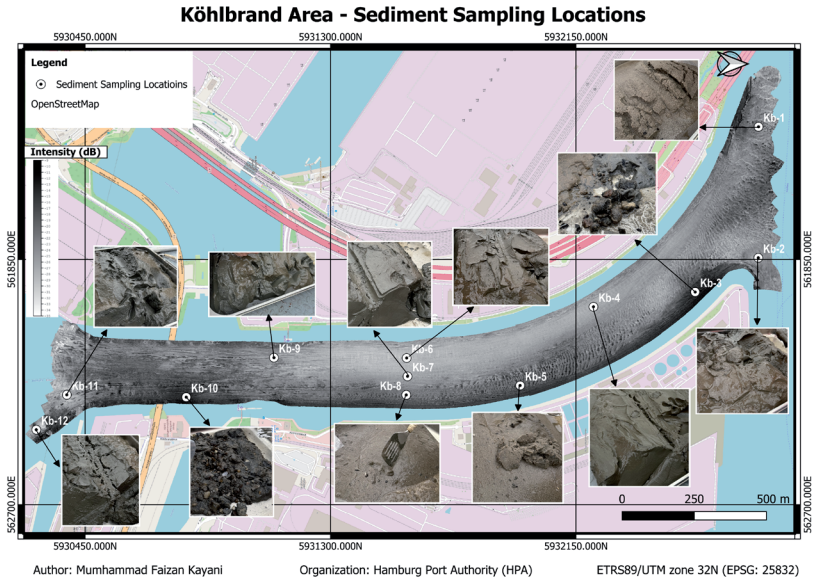

Fig. 3: Sediment sampling locations for Kb-1 to Kb-12 and images of the samples at each location in Köhlbrand

Backscatter mosaics were generated in CARIS HIPS and SIPS using normalised S7K data and the SIPS Backscatter WMA with Area-based AVG engine. A 0.20-m grid resolution was selected for single-frequency mosaics and 1-m resolution for multispectral backscatter to create mosaics of appropriate resolution using compensated 7,058 snippet records, default search radius settings and local absorption corrections. A processed bathymetric surface supported slope and angle-dependent corrections, while beam pattern and AVG corrections were applied to remove transducer artefacts and normalise intensity across incidence angles.

Sediment sampling

A sediment sampling campaign was conducted in which a total of 72 sediment samples were collected using the HPA vessel *Deepenschriewer 3,* equipped with a Van Veen grab sampler. After generating backscatter mosaics in HIPS and SIPS, 74 locations were marked in the selected seven areas. These locations were chosen to represent the full range of sediments, as shown by changes in backscatter intensity in Fig. 2. The selection is guided by histogram analysis of backscatter (dB) values, combined with the visual contrast (light and dark areas) visible on the mosaic. These sampling points were strategically marked to capture sediment variability and ensure diverse sediment coverage.

Köhlbrand area sampling

In the Köhlbrand area, twelve sediment samples were collected at marked locations, as shown in Fig. 2. These twelve locations are named with the abbreviation Kb, which represents the Köhlbrand area. In Fig. 3, sediment samples collected at locations Kb-1 to Kb-12 are shown. The same process was followed for all other areas.

Results and discussion

Bathymetric surface and backscatter mosaic

Final quality control confirmed that all the processed bathymetric surfaces met IHO S-44 Special Order accuracy requirements. Surface statistics are computed in HIPS and SIPS software using depth as an attribute layer with a bin size of 0.01 m. Fig. 4 and Fig. 5 show the maps of processed bathymetric surfaces and backscatter mosaics with their corresponding histograms for 200 and 400 kHz in the Köhlbrand area.

Multispectral backscatter

During this research, the significance of unavailable multispectral backscatter processing functionality for dual-head systems was highlighted, and continuous feedback and test data were provided to the Teledyne CARIS development team. As a result of this collaboration with CARIS, the HIPS and SIPS software, with its latest version 12.1.3, can now process multi-frequency data from dual-head systems. This is an important development for Hamburg port survey operations, particularly with all dual-head systems (T20-R and T50-R).

Multispectral backscatter data were not available for all survey areas due to technical limitations encountered during data processing in CARIS HIPS and SIPS, particularly related to the handling of dual-head systems and multispectral datasets. To address these limitations, the survey design was adapted to include the acquisition of backscatter data at a minimum of two different frequencies, with the research areas surveyed twice. As a re-

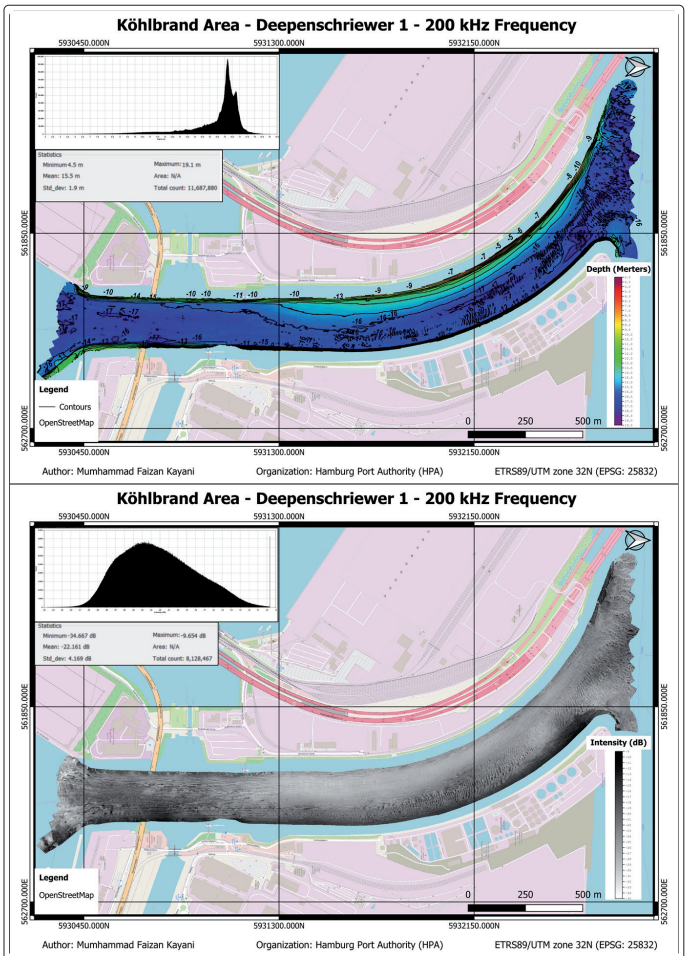

Fig. 4: Processed bathymetric surfaces and backscatter mosaics for the Köhlbrand area *(Deepenschriever 1)* at 200 kHz. The top map shows the 200-kHz bathymetry with its depth histogram, while the bottom map presents the corresponding 200-kHz backscatter mosaic map with intensity histogram

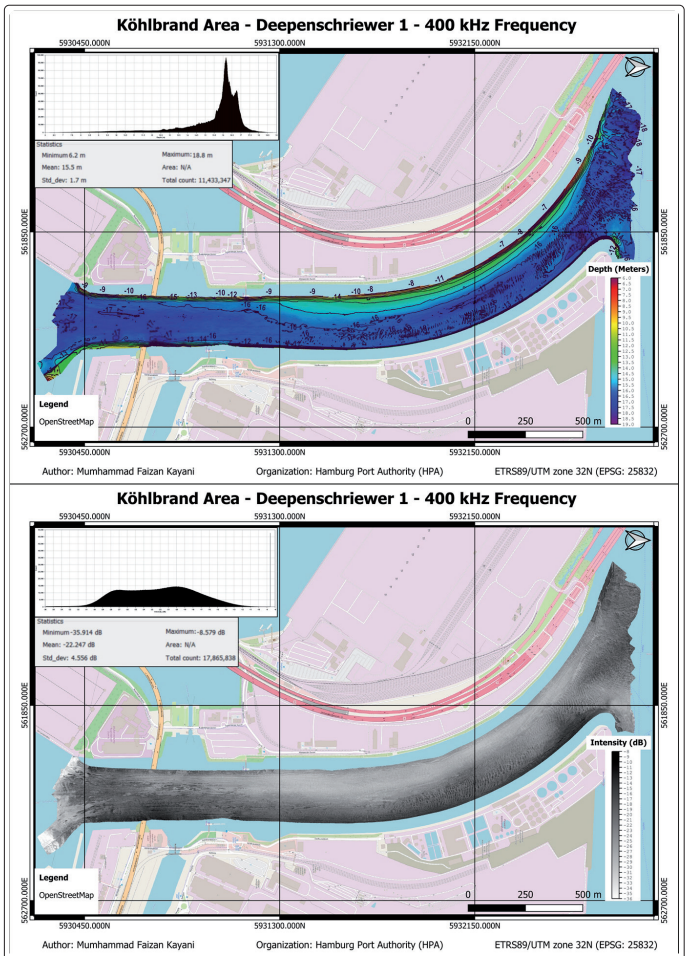

Fig. 5: Processed bathymetric surfaces and backscatter mosaics for the Köhlbrand area *(Deepenschriever 1)* at 400 kHz. The top map shows the 400-kHz bathymetry with its depth histogram, while the bottom map presents the corresponding 400-kHz backscatter mosaic map with intensity histogram

sult, direct multispectral comparisons between frequencies are only possible for a single dataset from the Strandhafen area.

With the new multispectral processing option, it is now possible to get three frequency layers (200 kHz, 300 kHz and 400 kHz) after generating the mosaic. Each frequency layer consists of two slightly different frequencies that come from the two heads of the dual-head multibeam system. The 200-kHz band includes data from 187 kHz and 213 kHz, the 300-kHz band from 287 kHz and 313 kHz, and the 400-kHz band from 387 kHz and 413 kHz. These small differences in frequency make it possible for the software to recognise which head the data comes from and to combine them correctly within each frequency band. A schematic illustration of the multispectral data acquisition concept using a dual-head system is shown in Fig. 6.

A multispectral backscatter mosaic shows frequency-dependent seabed details. At 200 kHz, the mosaic appears smooth, showing broad patterns because lower frequencies penetrate deeper and are less sensitive to small surface variations. The 300-kHz mosaic captures moderate seabed texture changes, while 400 kHz provides the sharpest detail, highlighting fine-scale roughness. In the combined RGB mosaic, 200 kHz is mapped to red, 300 kHz to green and 400 kHz to blue, emphasising differences in sediment response. Blue areas indicate coarser sediments, whereas red or brown areas cor-

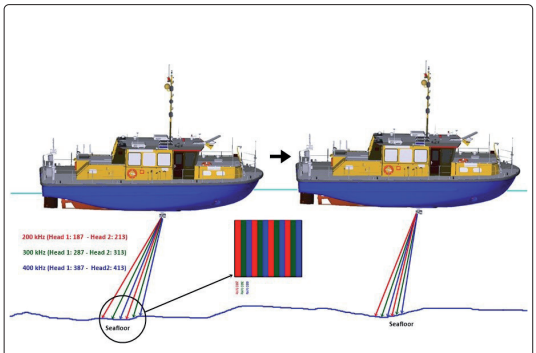

Fig. 6: Schematic illustration of the multispectral data acquisition concept from a dual-head configuration using 200 kHz (187 to 213), 300 kHz (287 to 313) 400 kHz (387 to 413) frequencies with *Deepenschriever 1* vessel (modified illustration from HPA n.d.)

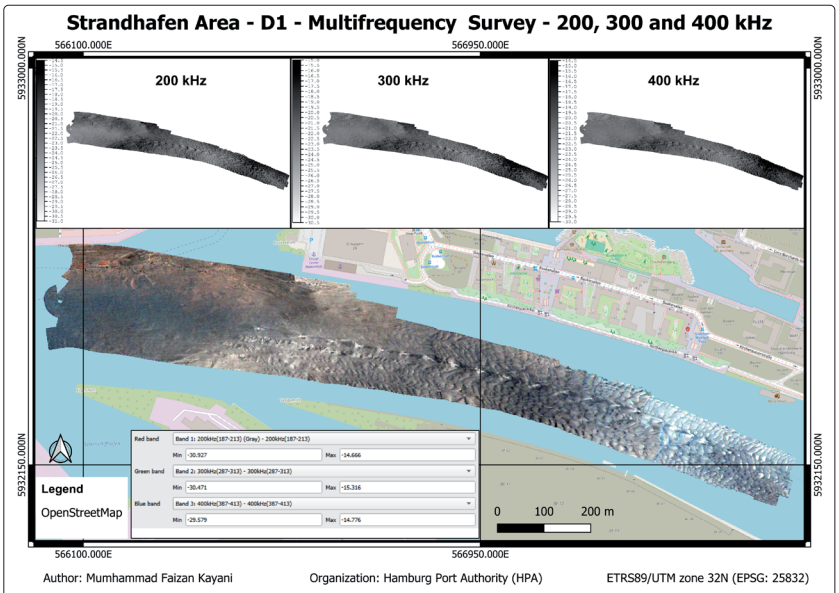

Fig. 7: Multispectral backscatter mosaic with layers 200 kHz, 300 kHz and 400 kHz

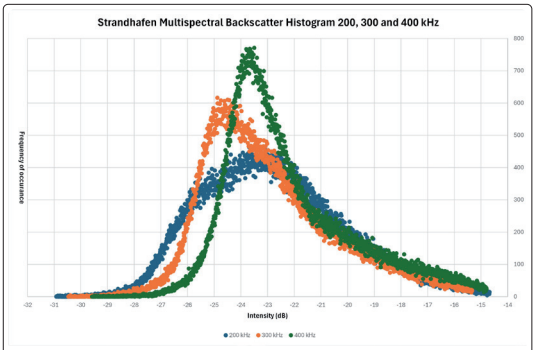

Fig. 8: Histogram comparison of 200-kHz, 300-kHz and 400-kHz backscatter mosaics layers in Strandhafen area (blue: 200 kHz, orange: 300 kHz, green: 400 kHz)

respond to finer-grained sediments. A combined multispectral backscatter mosaic map with layers at 200 kHz, 300 kHz and 400 kHz is shown in Fig. 7, and the histogram comparison is presented in Fig. 8.

Cumulative grain size distribution and mean grain size estimation

After receiving sieve analysis results from the laboratory, grain size data were first checked and corrected to ensure that cumulative percent-finer values increased with particle size. To convert laboratory results into a visual representation on a logarithmic scale and to determine median grain size (D50), the data were processed using forward and inverse splines based on Piecewise Cubic Hermite Interpolation (PCHIP) (Fritsch and Carlson 1980). PCHIP was implemented in Visual Studio using a Python script adapted from SciPy's open-source repository (SciPy Developers 2025), which was further modified.

The spline interpolation provided D50 values for all samples. The applied sieving method was designed for sediments larger than 20 µm, as the smallest sieve size was 20 µm. The resulting D50 values were then classified according to the Udden-Wentworth grain size scale. Fig. 9 shows spline curves for twelve samples from the Köhlbrand, and Table 1 lists their D50 values and corresponding sediment classifications.

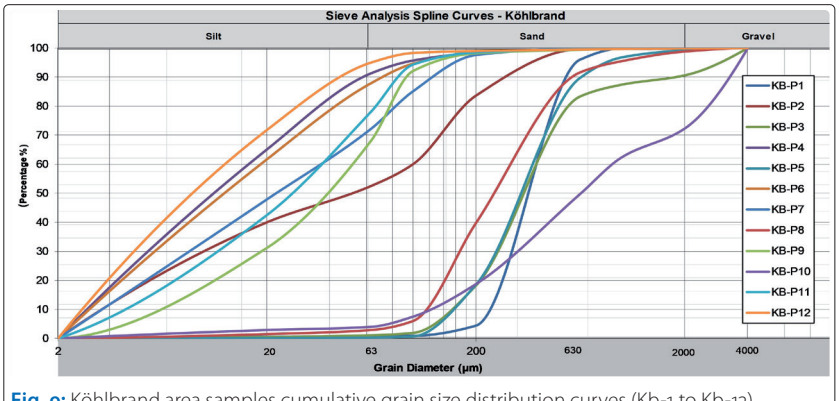

Fig. 9: Köhlbrand area samples cumulative grain size distribution curves (Kb-1 to Kb-12)

Name	D50	Udden-Wentworth Class (D50)
Kb-1	356.5 µm	Medium sand
Kb-2	52.11 µm	Coarse silt
Kb-3	339.14 µm	Medium sand
Kb-4	11.13 µm	Fine silt
Kb-5	329.41 µm	Medium sand
Kb-6	12.5 µm	Fine silt
Kb-7	22.63 µm	Medium silt
Kb-8	244.66 µm	Fine sand
Kb-9	39.47 µm	Coarse silt
Kb-10	636.91 µm	Coarse sand
Kb-11	25.92 µm	Medium silt
Kb-12	8.79 µm	Fine silt

Table 1: Summary of grain size diameters at each location and Udden-Wentworth classification in the Köhlbrand area

Estimation of mean backscatter values per location

To obtain reliable sediment classifications, accurate backscatter intensity (dB) values were extracted at each sampling location. The 200-kHz and 400-kHz backscatter mosaics were imported into QGIS as GeoTIFFs, and sampling points were added as delimited text. Because point coordinates may contain minor positional uncertainty, buffers were created around each location to include multiple pixels when calculating mean dB values using zonal statistics in QGIS.

Given the mosaic resolution of 0.20 m (pixel area = 0.04 m^2), buffer areas were calculated for a radius of 1 m using the circle area formula. This corresponded to approximately 78.5 pixels, respectively. A 1-m buffer was selected because it provides a sufficient number of pixels for stable averaging of intensity values at each sampling point.

Sediment classification using machine learning

A machine learning approach was used to classify sediments by predicting D50 values using a Random Forest regressor, trained on ground-truth and backscatter intensity data. The Random Forest model was implemented in the Python console of QGIS 3.34.1 with a script adapted from the scikit-learn open-source GitHub repository (Scikit-learn Developers 2025a), and it was further modified according to the workflow. The workflow is shown in Fig. 10.

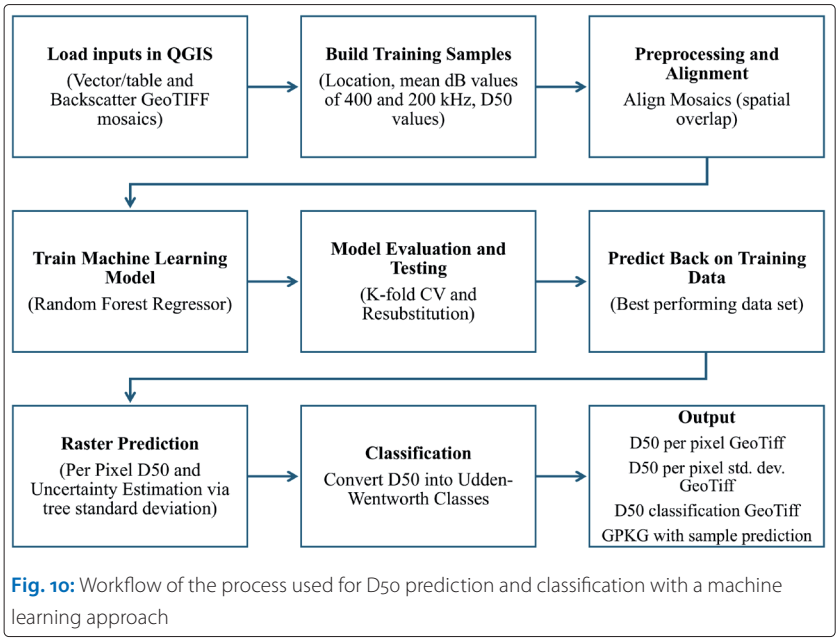

Fig. 10: Workflow of the process used for D50 prediction and classification with a machine learning approach

Stage 1: Preparing input data

The workflow began by preparing two input datasets: the first training dataset contains the mean backscatter intensity values of all valid 72 samples at 200 kHz and 400 kHz, ground-truth sediment labels, D50 values and their geographic coordinates in CSV file format. This is imported in QGIS as a delimited text layer. For the second dataset, 200-kHz and 400-kHz backscatter mosaics were exported as GeoTIFF rasters from CARIS HIPS and SIPS at a specified folder location.

Stage 2: Preprocessing and alignment

The modified Python script is executed in the QGIS Python console using a CSV file and path location to GeoTIFF rasters as input to initiate the training and prediction process. As the two mosaics did not perfectly overlap because they were from different surveys at 200 kHz and 400 kHz at slightly different times. The spatial intersection for both rasters was computed, using only overlapping pixels. The remaining non-overlapping area was not used as input data.

Stage 3: Training Random Forest regressor

During the training stage of machine learning, only samples with available mean_200, mean_400 and D50 values were used. This stage combines the two mean intensities into the feature matrix and the D50 values into the target vector. A Random Forest regressor with 500 trees was trained to learn the relationship between backscatter intensity and ground-truth grain size and make predictions on the training data.

Stage 4: Model evaluation and testing

Model's predictive performance was evaluated using both a re-substitution accuracy test and K-fold cross-validation for three setups: 200 kHz, 400 kHz and a combined 200 to 400 kHz frequency configuration. Both scripts were adapted from scikit-learn's open-source code (Scikit-learn Developers 2025b).

Re-substitution accuracy test

The purpose of testing three datasets was to evaluate the predictive performance on each dataset and use the best input dataset to train the model to achieve the most accurate results. These statistical results showed that, while both single-frequency setups performed reasonably well, the combination of 200 kHz and 400 kHz provided a more accurate and reliable prediction of D50, with a minimum RMSE of 102.69 µm, MAE of 36.29 µm and R^2 value of 0.89.

K-fold cross validation test

This test was run across the same three different setups. The statistical results from the K-fold cross validation test showed that with single-frequency input (200 kHz and 400 kHz), the model performed poorly on unseen data, as shown by high RMSE values and low R^2 values. When both 200-kHz and 400-kHz data were combined, the model performed relatively better by giving an RMSE of 287.08 µm, an MAE of 98.05 µm, and an R^2 of 0.12. Although the improvement was small, the combined values gave a better description of the data than the single-frequency values. This means that using both frequencies together gave better and more useful information than using only one frequency.

Stage 5: Raster prediction and classification

Among the test combinations, the combined setup (200 and 400 kHz) gave the best results in both tests. After this evaluation, the best-performing input setup (combined 200 and 400 kHz) was used to make predictions on the training data and to produce the final raster prediction. The trained model was then applied to the overlapping 200-kHz and 400-kHz mosaics so that each pixel's mean backscatter values could be used to predict its D50 value, and uncertainty was calculated as the standard deviation across all trees in

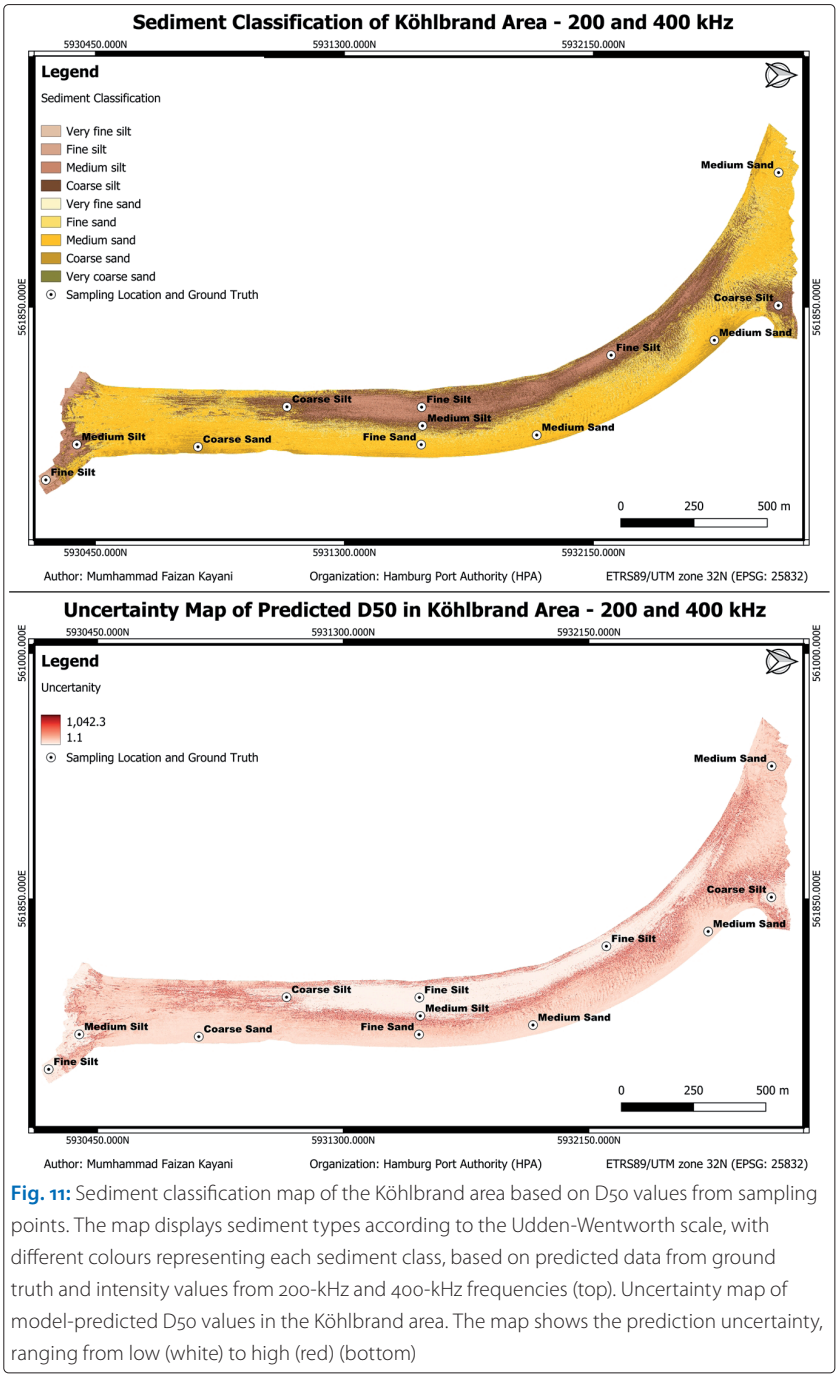

Fig. 11: Sediment classification map of the Köhlbrand area based on D50 values from sampling points. The map displays sediment types according to the Udden-Wentworth scale, with different colours representing each sediment class, based on predicted data from ground truth and intensity values from 200-kHz and 400-kHz frequencies (top). Uncertainty map of model-predicted D50 values in the Köhlbrand area. The map shows the prediction uncertainty, ranging from low (white) to high (red) (bottom)

the forest. The predicted D50 values were then post-processed into sediment classes using fixed Udden-Wentworth thresholds, generating a classification raster with integer class IDs.

Stage 6: Output

The workflow produced three raster outputs: a D50 prediction GeoTIFF, a standard-deviation GeoTIFF representing model uncertainty at each pixel and a D50 classification GeoTIFF as well as a corresponding Geo-package file.

Köhlbrand area sediment classification

In the Köhlbrand classification map, silts are mostly found in the western part of the area, whereas sands are more common in the middle and eastern parts, which matches the D50 classification. Some differences are observed near the boundaries, where the transition is happening between the sediment classes. These small mismatches are likely due to natural changes in the seabed and the limitations of the machine learning model.

The uncertainty map shows that most of the Köhlbrand area was predicted with low uncertainty. The silty region in the middle and the sandy region in the east are more consistent, which means the model worked well in those areas. Higher uncertainty is mainly found at the boundaries between classes, especially where fine silt and medium silt are located. This happens because the values in these areas are close to each other, which makes it harder for the model to separate them with high accuracy. In general, the results agreed with the ground-truth samples, but they also highlighted areas of high uncertainty (red), where the predicted performance is low.

Fig. 11 displays a sediment classification map of the Köhlbrand area with ground truth and a corresponding uncertainty map showing the model's prediction accuracy for the same area.

Comparison of the sedimentological model with machine learning predicted D50

In the Teledyne CARIS BASE EDITOR software, the existing sedimentological model at HPA and predicted D50 surfaces are used to generate a difference surface. The predicted D50 surface (B) is subtracted from the sedimentological model surface (A). This subtraction (A – B) produces a difference surface with both negative and positive values. Areas where A – B = 0 indicate no difference between the two surfaces, A – B > 0 indicates that the sedimentological model predicted a larger grain size than the predicted D50 surface, and A – B < 0 indicates that the predicted D50 surface predicted a larger grain size than the sedimentological model.

In the Köhlbrand area, the mean difference is –175.81 µm, which means that the predicted D50 values are overall larger than those from the sedimentological model. The standard deviation is ±267.88 µm, showing a wide range of differences. The largest difference is –1527.37 µm, where the predicted D50 is much coarser than the sedimentological model. The maximum difference is +187.91 µm, which means that the sedimentological model gave larger D50 values but only in a few areas.

In the Köhlbrand area, most of the eastern and southern parts are shown in blue, indicating that the predicted D50 values are coarser than those from the sedimentological model (A – B < 0). On the other hand, the central part shows more yellow to orange colours, meaning that the

sedimentological model gave similar or larger D50 values than those of the predicted model. The difference map between the predicted D50 and the sedimentological model in the Köhlbrand area is shown in Fig. 12.

Per-sample comparison sedimentological model vs. machine learning predicted D50

Köhlbrand area

The parity plot (Fig. 13) of the Köhlbrand shows that most values from the sedimentological model are below the 1:1 line. The sedimentological model gives smaller values in sandy sediments than the predicted D50. The difference is most prominent in the medium-to-coarse sand range, where the gap between the two values reached several hundred micrometers. The error metrics also support this, showing a mean absolute error (MAE) of 157.7 µm, a root mean square error (RMSE) of 212.1 µm and a very high mean absolute percentage error (MAPE) of 237.7 %.

The per-sample absolute difference shows these differences. Samples Kb-3, Kb-5 and Kb-10 have large differences, greater than 300 µm. On the other hand, samples Kb-11 and Kb-12 show very small differences, meaning that the sedimentological model gives closer results to the predicted D50 in the fine silt range. This shows that the sedimentological model struggles to represent sandy sediments.

Remaining survey areas

To assess the comparison across different regions of the Port of Hamburg, the predicted D50 values were compared with the ground-truth measurements for six other areas: Strandhafen, Köhlfleet, Waltershofer Hafen, Vorhafen, Norderelbe 7 and Reiherstieg. Table 2 provides an overview of MAE, RMSE and MAPE values.

Sedimentological model and predicted D50 vs. ground truth

Köhlbrand area

In the Köhlbrand area, the predicted D50 values show a similar trend to the ground-truth data and match quite well. Most samples have small differences, with an average error of about 63 µm. There are some noticeable changes at Kb-3 and Kb-10. At Kb-3, the predicted D50 is higher (110 µm) than the ground-truth value, whereas at Kb-10 it is lower by about 130 µm. These differences are primarily observed in areas where the sediments are coarser.

The sedimentological model gives lower D50 values than the ground truth, especially between Kb-1 and Kb-10. The largest differences occur at Kb-3 (370 µm) and Kb-10 (430 µm). This shows that the model underestimates coarse materials and smooths out local changes in the seabed. In finer

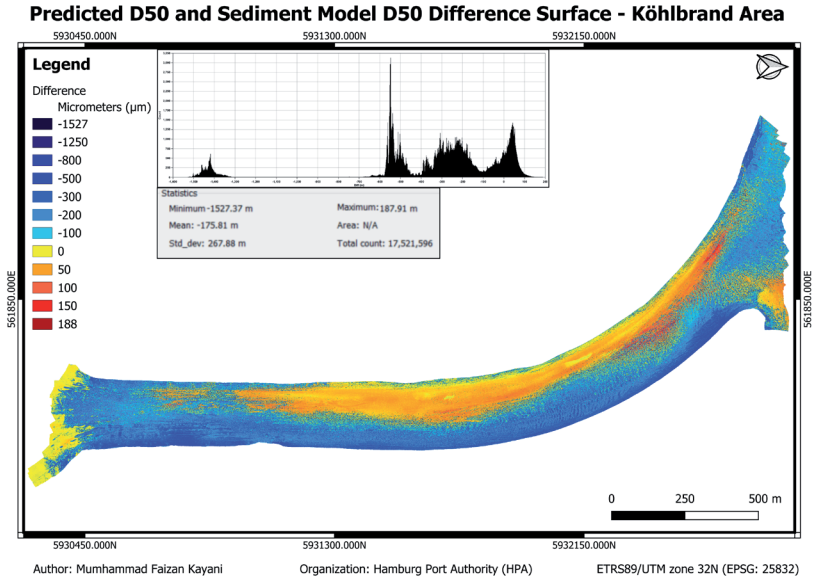

Fig. 12: Predicted D50 and sedimentological model D50 difference surface for the Köhlbrand area. Showing the difference between predicted values and existing sedimentological values, where blue colours represent areas of negative difference and orange to red colours show positive difference

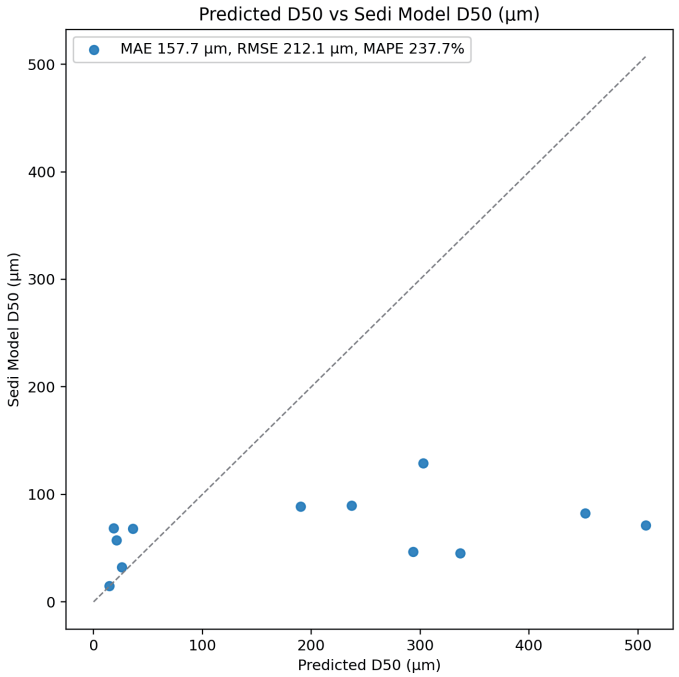

Fig. 13: Parity plot of sedimentological model vs. predicted D50 in Köhlbrand area

Area	MAE	RMSE	MAPE
Strandhafen	211.0 µm	237.1 µm	411.7 %
Köhlfleet	29 µm	70.5 µm	58.8 %
Waltershofer Hafen	136.9 µm	235.6 µm	464.0 %
Vorhafen	67.2 µm	151.3 µm	273.1 %
Norderelbe 7	152.7 µm	219.2 µm	238.8 %
Reiherstieg	81.5 µm	166.0 µm	250.9 %

Table 2: Comparison of predicted D50 and sedimentological model D50 with their error metrics

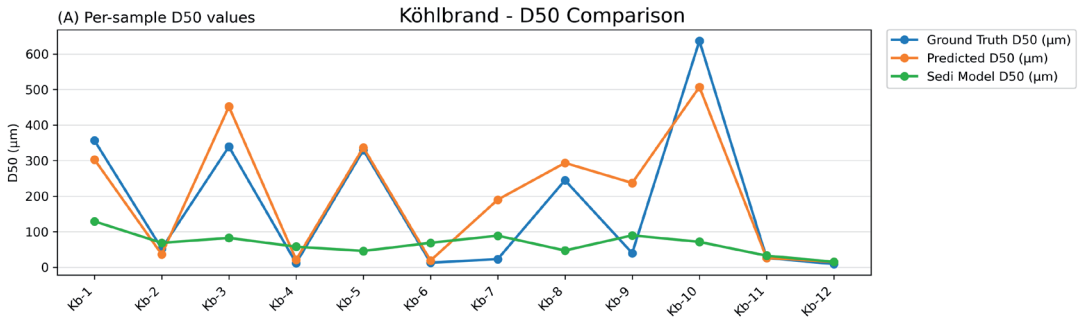

Fig. 14: Per-sample D50 values between the sedimentological model, predicted D50 and ground truth in the Köhlbrand area

areas such as Kb-2, Kb-4, Kb-11 and Kb-12, both models give similar results close to the ground truth. In the Köhlbrand area, the predicted D50 values agree more closely with the ground truth, while the sedimentological model performs better only in fine-sediment areas. Per-sample D50 values and the absolute difference between the sedimentological model, predicted D50 and ground truth are shown in Fig. 14.

Across all other survey areas

Across all the other investigated areas (Strandhafen, Köhlfleet, Waltershofer Hafen, Vorhafen, Norderelbe 7 and Reiherstieg), the predicted D50 values from the machine learning model generally show good agreement with the ground-truth measurements. Discrepancies predominantly occur in areas characterised by heterogeneous or coarser sediments. In contrast, areas dominated by homogenous or fine sediments show only minor differences, often below 20 to 50 µm, indicating stronger model performance under these conditions.

The HPA sedimentological model consistently gives lower D50 values than the ground truth, particularly underestimating coarse and sandy sediments, while performing more accurately in fine-grained environments.

Overall, both approaches demonstrate robust agreement in fine-sediment regions, whereas discrepancies increase with coarser sediment fractions, highlighting the limitations of the HPA sedimentological model in representing coarse-grained seabed conditions.

Conclusion

The results showed that normalised backscatter data from dual-head multibeam systems provide valuable additional information for hydrographic surveys. Based on the findings of this research, the data acquisition and processing workflow has been established as a straightforward procedure, with strong potential for future automation. In particular, the resulting high-resolution backscatter mosaics enable detailed seabed analysis and are well-suited for detecting even small-scale variations and changes in sediment characteristics.

The sediment classification results showed that the machine learning (ML) model performs well when trained and tested on the same data, achieving high accuracy and low error in the re-substitution test. Its generalisation to unseen data was limited, but combining 200 kHz and 400 kHz backscatter data improved performance, achieving the lowest errors (RMSE, MAE) and highest R^2.

In calm, fine-sediment areas such as Vorhafen, Köhlfleet and Reiherstieg, both the ML and HPA sedimentological models produced similar results. However, in coarse or mixed-sediment areas like Köhlbrand, Waltershofer Hafen, Strandhafen and Norderelbe 7, the ML model captured local seabed changes more accurately, whereas the sedimentological model oversimplified conditions. Overall, the ML model better represents coarse sediments and sediment mixtures, providing a more precise prediction of D50 values (mean absolute error 91 µm vs. 110 µm for the sedimentological model).

These results suggest that the HPA sedimentological model could be supported or replaced by a backscatter-driven ML approach, enabling faster, more accurate sediment mapping and better resolution of small-scale seabed changes. Future use of multispectral backscatter data (e.g., 200, 300, 400 kHz) combined with seabed texture information could further improve classification accuracy and enable the model to handle more complex seabed conditions. //

References

Fritsch, Fred N.; R. E. Carlson (1980): Monotone Piecewise Cubic Interpolation. SIAM Journal on Numerical Analysis, DOI: 10.1137/0717021

HPA (n.d.): D1 – 3D – WELT_INDEX-B. Hamburg Port Authority, internal PDF document, not publicly available

Menandro, Pedro S.; Benjamin Misiuk; Jens Schneider von Deimling; Alex C. Bastos; Craig J. Brown (2025): Multifrequency seafloor acoustic backscatter as a tool for improved biological and geological assessments – updating knowledge, prospects, and challenges. Frontiers in Remote Sensing, DOI: 10.3389/frsen.2025.1546280

Ohle, Nino; Ulrich Schmekel; Ivan Shevchuk; Moustafa Abdel-Maksoud; Carl-Uwe Böttner; Alex Kirichek (2024): New approaches in safe berthing and sailing through fluid mud at Hamburg Port. Proceedings of the 35th PIANC World Congress 2024, Cape Town, South Africa

SciPy Developers (2025): SciPy: PchipInterpolator (Version 1.16.2) [Source code]. GitHub, https://github.com/scipy/scipy/blob/v1.16.2/scipy/interpolate/_cubic.py#L160-L313

scikit-learn Developers (2025a): RandomForestClassifier (version 1.4.0) [Source code]. GitHub, https://github.com/scikit-learn/scikit-learn/blob/c60dae2060/sklearn/ensemble/_forest.py#L1571

scikit-learn Developers (2025b): KFold (version 1.4.0) [Source code]. GitHub, https://github.com/scikit-learn/scikit-learn/blob/c60dae2060/sklearn/model_selection/_split.py#L436

Sievers, Julian (2021): Erzeugung und Auswertung zweier oberflächensedimentologischer Modelle des Hamburger Hafens zum 01.05. und 01.11. des Jahres 2020. smile consult GmbH

DOI: 10.23784/HN133-09

The influence of seamount morphology on sediment accumulation and its potential reflection in the upper-ocean currents

An article by JOSY A. BERGMANN

Seamounts (SM) influence sedimentary depositions as well as oceanic currents, shaping the surrounding biota and increasing biological diversity as well as variability. This study investigates how seamount morphology steers sediment distribution and how these patterns may be reflected in upper water column current measurements. Five seamounts, located in two areas (SMA 16-17 and SMA 18-19-20), were underway surveyed during the MSM 140/2 transit cruise of the research vessel (RV) *Maria S. Merian,* using vessel-mounted multibeam echo sounder (MBES), sub-bottom profiler (SBP) and acoustic doppler current profiler (ADCP). The seafloor was characterised using automated geomorphon classification, while the sedimentary properties were analysed using automated MBES segmentation based on bathymetry data and backscatter intensities along with the evaluation of SBP echograms. In both study sites, the sediment accumulation correlates to the seamount morphology. The ADCP measurements show variability in zonal and meridional velocities within the upper 200 to 300 m, implying consistency with global currents but not sufficient to relate the measurements to the focus areas.

bathymetry | ocean currents | seamounts | sediment transport | underway survey
Bathymetrie | Meeresströmungen | Seamounts | Sedimenttransport | Transitvermessung

Seamounts (SM) beeinflussen Sedimentablagerungen und Meeresströmungen, wodurch sie das umgebende Ökosystem prägen und die biologische Vielfalt sowie Variabilität erhöhen. Diese Studie untersucht, wie die Morphologie von Seamounts die Sedimentverteilung steuert und wie sich diese Muster in Strömungsmessungen der oberen Wassersäule widerspiegeln können. Fünf Seamounts, die in zwei Studiengebieten (SMA 16-17 und SMA 18-19-20) liegen, wurden während der Transitfahrt MSM 140/2 des Forschungsschiffs (FS) *Maria S. Merian* mit einem schiffsmontierten Fächerecholot (MBES), Sub-Bottom Profiler (SBP) und einem Acoustic Doppler Current Profiler (ADCP) untersucht. Der Meeresboden wurde mit Hilfe einer automatisierten geomorphologischen Klassifizierung charakterisiert, während die Sedimenteigenschaften anhand einer automatisierten MBES-Segmentierung (basierend auf Bathymetriedaten und Rückstreuintensitäten) sowie der Auswertung von SBP-Echogrammen analysiert wurden. In beiden Untersuchungsgebieten korreliert die Sedimentakkumulation mit der Morphologie der Seamounts. Die ADCP-Messungen zeigen Schwankungen in den zonalen und meridionalen Geschwindigkeiten innerhalb der oberen 200 bis 300 m, was auf eine Übereinstimmung mit den globalen Strömungen hindeutet, jedoch nicht ausreicht, um die Messungen mit den Studienbereichen in Verbindung zu bringen.

Author
Josy Bergmann studies Hydrography at HafenCity University in Hamburg.

josy.bergmann@hcu-hamburg.de

Introduction

Seamounts represent one of the most predominant structures of the deep-ocean landscape (Mohn et al. 2018). The International Hydrographic Organization (2019) provides a standardised definition of seamounts as follows: »A distinct generally equidimensional elevation greater than 1,000 m above the surrounding relief as measured from the deepest isobath that surrounds most of the feature.« SMs influence local as well as global oceanic currents by redistributing energy from surface tides, blocking water flow and creating eddies (Buchs et al. 2014). Deep-ocean currents typically reach velocities of about 1 to 2 cm/s and are a driving factor for re-mobilising sediments, diffusing organisms and microplastics, and affecting benthic habitats (Turnewitsch et al. 2013; Frey et al. 2025). The interaction between deep-ocean

currents and sediment dynamics shapes the surrounding biota and increases biological diversity as well as variability (Iyer et al. 2012; Mohn et al. 2021).

Studies of Joo et al. (2020) and Gao et al. (2025) explored sediment distribution around seamounts in the Western Pacific, combining data from MBES with deep-towed camera systems. Joo et al. (2020) showed that high backscatter intensities and steep slopes are associated with exposed bedrock, while Gao et al. (2025) found an increase of sediment cover downslope from summit to flank and base. Integrating the influence of bottom currents on the sedimentary distribution, Frey et al. (2025) determined that areas of variable bedforms in the sediments are associated with bottom currents and topographic interactions. Wilckens (2023) also investigated on the interactions between ocean currents and sedimentary system, showing higher speeds and steeper slopes favour secondary flow.

During the transit cruise (MSM 140/2) of the *RV Maria S. Merian* from Brest, France to Rio de Janeiro, Brazil, several seamounts were surveyed underway at speeds of 10 to 12 knots, using vessel-mounted MBES, SBP and ADCP. This study focuses on two areas comprising five seamounts in order to investigate how seamount morphology influences sediment distribution and its potential reflection in upper-ocean currents. The seamount area (SMA) 16-17 consists of two previously charted seamounts (SM 16, SM 17), whereas the SMA 18-19-20 area includes three seamounts, of which two (SM 19, SM 20) had been charted prior to this survey and one (SM 18) had not. Both lie within the formation zone of the Brazil Current (BC), which originates south of 10°S, transporting warm, high-salinity Atlantic Tropical Water southwards within the upper 200 m (Pereira et al. 2014).

Methodology

Data acquisition

The EM124 (MBES by Kongsberg) operates at a fixed frequency of 12 kHz to collect bathymetric information of the seafloor. Given the absence of in-situ sound velocity profiles, data from the World Ocean Atlas 2023 were utilised instead (Garcia et al. 2024).

To gather profiles of the submarine strata a P70 (SBP by Teledyne) was used. The system operated with primary high-frequency (PHF) channels at 18 kHz and 21 kHz. Single acoustic pulses were transmitted at a pulse repetition interval of 100 ms, using a continuous wave pulse type.

The ADCP instrument used (OceanSurveyor by Teledyne) recorded the current velocities in the upper water column at operating frequencies of 38 kHz (depth range of approximately 700 m) and 75 kHz (depth range of about 1000 m). Both systems acquired data in single-ping narrowband mode.

Data processing

The software Qimera from QPS B.V. was utilised to post-process the acquired bathymetry data. The analysis on the morphology of the survey areas was done using the software FMGT by QPS B.V. as well as the software QGIS with the toolbox GRASS GIS and plug-in MarineTools. The tool r.geomorphon (GRASS GIS) was employed for automated classification of the terrain. Geomorphons present terrain forms, such as slopes, ridges, shoulders, valleys and flats, which are derived using a machine-vision approach based on an eight-tuple pattern of visibility neighbourhood. The MBES also recorded backscatter intensities, which were processed in FMGT to produce backscatter mosaics. The generated mosaics were used as an input for the MBES Segmentation (MarineTools). The MBES Segmentation creates a set of vector polygons that represent coherent regions derived from the statistics of the input data. From the bathymetry input, slope and terrain roughness derivatives are determined. Along with the backscatter mosaic, an Object Based Image Analysis is performed based on k-means clustering. Each class is assigned statistical attributes, namely the (normalised) mean and standard deviation of backscatter intensity, slope and terrain roughness (Le Bas n.d.).

The acquired echogram profiles of the SBP were replayed on board the *RV Maria S. Merian* using the acquisition software. For further analysis of stratification thickness, the software SonarWIZ by Chesapeake Technology was employed.

In MatLab, the GEOMAR Toolbox was used to post-process the ADCP data. Processing included data quality control, exclusion of bins with insufficient valid measurements (<25 %), correction for vessel motion and removal of hydroacoustic interference before averaging into 60 seconds ensembles.

Results

The geomorphon classification of SMA 16-17 (Fig. 1) reveals three peak areas. Each peak is surrounded by a concentric pattern of ridges, which transition outward into spurs and slopes. This geomorphic pattern is most developed around SM 16 and SM 17. The area around SM 17 is dominated by footslopes, marking the transition from SM 17 to the elevation opposite. Within this transition zone, a flat surface is primarily present.

In SMA 18-19-20 (Fig. 2) three peaks are identified. A pronounced valley structure prevails the area around SM 18 and is partially corroded by footslopes. This valley structure is bounded by hollow and slope structures, which are particularly evident in the central part of the survey swath. SM 20 is equally characterised by surrounding valley structure, whereas SM 19 shows contrasting morphology. The area between SM 18 and SM 19-20

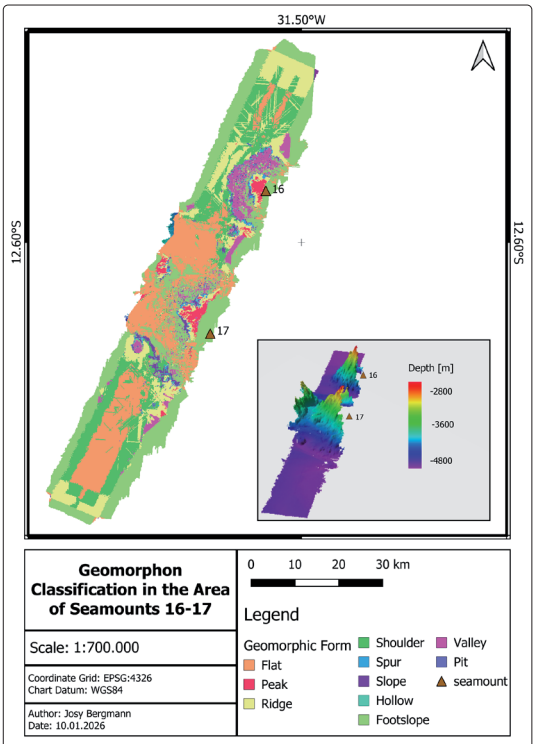

Fig. 1: Overview map of the classified geomorphons of SMA 16-17

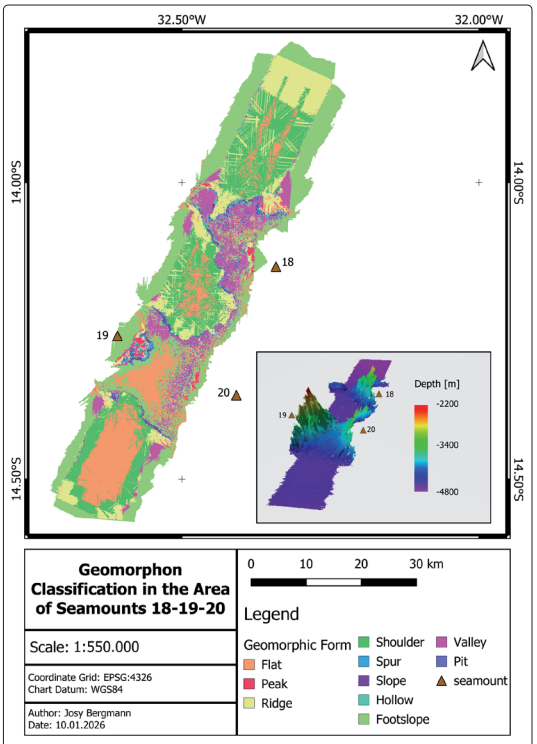

Fig. 2: Overview map of the classified geomorphons in SMA 18-19-20

is marked by ridges, which change into shoulder structures and ultimately into a flat area (Fig. 2).

In SMA 16-17, backscatter intensities range from –66 dB to –20 dB, and the MBES Segmentation resulted in eleven classes (Fig. 3). The lower backscatter values, between –48 dB and –55 dB, occur north and south of the seamount structures. The topographic highs of SM 16 and SM 17 are categorised into class 6.0, representing high mean backscatter values together with a low mean slope and higher mean roughness values. Areas surrounding the seamounts are assigned to class 19.0 with comparatively lower mean backscatter values, a moderate mean slope and high roughness values.

Within the SMA 18-19-20, the MBES Segmentation resulted in twelve classes. SM 18 and SM 20 are predominantly covered by class 5.0, which is characterised by higher mean backscatter, slope and roughness values. This is also observed for SM 19, although over a smaller spatial extent. The transition zone between SM 19 and SM 20 is primarily covered by class 0.0, presenting lower mean backscatter intensities and roughness values.

Approaching SM 16, the sub-bottom stratification shows a regular pattern of reflector layers (Fig. 4). At location (a), the penetration depth is 94.81 m and decreases towards the mount to approximately 45.25 m (location (b)). The steep elevation of SM 16 shows no signal penetration. Immediately south of SM 16, a depression with a penetration depth of 55.25 m (location (c)) is present. It has a regular, continuous reflection and a circularly bounded geometry. Between SM 16 and SM 17, a thin but continuous reflection layer is observed. This layer decreases from 30.29 m to 18.20 m towards SM 17, before no reflections are detected on the flanks of SM 17. The highest surveyed part of SM 17 shows partial reflections. Beyond SM 17, thin sub-bottom reflectors are observed with increasing thickness at a distance of about 40 km from SM 17.

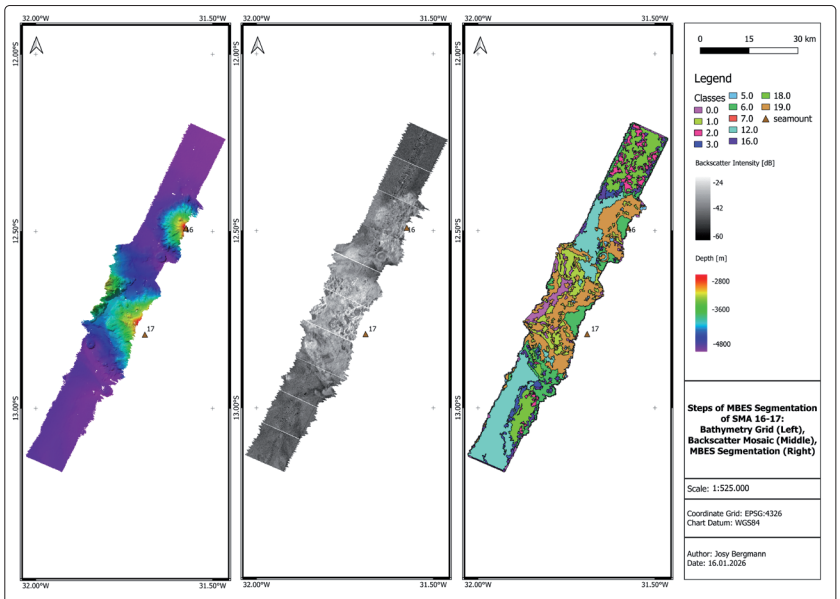

Fig. 3: Overview map of the bathymetry grid (left), the backscatter mosaic (middle) and the MBES Segmentation (right) of SMA 16-17

The echogram for the SM 18-19-20 survey area shows continuous, layered reflectors upon approaching SM 18 (Fig. 5). These reflections thin out and largely disappear when passing over the SM 18, where only weak to no sub-bottom penetration is observed. In the area between SM 18 and SM 19-20, there are layered reflections with a signal penetration depth of 97.84 m (location (a)). North of the transition zone between SM 19 and SM 20, no signal reflection can be seen. When reaching the highest part of the zone and continuing downslope, penetration depth partially increases on flatter parts and is characterised by strong continuous reflectors.

Between 1 November 2025, 20:21.53 UTC and 2 November 2025, 00:51.53 UTC, the study area of SM 16-17 was surveyed. SMA 18-19-20 were investigated on 2 November 2025, from 04:51.53 UTC to 08:21.53 UTC. Fig. 6 shows the zonal and meridional velocities of the 75 kHz ADCP from 31 October 2025, 21:00 UTC to 2 November 2025, 21:00 UTC. In the SM 16-17 area, zonal velocities range from –0.48 m/s to 0.25 m/s. Lower zonal velocities mainly occur in the upper 300 m of the water column, while comparatively higher values are observed below this depth. Meridional velocities in the SMA 16-17 increase over time, with higher values present in the upper 400 m and maximum of 0.36 m/s. In the SMA 18-19-20, greater zonal velocities are examined down to approximately 200 m, with a maximum of 0.37 m/s. The meridional velocities of this area decrease with time.

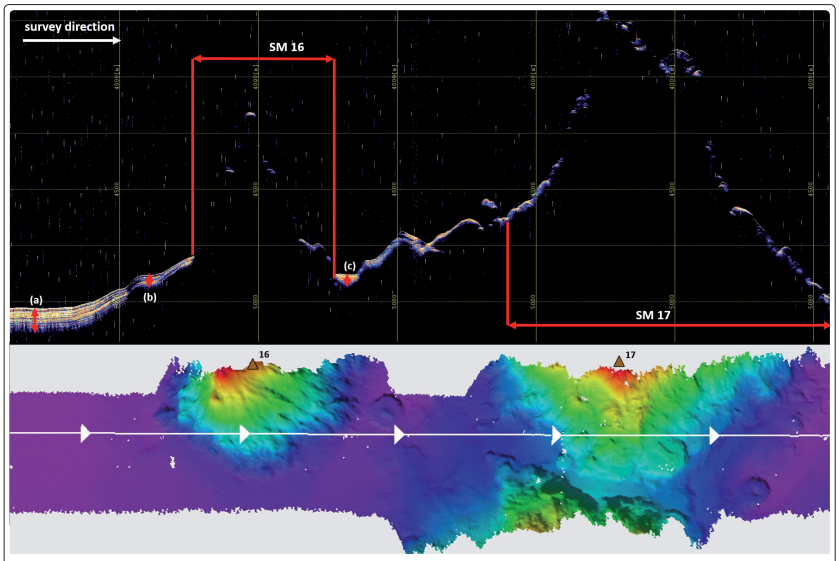

Fig. 4: Echogram profile of the sub-bottom stratification along with the DTM of SMA 16-17 (modified screen capture in Atlas Parastore)

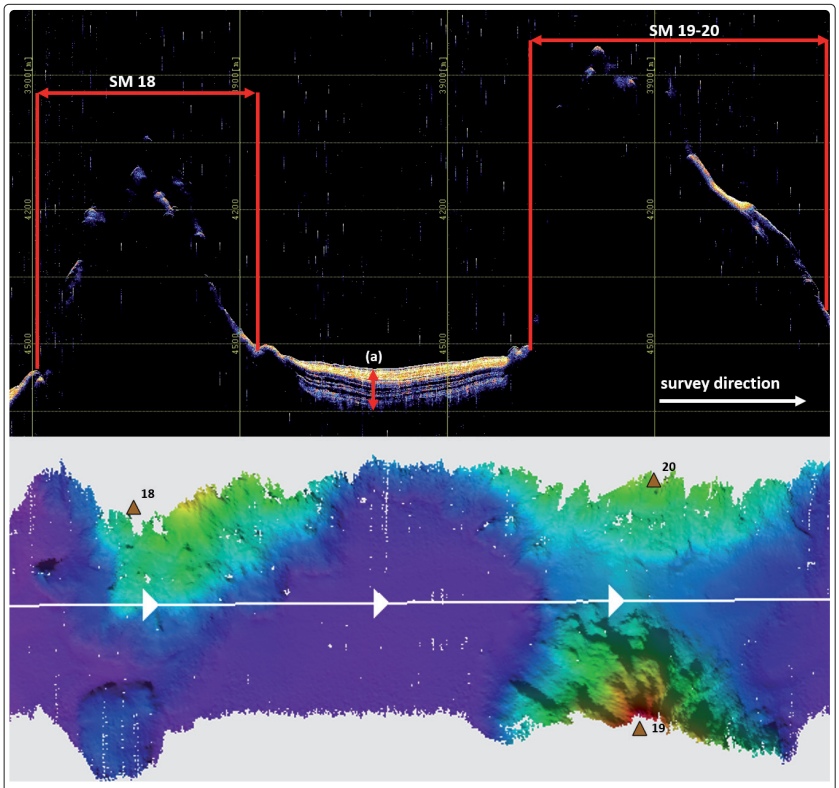

Fig. 5: Echogram profile of the sub-bottom stratification along with the DTM of SMA 18-19-20 (modified screen capture in Atlas Parastore)

Discussion

The observed sediment distribution in the focus areas of SMA 16-17 and SMA 18-19-20 show spatial coherence with seamount morphology, indicating depositional and erosional patterns. In SMA 16-17, sediments predominantly accumulate on shoulders and flats characterised by mean, low terrain roughness and relatively mean, low backscatter intensities, whereas the topographic highs show little to no sub-bottom penetration and are associated with higher backscatter values, indicating hard and exposed substrates (Joo et al. 2020). This contrast between sediment-covered flat regions and the weakly sedimented highs coincides with findings of Joo et al. (2020) and Gao et al. (2025). This suggests accelerating bottom currents over seamounts and steep relief, leading to erosion, while lower speeds are present on flatter surfaces, favouring sediment accumulation (Turnewitsch et al. 2013; Wilckens 2023). Immediately downstream of SM 16, a local entrapment of sediments within a ridge is observed, suggesting lee-side deposition where flow decelerates after passing the flank. SMA 16-17 is, comparatively, topographically open structured (cf. SMA 18-19-20), as the area in-between SM 16 and SM 17 is not bound by slopes, ridges and hollows, but rather dominated by elongated flats, bisected by footslopes towards SM 17. Additionally, water can flow in zonal directions through both seamounts, creating a well-connected topography, which may act as transport pathway rather than a sedimentary depot, explaining the observed thin sediment layer beyond the local entrapment. As SM 17 forms a complex with the opposing elevation, it acts as a morphological barrier that limits sediment accumulation south

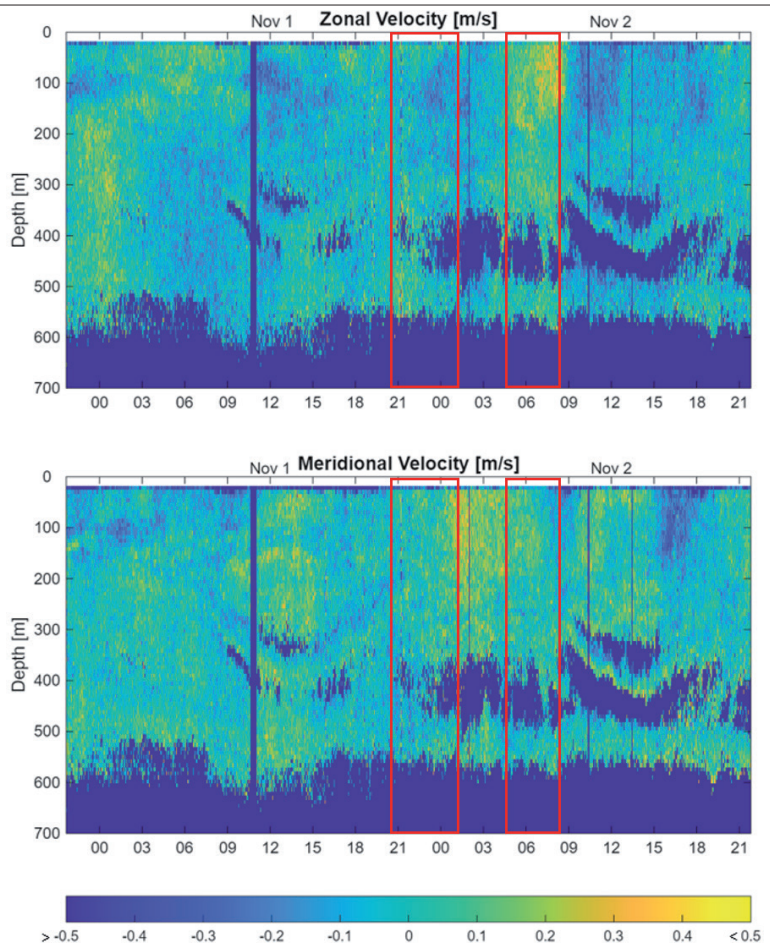

Fig. 6: Plots of zonal and meridional velocities of the 75 kHz ADCP system spanning from 31 October 2025, 21:00 UTC to 2 November 2025, 21:00 UTC (own representation in MatLab)

of the seamount. Increased sediment thickness is first observed about 40 km downstream along the track, where the flow field weakens again as the seafloor becomes more uniform. In contrast, the SMA 18-19-20 exhibits a morphological enclosed structure, in which the mounts are bounded by pronounced spurs, slopes and hollows. Between SM 18 and SM 19-20, the area is dominated by shoulders as well as flats, and the echogram exhibits thick, regularly layered sediment accumulation, indicating sediment entrapment within the basin. This enclosed topography might alter the bottom current pathway through local recirculation, which traps suspended particles within the basin (White and Mohn 2004; Turnewitsch et al. 2013). Once such circulation is established, the current repeatedly reworks the sediment but does not transport it further (Wilckens 2023). In addition, information on the sediment types is important to determine whether observed currents are capable of transporting the material. This was investigated by performing an Angular Response Analysis of MBES backscatter intensities but the method did not deliver reliable results. The measured current velocities cannot be used to directly characterise and validate due to the limited depth range of the ADCP. Nevertheless, the zonal and meridional velocities show variability in the upper 200 m of the water column, specifically in the zonal velocities of SMA 18-19-20 and in the meridional velocities between SMA 16-17 and SMA 18-19-20. Because the study areas are located within the transformation zone of the BC, which transports water southward in the upper 200 m of the water column (Pereira et al. 2014), this variability likely reflects the influence of the BC. To specifically account for the flow directions and quantity of SMA 16-17 and SMA 18-19-20, near bottom current measurements are required. As bottom currents are fluctuating, the observations need to be performed over longer periods of time, e.g. using moored ADCP systems. An alternative approach is the usage of the ARGO float network (cf. Frey et al. 2025).

Conclusion

The results suggest that sediment accumulation is influenced by the morphology of the seamounts. In both sites, the slopes of the mounts showed little to no sediment accumulation, indicating erosion due to accelerated bottom currents. Sediment depositions are dominant on flats of the luv-side before the seamounts, and local entrapments on the lee-side after currents decelerate downslope. SMA 16-17 is characterised by a rather openly structured topography where the area between SM 16 and SM 17 likely acts as sediment pathway. An enclosed topography is exhibited for SMA 18-19-20, suggesting sediment entrapment because of local recirculating bottom currents. The assumptions made on the interaction between bottom currents and sediment depositions could not be validated through ADCP measurements, as no coherent velocities were observed and the measurements likely reflect the southward-flowing BC rather than local seamount driven currents. This study can be viewed as limited as the collected data during MSM 140/2 were acquired during an underway survey, which limited the coverage in terms of survey directions, temporal resolution, survey speed and the possibility to map the seamounts with their surroundings to full spatial extent. //

References

Buchs, David M.; Kaj Hoernle; Ingo Grevemeyer (2014): Seamounts (chapter 34). Encyclopedia of Marine Geosciences. Springer Netherlands, DOI: 10.1007/978-94-007-6644-0_34-1

Frey, Shannon E.; Martin Jutzeler; Rebecca J. Carey; Peter T. Harris (2025): In-situ sedimentary evidence of complex bottom currents at a modern deepwater seamount. Communications Earth & Environment, DOI: 10.1038/s43247-025-02690-7

Gao, Wei; Heshun Wang; Yongfu Sun; Weikun Xu; Yuanyuan Gui (2025): Sediment Distribution and Seafloor Substratum Mapping on the DD Guyot, Western Pacific. Journal of Marine Science and Engineering, DOI: 10.3390/jmse13101904

Garcia, Hernan E.; Zhankun Wang; Courtney Bouchard et al. (2024): World Ocean Atlas 2023: Volume 3: Dissolved Oxygen, Apparent Oxygen Utilization, and Dissolved Oxygen Saturation and 30-year Climate Normal. DOI: 10.25923/rb67-ns53

IHO (2019): Standardization of Undersea Feature Names: Guidelines, Proposal Form, Terminology. Publication B-6, International Hydrographic Organization

Iyer, S. D.; C. M. Mehta; P. Das; N. G. Kalangutkar (2012): Seamounts – characteristics, formation, mineral deposits and biodiversity. Geologica Acta, DOI: 10.1344/105.000001758

Jasiewicz, Jarek; Tomek Stepinski (2025): r.geomorphons. https://grass.osgeo.org/grass84/manuals/r.geomorphon.html

Joo, Jongmin; Seung-Sep Kim; Jee Woong Choi et al. (2020): Seabed Mapping Using Shipboard Multibeam Acoustic Data for Assessing the Spatial Distribution of Ferromanganese Crusts on Seamounts in the Western Pacific. Minerals, DOI: 10.3390/min10020155

Le Bas, T. (n.d.): MBES Segmentation: Manual. Southampton, UK

Mohn, Christian; Anneke Denda; Svenja Christiansen et al. (2018): Ocean currents and acoustic backscatter data from shipboard ADCP measurements at three North Atlantic seamounts between 2004 and 2015. Data Brief, DOI: 10.1016/j.dib.2018.01.014

Mohn, Christian; Martin White; Anneke Denda et all (2021): Dynamics of currents and biological scattering layers around Senghor Seamount, a shallow seamount inside a tropical Northeast Atlantic eddy corridor. Deep Sea Research Part I: Oceanographic Research Papers, DOI: 10.1016/j.dsr.2021.103497

Pereira, Janini; Mariela Gabioux; Martinho Marta-Almeida at all (2014): The Bifurcation of the Western Boundary Current System of the South Atlantic Ocean. Brazilian Journal of Geophysics, DOI: 10.22564/rbgf.v32i2.456

Turnewitsch, Robert; Saeed Falahat; Jonas Nycander et al. (2013): Deep-sea fluid and sediment dynamics – Influence of hill- to seamount-scale seafloor topography. Earth-Science Reviews, DOI: 10.1016/j.earscirev.2013.10.005

White, Martin; Christian Mohn (2004): Seamounts: A review of physical processes and their Influence on the seamount ecosystem. Oceanic Seamounts: An Integrated Study, https://epic.awi.de/id/eprint/37314/17/OASIS_Oceanography.pdf

Wilckens, Henriette (2023): Contourite development: Analysing the interaction between bottom currents and sedimentary systems. Dissertation, University of Bremen

DOI: 10.23784/HN133-10

Validation of altimetry-derived seamount morphology using a multibeam echo sounder in the Atlantic Ocean

An article by JENNICA FREDERICK

High-resolution mapping of the global seafloor remains incomplete, with large areas mapped using global satellite altimetry models. These models are often used to identify and describe seamounts, although their capability to show the morphology of seamounts accurately is unclear. This study evaluates how well satellite altimetry models derived from vertical gravity (VG) anomalies represent seamount morphology compared to multibeam echo sounder (MBES) data. Eleven uncharted seamounts in the Atlantic Ocean were surveyed during a transit cruise between France and Brazil using a hull-mounted MBES. Seamount height, basal radius and base depth were computed from MBES data and then compared with values from a global seamount catalogue based on satellite altimetry. MBES-derived heights exceeded altimetry estimates for seven of the eleven seamounts, with height differences ranging from approximately 200 m to over 1200 m. The height to basal radius ratio varied widely for MBES data (0.08 to 0.39), while altimetry-derived seamounts exhibited a constant ratio of 0.14. These results show the limitations of altimetry-derived models for describing the morphology of seamounts, especially for steep features, and highlight the importance of ship-based bathymetric surveys for accurate seafloor characterisation.

seamounts | satellite altimetry | MBES | vertical gravity gradient (VGG) | bathymetry
Seamounts | Satellitenaltimetrie | MBES | vertikaler Schwerkraftgradient (VGG) | Bathymetrie

Die hochauflösende Kartierung des globalen Meeresbodens ist nach wie vor unvollständig, wobei große Gebiete anhand globaler Satellitenaltimetriemodelle kartiert werden. Diese Modelle werden häufig zur Identifizierung und Beschreibung von Seamounts verwendet, obwohl ihre Fähigkeit, die Morphologie von Seamounts genau darzustellen, unklar ist. In dieser Studie wird bewertet, wie gut Satellitenaltimetriemodelle, die aus vertikalen Gravitationsanomalien abgeleitet wurden, die Morphologie von Seamounts im Vergleich zu Fächerecholotdaten (MBES) darstellen. Elf nicht kartierte Seamounts im Atlantik wurden während einer Transitfahrt zwischen Frankreich und Brasilien mit einem am Rumpf montierten MBES vermessen. Die Höhe, der Basisradius und die Basistiefe der Seamounts wurden aus den MBES-Daten berechnet und dann mit den Werten aus einem globalen Seamount-Katalog auf der Grundlage von Satellitenaltimetrie verglichen. Die aus MBES abgeleiteten Höhen lagen bei sieben der elf Seamounts über den altimetrischen Schätzungen, wobei die Höhenunterschiede zwischen etwa 200 m und über 1200 m lagen. Das Verhältnis von Höhe zu Basisradius variierte bei den MBES-Daten stark (0,08 bis 0,39), während die aus Altimetrie abgeleiteten Seamounts ein konstantes Verhältnis von 0,14 aufwiesen. Diese Ergebnisse zeigen die Grenzen von altimetriebasierten Modellen zur Beschreibung der Morphologie von Seamounts, insbesondere bei steilen Strukturen, und unterstreichen die Bedeutung von schiffsgestützten bathymetrischen Vermessungen für eine genaue Charakterisierung des Meeresbodens.

Author
Jennica Frederick studies Hydrography at HafenCity University in Hamburg.

jennica.frederick@hcu-hamburg.de

1 Introduction

Seamounts are underwater volcanic structures that are found on the seafloor of the oceanic crust and reach a height of at least 100 m (Staudigel and Clague 2010). They are important features in the oceans that are studied by many different disciplines like geology, oceanography, biology and ecology (Wessel et al. 2010). They are also local hubs for species diversity and underwater ecology (Iyer et al. 2012). The general knowledge on seamounts and, more generally, on the oceans is still very limited. Large areas of the seafloor are

still not well mapped, and many seamounts have only been found indirectly with satellite-derived bathymetric models. Satellite altimetry has become an important tool for seafloor mapping, especially in areas where ship-based measurements are unavailable. Satellite altimetry measures sea surface height, from which variations in the Earth's gravitational field are calculated and are then used to calculate the morphology of the seafloor at a larger scale (Gevorgian et al. 2023a). This method is therefore used to estimate the global distribution of seamounts and collect this data in global seamount catalogues. However, the resolution of satellite altimetry data is limited (~6 km) and smaller seamounts measured with this method may not be represented accurately.

Measuring seamounts more accurately requires multibeam echo sounders (MBES) which offer high-resolution bathymetric data (100 to 200 m) (Gevorgian et al. 2023a). Comparing altimetry-derived seamount models with MBES data allows the assessment of the reliability of global seamount catalogues. This research investigates how well altimetry-derived models describe the morphology of seamounts in the Atlantic Ocean when compared with MBES data. The aim of this study is to compare the morphological parameters, height, radius and base depth of uncharted seamounts between satellite altimetry data and bathymetric data from MBES.

2 Theoretical principles

2.1 Seamounts

Menard (1964) defined seamounts as isolated volcanic structures at least 1000 m high from their base located on the ocean floor. In 2010, Staudigel and Clague (2010) defined seamounts as any isolated topographic feature on the seafloor taller than 100 m. Seamounts can be as small as 10 m high domes or as huge as several kilometres-tall structures and sometimes they have flat circular summits or steep external slopes and collapsing features (Iyer et al. 2012; Wessel et al. 2010).

The morphology of seamounts is usually described with parameters such as height and basal radius. Small seamounts have a slope angle proportionate to their maximum height and tend to be much flatter (Gevorgian et al. 2023a). Although there are differences in shape and flatness (height-to-basal radius ratio), Smith (1988) observed a constant relationship between height and basal radius where the summit height of seamounts is approximately one fifth of the basal radius.

Seamount mapping is needed to advance ecological knowledge, understanding volcanic and tectonic processes and higher resolution bathymetric mapping. The majority of seamounts have not yet been surveyed with MBES (Wessel et al. 2010). Global seafloor mapping requires broad multibeam coverage, which is costly and time-consuming. It is therefore important to use indirect mapping methods for the areas between MBES survey tracks. These areas are mapped using global satellite altimetry models derived from vertical gravity (VG) anomalies, which have lower resolution and accuracy (Gevorgian et al. 2023a).

2.2 Satellite altimetry

Satellite altimetry determines the height of the sea surface by measuring the time it takes for a radar pulse to travel from the orbiting satellite to the sea surface and back (Tarpanelli and Benveniste 2019). An equipotential surface called the geoid is approximated by measuring the mean sea surface height with satellite altimeters. Spatial variations in the sea surface height indicate variations in the Earth's gravitational field, which is influenced by mass differences such as the seafloor topography (Kim and Wessel 2011). The density contrast between water and bathymetric structures is the primary cause of the spatial variations in the gravitational field since the gravity field is locally enhanced over bathymetric features (Kim and Wessel 2011; Wessel et al. 2010). Gravity anomalies are derived from the sea surface height measurements and are processed into vertical gravity gradient (VGG) grids that are used to detect seamounts (Gevorgian et al. 2023a). VGG suppresses long-wavelength trends while amplifying short-wavelength signals, such as those seen over seamounts (Kim and Wessel 2011).

However, satellite altimetry has several limitations. One is upward continuation where short wavelengths are attenuated more than long wavelengths in the gravitational signal, which attenuates exponentially with distance from the bottom (Wessel et al. 2010). Seamounts that have a diameter less than the mean ocean depth (~4 km) are then smoothed and attenuated. Another limitation is sediment cover where sediment on the seafloor often covers older tiny seamounts. Despite not being obvious in the topography, the gravity anomaly will still be visible above the buried seamount (Gevorgian et al. 2023a). Sediment thickness on older seafloor can be more than 1 km, hiding many tiny seamounts underneath (Wessel et al. 2010).

2.3 Global seamount catalogue

The global seamount distribution catalogue used in this study is based on VGG grids derived from marine gravity models (Kim and Wessel 2011). The original global seamount catalogue created by Kim and Wessel (2011) used the 1-min Mercator VGG grid to find 24,643 seamounts with heights higher than 100 m. An updated version used an improved VGG grid which found 19,325 additional seamounts (Gevorgian et al. 2023b). The morpho-

logical parameters of the seamounts were estimated using Gaussian fitting methods which give information on the height, basal radius and base depth.

3. Methodology

3.1 Data acquisition

The data was collected during the MSM140/2 transit cruise on the Atlantic Ocean from Brest (France) to Rio de Janeiro (Brazil) on the *Maria S. Merian* research vessel. The vessel left Brest on 17.10.2025 and arrived in Rio de Janeiro on 05.11.2025. Eleven seamounts were surveyed along the way (Fig. 1). The Kongsberg EM-124 MBES was used to record the seafloor bathymetry. The frequency used was fixed at 12 kHz with an opening angle of 150°. Modelled sound velocity profiles obtained from World Ocean Atlas 2023 were regularly imported into the acquisition software to correct the refraction of the sound pulses through the water column.

During the transit, the latest global seamount catalogue by Gevorgian et al. (2023b) was used. This allowed the identification of eleven uncharted seamounts along the survey track. Their coordinates are found in Table 1.

3.2 Data processing

Quality check and processing of the MBES data was conducted on board using Qimera. Seamount morphology was analysed in QGIS. Contour lines at 100-m intervals were added, and terrain profiles were drawn through each seamount to determine their base depth, summit depth and height. The base radius for all seamounts was calculated by drawing polygons around the base contour and using the formula $r = \sqrt{Area : \pi}$. The height-to-base radius ratio ($h : r_b$) was then calculated for each seamount. The parameters height, base radius, base depth and height-to-base ratio were compared with the values from the VGG-based global seamount catalogue.

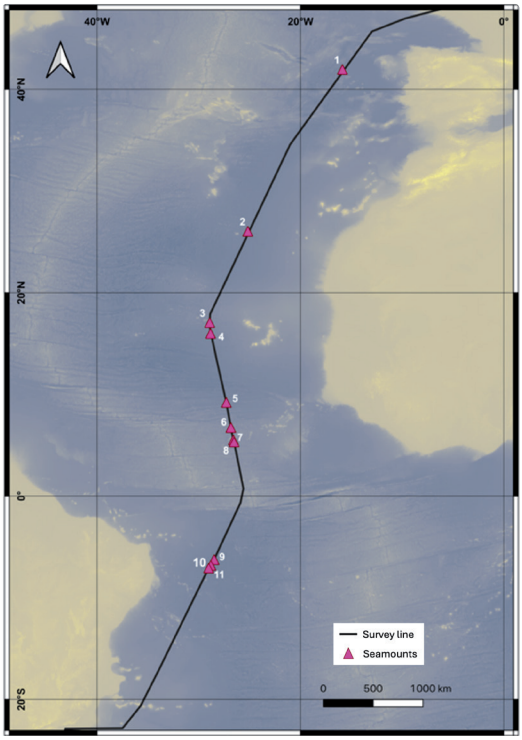

Fig. 1: Survey track of the MSM140/2 transit with the location of the eleven surveyed seamounts (representation in QGIS)

4 Results

Seamount heights measured from MBES ranged from 560 m (seamount 4) to 2,571 m (seamount 11), while altimetry-derived heights ranged from 1,000 m to 2,000 m. Seven of the eleven seamounts had MBES-derived heights higher than altimetry estimates. Base depths measured with MBES varied between –5,802 m (seamount 9) and –4,559 m (seamount 8), with equivalent altimetry base depths between –5,570 m and –4,200 m. The basal radius of the seamounts, measured from MBES data, ranged from 5.7 km (seamount 3) to 12.6 km (seamount 10). The altimetry-derived basal radius ranged from 7.2 km to 14.6 km. The calculated height-to-base ratios from MBES data ranged between 0.08 (seamount 5) and 0.39 (seamount 7). The height-to-base ratios from the altimetry-derived catalogue were equal to 0.14 for all seamounts. Table 2 summarises the results and the corresponding values from the altimetry-derived seamount catalogue (Gevorgian et al. 2023b).

5 Discussion

The results show that altimetry-derived models do not fully represent the morphological characteristics of the surveyed seamounts. The comparison between MBES and altimetry-derived data demonstrates significant differences in base depth, height and morphological ratios. Altimetry-derived base depths are consistently shallower than MBES measurements, with MBES depths on aver-

Seamount	Longitude	Latitude
1	–15.875°	41.958°
2	–25.175°	26.042°
3	–28.925°	17.058°
4	–28.842°	15.992°
5	–27.292°	9.208°
6	–26.842°	6.742°
7	–26.592°	5.525°
8	–26.525°	5.325°
9	–28.492°	–6.242°
10	–28.808°	–6.808°
11	–29.025°	–7.075°

Table 1: Coordinates of the eleven surveyed uncharted seamounts

Seamount	MBES height	Altimetry height	MBES base depth	Altimetry base depth	MBES base radius	Altimetry base radius	MBES height-to-base ratio (h/r_b)	Altimetry height-to-base ratio (h/r_b)
1	1,506.68 m	1,300 m	−5,556.13 m	−5,332.758 m	11.213 km	9.461 km	0.13	0.14
2	1,952.24 m	1,300 m	−5,341.15 m	−5,183.175 m	8.015 km	9.461 km	0.24	0.14
3	801.42 m	1,000 m	−4,933.78 m	−4,824.575 m	5.666 km	7.278 km	0.14	0.14
4	560.34 m	1,800 m	−5,184.06 m	−5,092.997 m	6.206 km	13.100 km	0.09	0.14
5	930.97 m	1,500 m	−5,422.61 m	−5,188.081 m	11.518 km	10.917 km	0.08	0.14
6	1,050.28 m	1,700 m	−4,722.68 m	−4,372.370 m	8.774 km	12.373 km	0.12	0.14
7	2,384.85 m	1,200 m	−4,595.86 m	−4,200.837 m	6.121 km	8.734 km	0.39	0.14
8	2,532.98 m	1,700 m	−4,559.25 m	−4,269.173 m	8.100 km	12.373 km	0.31	0.14
9	1,768.01 m	1,500 m	−5,801.65 m	−5,570.354 m	9.317 km	10.917 km	0.19	0.14
10	1,833.98 m	1,600 m	−5,550.73 m	−5,357.896 m	12.587 km	11.645 km	0.15	0.14
11	2,571.07 m	2,000 m	−5,666.27 m	−5,402.928 m	10.194 km	14.556 km	0.25	0.14

Table 2: Morphological parameters from MBES and altimetry data

age approximately 230 m deeper. This difference can be explained by upward continuation of the gravity field, which results in the gravity-derived model smoothing the bathymetry and underestimating true depths.

Altimetry often underestimates values, as seen in the heights of seamounts 7 and 8. Their basal diameters (12 km and 16 km) are close to the VGG resolution limit, which probably causes spatial smoothing and lower height estimation. Their MBES-derived height-to-base ratios (0.39 and 0.31) indicate steep morphology, while the altimetry model has a constant ratio of 0.14. This comparison shows the limitations of VGG-based models for representing the true morphology and steepness of seamount structures. Fig. 2 shows the visual comparison of seamounts 7 and 8 between altimetry and MBES data.

Seamount 5 shows an opposite behaviour in height estimation, where altimetry overestimates the actual height measured by MBES. Seamounts smaller than 1 km are generally difficult to detect using VGG because their gravity signals are weak and more strongly affected by upward continuation. However, a locally stronger gravity signal may be caused by the capacity of altimeters to detect buried volcanic structures beneath sediment cover. In this case, the altimetry model interprets the feature as higher than it actually is while MBES measures the actual bathymetric surface. The very low height-to-base ratio of 0.08 supports this interpretation, as it indicates a very flat and wide structure that may have undergone long-term sedimentation. Fig. 3 shows the visual comparison of seamount 5 between altimetry and MBES data.

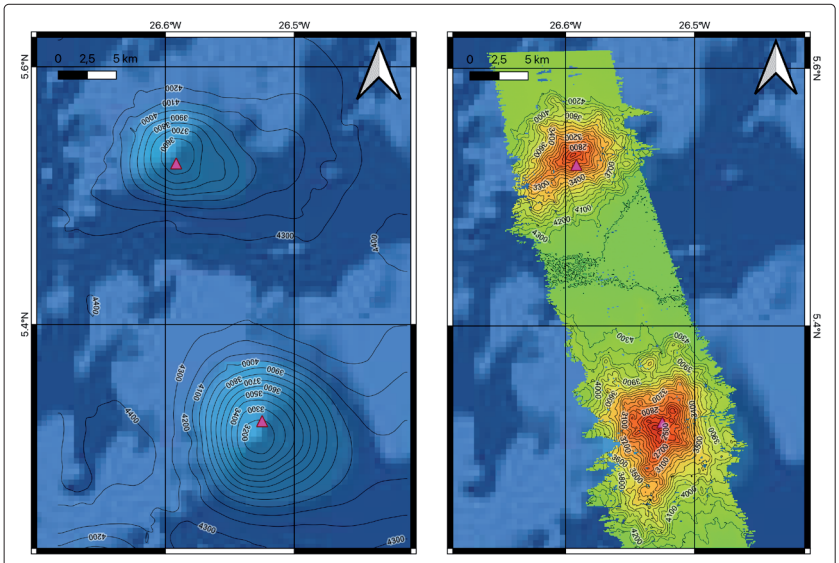

Fig. 2: Seamounts 7 and 8 with 100 m depth contour lines shown by altimetry model GEBCO (left) and MBES data (right) (representation in QGIS)

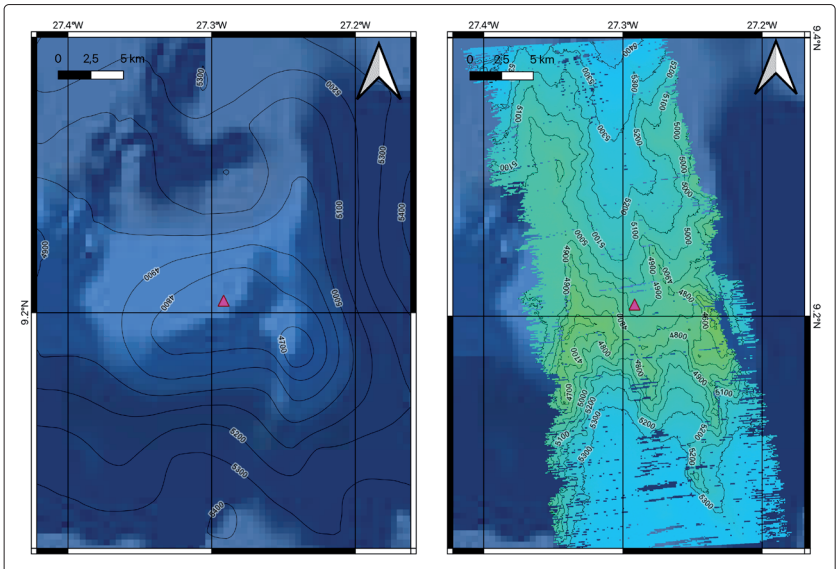

Fig. 3: Seamount 5 with 100-m depth contour lines shown by altimetry model GEBCO (left) and MBES data (right) (representation in QGIS)

6 Conclusion

This study evaluated the validity of altimetry-derived seamount morphology by comparing the parameters from the VGG-based catalogue to MBES data for eleven uncharted seamounts in

the Atlantic Ocean. The results show significant differences in height, base depth and height-to-base ratio between the two datasets. The altimetry-derived base depths are shallower, and the steep seamounts have underestimated heights due to spatial smoothing. In contrast, other seamounts showed an overestimation of height in the altimetry model, possibly related to sediment-covered structures which influence the gravity signal. The MBES data show that the height-to-base ratios vary widely, ranging from very flat and wide to steep and narrow morphologies, which are not represented in the constant ratio used in the global catalogue. While satellite altimetry is important for global seamount detection, morphological characterisation requires high-resolution multibeam surveys to accurately represent seafloor features. //

References

GEBCO (2026): General Bathymetric Chart of the Oceans. www.gebco.net

Gevorgian, Julie; David Sandwell; Yao Yu; Seung-Sep Kim; Paul Wessel (2023a): Global Distribution and Morphology of Small Seamounts. Earth and Space Science, DOI: 10.1029/2022EA002331

Gevorgian, Julie; David Sandwell; Yao Yu; Seung-Sep Kim; Paul Wessel (2023b): Global Distribution and Morphology of Small Seamounts [Data set]. Zenodo. DOI: 10.5281/zenodo.7718512

Iyer, S. D.; C. M. Mehta; P. Das; N. G. Kalangutkar (2012): Seamounts – characteristics, formation, mineral deposits and biodiversity. Geologica Acta, DOI: 10.1344/105.000001758

Kim, Seung-Sep; Paul Wessel (2011): New global seamount census from altimetry-derived gravity data. Geophysical Journal International, DOI: 10.1111/j.1365-246X.2011.05076.x

Menard, Henry W. (1964): Marine Geology of the Pacific. McGraw-Hill

Smith, Deborah K. (1988): Shape analysis of Pacific seamounts. Earth and Planetary Science Letters, DOI: 10.1016/0012-821X(88)90143-4

Staudigel, Hubert; David Clague (2010): The Geological History of Deep-Sea Volcanoes: Biosphere, Hydrosphere, and Lithosphere Interactions. Oceanography, DOI: 10.5670/oceanog.2010.62

Tarpanelli, Angelica; Jérôme Benveniste, J. (2019): Chapter Eleven – On the potential of altimetry and optical sensors for monitoring and forecasting river discharge and extreme flood events. Extreme Hydroclimatic Events and Multivariate Hazards in a Changing Environment, DOI: 10.1016/B978-0-12-814899-0.00011-0

Wessel, Paul: David T. Sandwell; Seung-Sep Kim (2010): The Global Seamount Census. Oceanography, DOI: 10.5670/oceanog.2010.60

World Ocean Atlas (2023): World Ocean Atlas 2023. Ocean Data View, https://odv.awi.de/data/ocean/world-ocean-atlas-2023

SUBSEA EUROPE
SERVICES

Powering Energy. Enabling Science

Equipment. Expertise. Integration.

From sonars and ADCPs to crewed and autonomous survey platforms, our marine technology drives offshore energy and ocean science operations across Europe. Whether purchasing, renting, or integrating equipment, our expert team ensures fast delivery and responsive support, keeping your next project on time and on budget.

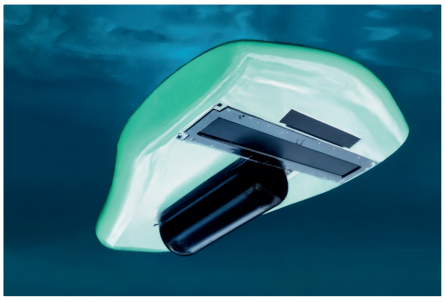

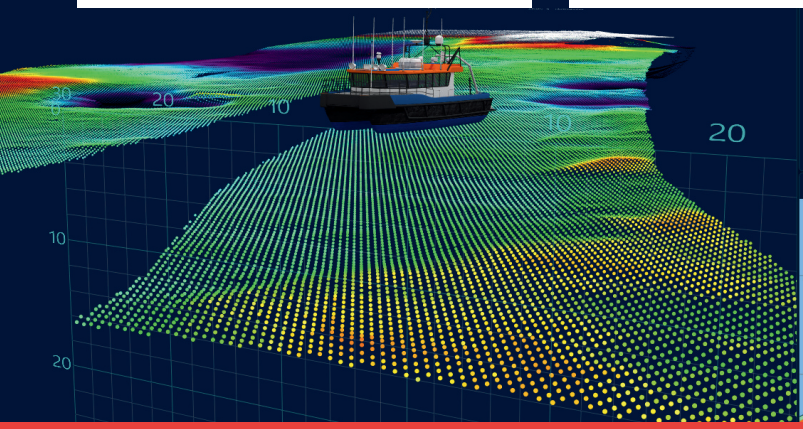

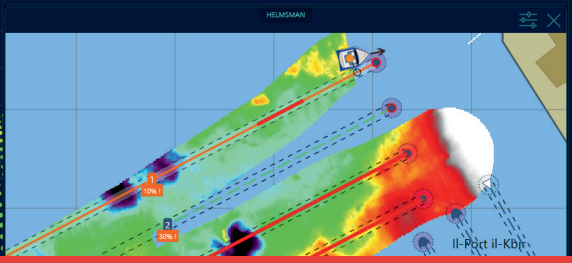

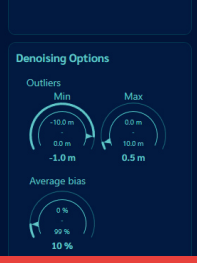

Now stocking Voxometer from R3 Vox and Origin ADCP from Sonardyne
Contact our expert team today: **sales@subsea-europe.com**

MacArtney
UNDERWATER TECHNOLOGY

Consulting

Ocean engineering from space into depth

Realise your projects in cooperation with our hydrographic services

Our hydrography engineers are happy to develop systems tailored exactly to your needs and to provide professional advice and support for setting up your systems and training your staff.

MacArtney Germany benefits from being part of the MacArtney Group and enjoys unlimited access to cutting-edge engineering competences and advanced facilities.

CTDs & SVPs

Acoustic sensors

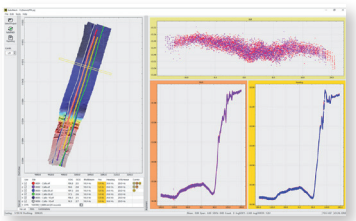

Software

Position and motion sensors

Integration

Denmark | Norway | Sweden | United Kingdom | France | Italy | Netherlands | Germany
USA | Canada | South America | Australia | Singapore | China